UNIVERSIDAD COMPLUTENSE DE MADRID

FACULTAD DE CIENCIAS FÍSICAS


# TESIS DOCTORAL

Unification of nonclassical signatures under the concept of quantum coherence

Unificación de efectos no clásicos bajo el concepto de coherencia cuántica

MEMORIA PARA OPTAR AL GRADO DE DOCTOR

PRESENTADA POR

Laura Ares Santos

DIRECTOR

Alfredo Luis Aina

# Unification of nonclassical signatures under the concept of quantum coherence

## Unificación de efectos no clásicos bajo el concepto de coherencia cuántica


Memoria para optar al grado de Doctora
presentada por

Laura Ares Santos

**UNIVERSIDAD COMPLUTENSE DE MADRID**
FACULTAD DE CIENCIAS FÍSICAS

Director
Alfredo Luis Aina

Programa de Doctorado en Física

*A mis abuelos*

# Agradecimientos

No hay folio en blanco que no produzca tanta ilusión como miedo. Confío en que nadie necesite leer esto para saber lo importante que es para mi y, a su vez, me honra la oportunidad de resaltarlo. A cientos de km, a destiempo, a veces incluso sin ser notados. Gracias a todos por no dejarme sola mientras me alejaba. Porque la coherencia, incluso en el lenguaje, está sobrevalorada.

A todos los Alfredos. Al que siempre escucha. Al que entiendo y, sobre todo, al que no. Al que comparte con generosidad sus ideas aunque yo haga de poli malo... Al de paciencia inagotable. Mi agradecimiento infinito por su confianza y su cariño. Por la complicidad y el sentimiento de equipo. También por demostrar que puede construirse un mundo en el que investigar lo que te hace feliz. Es un privilegio el tiempo compartido y un honor ver mi nombre junto al tuyo. Lo que he aprendido de ti no cabe en ninguna memoria.

A mi familia. El sitio al que volver, desde donde crecer. Por enseñarme que siempre tiene que haber hueco para uno más. A mi madre, por mostrarme lo que puede el amor. A mi padre, por enseñarme a mirar a las estrellas. Incansables, gracias por vuestro esfuerzo y vuestra paciencia conmigo. Si algo hay de bueno en este trabajo, es vuestro. A mi hermana, ejemplo, norte y compañera de vida, por su lealtad pura. Gracias a los tres por *escoltarme* por un camino que ni yo entendía. También agradezco a mis tíos la confianza y el apoyo que siempre me demuestran.

Dani, el chico del café, por caminar por este filo conmigo. Experto en señalar los arcoíris escondidos en las nubes de tormenta y en los charcos de aceite. Por los grillos, las pizzas y los arándanos. Ángela, por las lágrimas

compartidas, y Mario, por los habrazos a tiempo. Hermanos mayores a todas luces, siempre os deberé un café. A Gerardo, ejemplo a seguir con carácter retroactivo, aunque estemos condenados a no entendernos. Sara y Noelia, mis catalizadores, por los cafés eternos. También por todas las cosas que no habría hecho sin vosotras. A Verónica, por darme perspectiva y por compartir conmigo los consejos de Inma. A la becaría, por acogerme y dejarse acoger haciendo de ese despacho un lugar amable y seguro. Gracias, Óscar, por los cafés como excusas para parar y las ideas como punto de partida para seguir. Siempre con algo positivo que ofrecer, no me imagino esta etapa sin ti.

A mi otra familia: sin El Comando la física y el mundo perderían casi toda su luz. Han sido infinitas ayudas *infinitesimales*, pero, sobre todas ellas, gracias por estar (y ser) incondicionalmente. Por hacerme mejor con cada broma, debate o concierto. Por llenar estos 10 años de recuerdos dignos de ser citados uno a uno [113, 114, 115, 136, 139, 151, 165, 166, 170][1]. En especial a Paloma, por los lunes muy lunes y los viernes muy viernes. Un honor compartir este camino contigo.

Cómo olvidarme de Pablo y su maldita costumbre de preguntar de vez en cuando quién soy, o si soy feliz. Este trabajo me hace más ilusión gracias a ti. Gracias, Jose. Entre *todo*, por aguantar los momentos de lucidez que surgen con la segunda cerveza. Por sujetarme. A José Manuel, de quien aprendo tanto, aunque no siempre entienda. Refugio de mi pesimismo viernes tras viernes. A Isabel, por aquel paseo por el canal, y Diana, por confiar en mi más que yo misma. Gracias por seguir formando parte del recorrido, todo sería mucho más triste sin vosotras.

To Prof. Sperling, who carries all the kindness and courtesy of the world on his shoulders, thank you for showing me the beauty of the quantum world when it becomes tangible. I acknowledge him, Prof. Silberhorn, and the Integrated Quantum Optics Group at Paderborn University for the welcome when frontiers were still closed. Thanks, Nidhin, for the data acquisition that made our work possible. Dr. Marcos, for the gift of Lille (et du Cheval Blanc). You make me a better scientist. Finally, I want to acknowledge the optics department at the Complutense University of Madrid for allowing my development also as an educator, and the financial support from the European Social Fund and the Spanish Ministerio de Ciencia Innovacion y Universidades, Contract Grant No. BES-2017-081942.

[1] Si el Pablos se doctora, yo también puedo.

# Resumen

La coherencia cuántica es la consecuencia tangible del principio de superposición, por lo que debe estar completamente enraizada en todos los efectos cuánticos. La característica común a todos estos comportamientos de la naturaleza no explicables por las teorías clásicas se define como no clasicidad. Al ser ambos conceptos bastante escurridizos, pueden encontrarse varias interpretaciones de la coherencia y la no clasicidad. Esto hace que su conexión sea a veces trivial y a veces contradictoria.

El objetivo principal de esta tesis es encontrar conexiones entre los principales efectos no clásicos y la coherencia, analizando si esta última puede considerarse el único fenómeno subyacente a todo comportamiento cuántico. Durante el proceso, investigamos los vínculos entre las potenciales causas de la no clasicidad, como la complementariedad, el proceso de medida y la separabilidad estadística, pero también los vínculos entre diferentes efectos no clásicos, como el entrelazamiento, la polarización no clásica o la super resolución. Dado que la coherencia cuántica es un concepto presente en varios contextos, enfocamos su estudio desde distintas perspectivas: como recurso, como magnitud medible experimentalmente y como característica fundamental en metrología. Se incluye en este análisis la naturaleza cuántica de los detectores como pareja ineludible en toda observación cuántica.

En este trabajo, la no clasicidad se define como la falta de una distribución de probabilidad conjunta para observables incompatibles legítima. El mecanismo para obtener dicha distribución consiste en realizar una medición conjunta de ciertas versiones no ideales de los observables incompatibles a estudiar. Esto siempre es posible para cierto grado de imprecisión en la medida. Puesto que se conoce la no idealidad utilizada, esta puede invertirse, permitiendo inferir la distribución completa. Los signos de no clasicidad surgen cuando esta distribución invertida resulta ser patológica.

Este protocolo de medidas no ideales de observables incompatibles seguido de la correspondiente inversión de datos se aplica a experimentos tipo Bell, mostrando la equivalencia exacta entre el fallo de los modelos de variables ocultas y nuestra misma definición de no clasicidad. También nos permite trasladar el teorema de Bell a estados con un único subsistema. Además, mostramos que la no clasicidad de los detectores surge como condición necesaria para estas y otras señales típicas de comportamientos cuánticos.

En la búsqueda de una unificación de los fenómenos cuánticos basada en la coherencia, utilizamos una teoría de coherencia-no clasicidad para revelar una equivalencia

fundamental entre la polarización no clásica y el entrelazamiento multifotónico. Esta teoría se evalúa también experimentalmente mediante tomografía de polarización de un estado de vacío comprimido de dos modos. Además, introducimos una nueva teoría de la coherencia directamente enraizada en un contexto metrológico, proporcionando una relación notablemente sencilla entre la resolución de los procesos de detección de una señal y las propiedades de coherencia de los elementos de la medida. Como resultado especialmente significativo en el contexto de la coherencia, descubrimos que la coherencia de los detectores tiene la misma influencia en la resolución que la coherencia de la sonda. En el ámbito de las teorías de recursos estudiamos cómo las principales operaciones en óptica cuántica, desplazamiento, compresión y división del haz, influyen en la cantidad de coherencia de varios estados, mostrando una dependencia inesperada de la coherencia con la intensidad de la luz, y una dependencia más natural con la compresión.

En cuanto a los vínculos entre coherencia y no clasicidad, se desarrolla una relación geométrica entre sus cuantificadores en el marco de las teorías de recursos. Finalmente la dependencia con el cuantificador es eliminada y se estable una relación unívoca entre las coherencias de la matriz densidad y la falta de una distribución conjunta para observables incompatibles, nuestra definición de no clasicidad en si misma.

A partir de los diversos resultados obtenidos, concluimos que el mecanismo más adecuado para detectar la no clasicidad y analizar sus causas es la medida conjunta no ideal de observables incompatibles. También concluimos que es esencial tener en cuenta las propiedades del detector los análisis cuánticos. Por último, resolvemos que la coherencia y la no clasicidad surgen como conceptos equivalentes a un nivel muy fundamental.

Para concluir, destacamos la consistencia del planteamiento general de este trabajo: parte de una definición inequívoca de no clasicidad, expone un mecanismo para detectarla y analizar sus causas y, en última instancia, permite concluir que la causa fundamental de la no clasicidad es la coherencia.

# Abstract

Quantum coherence is the measurable consequence of the superposition principle, so it must be completely rooted in all the quantum effects. The feature common to all these behaviors of nature not affordable by classical theories is defined as nonclasicality. Being both rather elusive concepts, several interpretations of coherence and nonclassicality can be found. This makes their link sometimes trivial and sometimes contradictory.

The main objective of this thesis is to find connections between the main signatures of nonclassical effects and coherence, analyzing if the latter can be considered the sole phenomenon underlying every quantum effect. During the process, we investigate the links between different potential causes of nonclassicality, such as complementarity, measurement process, and statistical separability, but also between different nonclassical effects, such as entanglement, nonclassical polarization, or sub-shot noise resolution. Since quantum coherence is a concept present in several contexts, we face it from different perspectives: as a resource, as an experimentally measurable magnitude and as a fundamental feature in metrology. We include in this picture the quantum nature of detectors as the unavoidable partner in every quantum observation.

In this work, nonclassicality is defined as the lack of a legitimate joint probability distribution for incompatible observables. The mechanism to obtain such joint distribution is to perform a joint measurement of nonideal versions of the incompatible observables under study, which is always possible for some degree of added fuzziness. As far as the nonideality utilized is known, it can be inverted, allowing to infer the complete distribution. Quantumness emerges when this inverted distribution turns out to be pathological.

This protocol of nonideal measurements of incompatible observables followed by suitable data inversion is applied to Bell-type analyses in bipartite systems, showing the exact equivalence between the failure of hidden-variable models and our very definition of nonclassicality. It also allows us to translate Bell's theorem to single systems. Furthermore, we show that the quantumness of detectors arises as a necessary condition for these and other typical quantum signatures.

Looking for a unification of quantum phenomena based on coherence, we utilize a coherence-nonclassicality theory to reveal a fundamental equivalence between nonclassical polarization and multi-photon entanglement. This theory is also experimentally evaluated by polarization tomography of a two-mode squeezed vacuum state. As a

further development, we introduce a new theory of coherence directly rooted in a metrological context, providing a remarkably simple relationship between the resolution of signal detection processes and the coherence properties of the measurement elements. As a particularly meaningful result in the coherence context, we find out that the coherence of the detectors has the same influence on the resolution as the coherence of the probe state. We study how the principal operations in quantum optics, displacement, squeezing and beam splitting, alter the amount of coherence for several states, showing an unexpected dependence on coherence with light intensity and a more natural dependence on squeezing.

Regarding the links between coherence and quantumness, a distance-based relation between nonclassicality and coherence quantifiers is developed within the framework of resource theories. Moreover, the dependence on the quantifier is finally removed, and we establish a univocal relation between the coherences of the density matrix and the lack of a joint distribution for incompatible observables, our very definition of nonclassicality.

From the diverse results obtained, we conclude that the most adequate mechanism to detect nonclassicality and analyze its causes is the nonideal joint measurement of incompatible observables. We also conclude that the properties of the detector have to be taken into account in quantum analyses. Finally, we resolve that coherence and nonclassicality have emerged as equivalent concepts at a very fundamental level.

To conclude, we remark on the consistency of the general approach of this work: it starts from an unambiguous definition of nonclassicality, exposes a mechanism to detect it and to analyze its causes, and, ultimately, allows the conclusion that the fundamental cause of nonclassicality is quantum coherence.

# Contents

# Introduction

*De no hablar hasta saber, nunca diríamos nada.*

*A. L. A.*

Quantum theory is one of the most fascinating proposals that physics has ever made. Behind its extremely accurate precision in predicting the behaviour of nature, surprisingly, one finds a probabilistic theory. Moreover, a probabilistic theory in an intrinsic sense, unavoidable, not regarding lack of knowledge but built by probabilities themselves. It makes statistics, correlation, and inference basic tools for describing reality.

Leaving aside aspects of interpretation, which could be considered rather philosophical, the fundamental concepts behind the quantum theory, such as the definitions of measurement and quantumness, are still under discussion [1, 2]. Moreover, from the postulates to the superposition principle, the quantum theory itself is composed of an intricate set of elements whose physical meanings and links are not always as clear as we can see in other theories [3, 4]. The utmost discussion in this direction could be searching for the main ingredient of the quantum theory. Is it the measurement process? Is it complementarity? Is it the superposition principle? In the most probable scenario, where a complete identification between those elements cannot be made, remains legitimate the question about the potential links between these concepts [5, 6]. To contribute to answering this question, the purpose of this work is to discern the proper relation between quantum coherence and the main signatures of nonclassicality introduced so far.

The lack of a consensual, neither definite nor final, interpretation of these concepts obscures the links already established in the literature [7, 8]. In a similar way as optical coherence manages classical randomness in classical optics, quantum coherence is a property of nature essentially defined in a scenario driven by quantum randomness to encompass all the consequences of the superposition principle. However, when these consequences are specific enough, they are usually disengaged, even if they are included by definition under the concept of coherence. Sometimes, this prevents us from a general approach that may provide a common interpretation for some quantum effects.

The concept of nonclassicality was born to enclose the observations that classical theories cannot explain, being the ultimate reason for the introduction of such a curious theory. Historically, the definition of classicality has been linked to the incoherent superposition of coherent states. The definition itself labels *deus ex machina* the classical-like states. This preference is based on their performance in certain scenarios, however, these circumstances are by no means universal, which makes the choice of classical states still a particular, biased decision. Consequently, a definition of nonclassicality that does not require any predetermined classical set of states is proposed. This definition states that it is always necessary to appeal to incompatible observables to disclose nonclassicality. This is because classical physics can mimic the statistics of every single quantum observable by a series or particular initial conditions [9]. Accordingly, this approach recognizes much more importance than usual to the measurement and presents quantumness as a phenomenon, not only as a property of the state.

The deeper knowledge about how nature works, the more advantage we can take of it. The accuracy with which quantum mechanics models the more subtle processes allowed us to develop technologies previously reserved for science fiction [10]. For example, quantum metrology is one of the pioneer areas of application of the advantages of quantum features. Actually, quantum mechanics turned out to be both, *the cause of and solution to all of the sensitivity's problems*: When the detection processes achieved the scales of the quantum fluctuations, the use of states with reduced fluctuations allowed to further increase the sensitivity of the experiments. However, once again, the efforts to exploit the properties of nature that quantum theory brings to light, either to use or to analyze them, have led to considerable fragmentation in their analysis [11]. In this context, coherence is understood as the main resource regarding exploiting quantumness, and, despite this, there is no definitive relationship between these two properties. The absence of an explicit, unambiguous relation between sensitivity and coherence brings one mayor aim of this work concerning coherence: to connect the metrological resolution and quantum coherence of the signal detection process.

However, the value of coherence should not be reduced to its usefulness. Quantum coherence appears as the fundamental resource for quantum technologies, but precisely because without it, all is classical physics. In the same spirit that without classical coherence, all optics is geometrical optics. Therefore, we are also interested in analyzing the fundamental meaning of coherence. To this end, we focus on the basis-dependence of the measures of coherence. This commitment will guide us to define and quantify nonclassicality through the quantifiers of coherence by a geometrical relation between them.

Regarding nonclassicality, the first objective is to analyze the relevance of some elements -such as complementarity, statistical separability, and detector contribution- involved in the emergence of quantum signatures. The aim is to provide a unified picture embracing all of them, able to reveal any kind of structure. This leads us to

the second goal, which is to analyze the relationship between different nonclassical signatures themselves. The last and central objective of this work is to establish a direct, practical, and fundamental relation between the very roots of coherence and nonclassicality disclosed in the previous objectives.

The mechanisms utilized to achieve the objectives of this thesis are general enough to allow the study of several elements through the same tool. The main ones are the nonideal measurement of incompatible observables, the theory of quasiprobability distributions, and the framework of resource theories.

# Nonclassicality

*HEISENBERG: ¡Porque supuse que no valía la pena hacerlo!*
*BOHR: ¿Supusiste? ¡Tú nunca suponías las cosas!*
*Copenhague, Michael Frayn.*

## 1.1 Introduction to nonclassical features

Non-classical phenomena are experiences that cannot be explained by means of classical theories, in particular by classical electromagnetism when talking about quantum optics [12]. The black-body radiation and the photoelectric effect are irrevocably the seeds of quantum theory. Those experiments accounted for the need to discretize some variables to understand the behaviour of nature. Nowadays, the physical understanding of these experiences has changed. Those phenomena can be essentially explained by semiclassical theories, where quantumness can be ascribed only to matter instead of the electromagnetic field, as originally inferred [13]. In any case, there is no fully classical theory explaining these experiences. Although semiclassical theories may be interpreted as incomplete or even biased, they are still an important tool for approaching intricate problems and understanding the quantum-classical borderline [14, 15]. In this respect, the semiclassical explanation of the photoelectric effect is the perfect example of the self-evaluation of quantum theory.

Further typical nonclassical effects are those attributed to the vacuum fluctuations [12]. They generate a manifold of amazing effects such as spontaneous emission, Lamb shift and the Casimir effect, among other examples. If we focus on the specific quantization of the electromagnetic field, there are some emblematic quantum manifestations that we should highlight: the anti-photon correlation and the Hong-Ou-Mandel effect, the subPoissonian photo-counting statistics, the photon antibunching and the quadrature squeezing [16], which will be further analyzed in this work.

Nevertheless, strictly speaking, subPoissonian statistics, antibunching and quadrature squeezing are not quantum signatures by themselves. This is because any probability distribution for a single-observable can be achieved in classical physics. These features are commonly considered nonclassical signatures because they cannot be displayed by the states usually defined as classical in quantum optics, as we are about to see.

It was considered that the fundamental evidence for the lack of classical explanation could be the impossibility of defining a proper phase-space probability distribution for certain states. The success of the phase-space description in classical theory motivated the translation of this representation to quantum mechanics [17, 18]. However, infinite quasiprobability distribution can be established due to the commutation relations between operators [19]. Moreover, not all of them have equivalent pathologies or even pathologies at all.

Since the original works of Glauber and Surdashan [20, 21, 22], and being still widely accepted [23, 24], the definition of nonclassicality in quantum optics have rested on the Glauber-Surdashan $P(\alpha)$ function on a more or less consensual way. This choice is rooted in the fact that the $P(\alpha)$ allows to compute the expectation value of normally ordered operators just like a classical phase-space function, resting the importance of the normal ordered in the operation of photoelectric detectors.

Additionally, $P(\alpha)$ allows the representation of the density in terms of coherent states of the harmonic oscillator, $|\alpha\rangle$,

$$\rho = \int d^2\alpha P(\alpha)|\alpha\rangle\langle\alpha|. \tag{1.1}$$

Therefore, it is considered classical-like any incoherent combination of Glauber-coherent states, this is, any state with a well-behaved $P(\alpha)$ as a probability distribution on phase space. On the contrary, a $P(\alpha) < 0$ or any other pathology implies that the state cannot be expanded as a convex combination of coherent states. Now we can see that subPoissonian statistics or quadrature squeezing imply nonclassical behaviour, since both features require statistics less fluctuating than the statistics of coherent states.

However, the concept of a preferred set of states considered classical by definition could not be so attractive. This is why the definition of nonclassicality to be considered in this work is slightly different. We maintain the idea of the failure of a joint probability distribution as the essential signature of quantumness, however, we do not privilege any set of variables and we consider nonclassicality the failure to obtain by any means a joint probability distribution, or its pathological behavior, for any two incompatible observables [25, 26]. This definition includes as a particular case the pathological $P(\alpha)$, which implies the absence of a joint probability distribution for the quadrature observables. However, by choosing a different set of incompatible observables, even Glauber-coherent states can lack a well-behaved joint statistics [26, 27]. All

the experiences introduced in this section as nonclassical effects reflect, in one way or another, the lack of a joint probability distribution for different incompatible observables. Consequently, we may refer to them as indirect signatures of nonclassicality.

### 1.1.1 Joint measurements of incompatible observables

Incompatible observables cannot be measured in the same experiment. Since they do not have common eigenvectors, states with both variables well defined, we cannot obtain the value of both magnitudes in the same (individual) experiment respecting the Born's rule. What we can do is to measure each magnitude in different repetitions and then we would have their individual statistics. But this is not a joint statistics.

We consider that this lack of joint distributions is actually the central fact of quantumness. Consequently, we look for procedures to approach such a potentially pathological probability distribution. It seems quite problematic to directly measure a not legitimate statistics (how to find negative probabilities when repeating an experiment?). The technique applied in this work is based on the indirect observation of the distribution under study. To this end, a nonideal, inaccurate, unsharp measurement is performed, followed by the corresponding data inversion based on our knowledge of the arrangement. In this section, we briefly introduce the theoretical concepts behind generalized measurements.

#### 1.1.1.1 Positive Operator-Valued Measurements

There are two possible dynamics in the standard quantum theory. The Schrödinger equation describes the continuous, deterministic evolution of an isolated system. Known the initial state and the Hamiltonian of the system, it gives the final state univocally. On the contrary, the description of the evolution in a measurement process is sharp and nondeterministic. In an ideal formulation, the projection postulate, fully phenomenological, establishes the state after the measurement as the eigenvector associated with the result. The discontinuity in the dynamics caused by the reduction of the state is a controversial element in quantum theory, which gives rise to the measurement problem: How to reconcile these two kinds of evolution. When a measurement is performed, going deep enough there is, one way or another, the observed system interacting with an *external* detector, giving rise to the mentioned discontinuity. However, we may also consider both, observed system and detector, as an entangled system whose corresponding evolution would be driven by the deterministic Schrödinger equation. Therefore, at what point does the discontinuity occur and why?

The relationship between states and the outcomes of measurements is just a matter of probabilities in quantum mechanics[1]. A physical magnitude, an observable, is

[1] Actually, the kind of objective, irreducible quantum uncertainty beyond human and nonhuman knowledge.

described by a self-adjoint operator, $A = A^\dagger$, whose eigenvectors $\{|a\rangle\}$ form an orthonormal basis of the Hilbert space [28, 29, 30]. This can be represented by the closure relation

$$\sum_a |a\rangle\langle a| = \sum_a \Pi(a) = \mathbb{1} \tag{1.2}$$

where $A$ is assumed non-degenerate and discrete for simplicity, and $\Pi(a) = |a\rangle\langle a|$ is a projection operator. The orthogonality between projectors corresponding to different eigenvectors is immediate. The spectral decomposition of the observable is

$$A = \sum_a a\Pi(a), \tag{1.3}$$

where $|a\rangle$ is the eigenvector of $A$ related to the eigenvalue, $a$. When measuring an observable, $A$, Born's rule establishes that the probability of finding a certain value, $a$, is

$$P(a) = \mathrm{tr}[\rho\Pi(a))] \tag{1.4}$$

being the only possible outcomes the eigenvalues of the observable. The measurement described is represented by a Projective Valued Measurement (PVM), $\{\Pi(a)\}$.

However, not all realistic experiments can be represented by a self-adjoint operator. It was shown that the probability distribution of the outcomes, $b$, of the most general measurement allowed by the quantum theory can be described in the same way as in Eq. (1.4) [31, 32],

$$P(b) = \mathrm{tr}[\rho E(b))], \tag{1.5}$$

as long as the elements of the measurement, $E(b)$, are not necessarily orthonormal projectors but only positive operators. These operators form a Positive Operator-Valued Measurement (POVM), $\{E(b)\}$, which is a generalization of the concept of observable [29]. Its elements generate a non-orthogonal decomposition of the identity, $\sum_b E(b) = \mathbb{1}$. One remarkable characteristic is that the number of outcomes can be higher than in a PVM, this is higher than the dimension of the space.

One example of measurement represented by a POVM is a realistic photodetector such as that in [30]. It is worth noting that when we make a PVM over a system coupled to an auxiliary system in a fixed state, the measurement resulting on the initial system is described by a POVM. This is related to the Naimark extension, which says that we can always extend a non-orthogonal resolution of the identity to an orthogonal one in a higher dimensional Hilbert space [32].

#### 1.1.1.2 Generalized measurements

The formalism of POVMs is the perfect framework to describe non-ideal measurements such as the realistic detector mentioned above. The concept of nonideal or inaccurate

[30] refers to the possibility of relating the measurement elements of the POVM, $E(b)$, to the measurement of the corresponding ideal PVM, $\Pi(a)$. This inversion can be made utilizing some fixed, known matrix, $\mu(a,b)$,

$$E(b) = \sum_a \mu(a,b)\Pi(a). \tag{1.6}$$

Recalling the case of the detector, this idea will be equivalent to relating the statistics of a non-ideal detector to the statistics of an ideal one. The key concept is that we cannot relate the individual result of an experiment, but we can connect both statistics.

The nonideality should not be understood as classical noise erasing information but as a quantum mechanical process itself. It is determined by the experiment, therefore known, and the information is enclosed in the matrices $\mu(a,b)$, called inversion matrices in the following. This kind of matrices has inverse, $\mu(a,b)^{-1}$, as long as the non-ideal process is reversible. To ensure the existence and uniqueness of the inverse, the POVM and the PVM must have the same number of elements [30]. Under these conditions, $\mu(a,b)^{-1}$ can be related as

$$\Pi(a) = \sum_b \mu(a,b)^{-1} E(b), \tag{1.7}$$

thus, the probability distribution of the exact observable is actually obtainable. This process constitutes the *inversion procedure*. Now, it is described how to utilize this procedure to make non-ideal measurements of incompatible observables.

We start by exposing how a POVM can be utilized to make joint measurements of other POVMs. Let $\{E(b)\}$ and $\{F(c)\}$ be POVMs, they can be jointly measured if it exists a measurement procedure characterized by a POVM, $\{G(b,c)\}$, such that the elements of the individual ones can be recovered [30],

$$E(b) = \sum_c G(b,c), \qquad \text{and} \qquad F(c) = \sum_b G(b,c). \tag{1.8}$$

From the measurement of $\{G(b,c)\}$ we obtain a joint statistics for $b$ and $c$,

$$\tilde{p}(b,c) = \mathrm{tr}[\rho G(b,c)]. \tag{1.9}$$

The main point allowing the joint measurement is that $\{E(b)\}$ and $\{F(c)\}$ are POVMs [30]. As we have seen Eq. 1.7, these POVMs can be chosen in such a way that they represent non-ideal measurements of certain non-commuting observables. In this manner, the concept of non-ideal joint measurement is obtained by combining both ideas, see Fig. 1.1. It is, therefore, possible to define the elements of the joint POVM such as the individual POVMs are non-ideal measurements of non-commuting

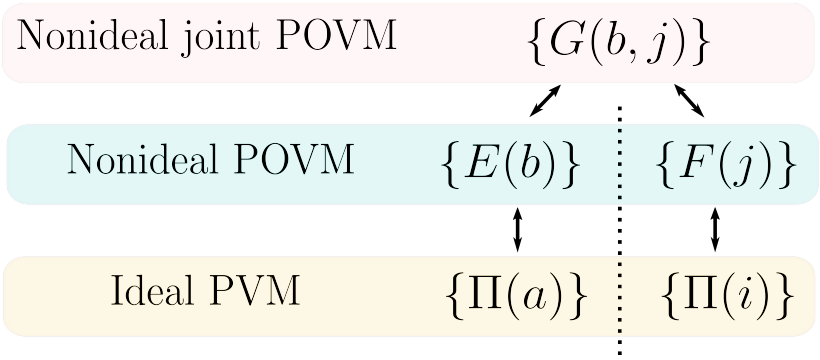


Figure 1.1: Scheme of the relation between ideal, non ideal and joint measurements.

observables,

$$\begin{aligned} \textstyle\sum_c G(b,c) = E(b) = \textstyle\sum_a \mu(a,b)\Pi(a). \\ \textstyle\sum_b G(b,c) = F(c) = \textstyle\sum_a \mu(a,b)\Pi(j). \end{aligned} \tag{1.10}$$

This is why we refer to this observation procedure as an indirect measurement: We do not jointly measure the non-commuting observables directly, but two POVM generated from them, their inaccurate versions.

This scheme can be utilized to obtain the complete inaccurate probability distribution of the two observables. It is remarkable that the total probability distribution obtained from the joint measurement has more information than the two exact marginals, and it may contain (depending on the actual experiment) information about the correlations between the observables. This information cannot be properly defined within the theory. Experimental implementations for these measurements were soon proposed [33, 34].

As long as we know the characteristics of the experiment, and thus the nonideality matrices (1.7), we can obtain from the statistics of the nonideal joint measurement the marginals corresponding to the probability distributions of the individual, exact, observables.

$$p(a) = \sum_b \mu(a,b)^{-1} \mathrm{tr}[\rho \sum_c G(b,c)]. \tag{1.11}$$

Moreover, as we will see, we can obtain the complete probability distribution of two or more incompatible observables by inferring the statistics from indirect measurements via this data inversion. This procedure always provides the legitimate joint probability distribution of the observables at hand in classical physics [35]. On the contrary, in quantum physics, the retrieved probability distribution may show pathologies when the observables do not commute. These pathologies are our basis for nonclassicality.

### 1.1.2 Fine's theorem and Bell's inequalities

Alternatively to inferring the complete probability distribution, it might be useful from an experimental point of view, a way of tracing back the pathologies in the statistics to some combination of measurable correlations and moments [36]. In this kind of experiments, a measurement of different correlations is performed, and some bounds are imposed by classical theories. Bell/CH's inequalities [37, 38] are the best example of this approach. A. Fine [25] demonstrated that any violation of these inequalities corresponds to a lack of a joint distribution for the observables involved. Therefore, it becomes an example of our approach.

#### 1.1.2.1 Bell's theorem: the role of separability

Originally, Bell's inequalities were derived not to test the existence of a joint probability distribution, but to examine whether a particular classical model underlies the results of certain quantum experiments.

The classical model proposed by Bell [39] translates to mathematical conditions the concerns exposed by Einstein, Podolsky and Rosen, [40]. In this manner, those requirements become experimentally testable: Bell's theorem implies that if the model is applicable to the statistics of the experiment, then some bounds to some function of correlations will never be exceeded. On the contrary, violations of Bell-like inequalities imply that the model is not applicable and, therefore, the failure of at least one of the hypotheses on which it is based.

The type of experiment is the measurement of two observables on each subsystem of a bipartite system, for example, we may call $X, Y$ the observables measured on subsystem A and $U, V$ those on subsystem B. The system is typically represented by two entangled 1/2-spin particles or polarized photons. This model includes a set of variables that would completely determine the state of the system, these are the hidden variables, $\lambda$, with probability distribution $p(\lambda)$. It also considers the measurements performed on each subsystem statistically independent. This includes that the results in one subsystem cannot influence the results in the other, but neither can influence the election of measurements (the results on one subsystem cannot depend on which measurement is being performed in the other subsystem). These hypotheses are usually referred to as reality, locality and non-contextuality conditions. All these conditions are translated into the following model

$$p(x,u) = \int d\lambda p(\lambda) p(x|\lambda) p(u|\lambda), \tag{1.12}$$

where $x, y, u, v$ are the outcomes of the corresponding observables. We also refer to this model as separable due to the factorization of the conditional probabilities, $p(y|\lambda)p(x|\lambda)$. Experimental violations of Bell-like inequalities have been reported in

recent years to the point that they are generally without loopholes [41, 42, 43]. Therefore, we conclude that Bell's realistic, local, non-contextual model is not applicable to quantum statistics. However, only by testing this model we cannot specify which hypothesis (or hypotheses) fails.

At this point arise two main concerns related to the mathematical translation of the hypotheses. First, does separability truly account for locality? Or is it an assumption by itself? [44, 45, 46] The second one points to Fine's theorem. This is, can we obtain any information about the hypotheses of a model for a probability distribution when the tested probability distribution does not exist at all? [47, 48, 49, 50]. This can be related to the question of whether there is room for contextuality and nonlocality without complementarity, see [51] and references therein.

### 1.1.3 Chapter outline

This chapter utilizes the joint measurement of incompatible observables (JMIO) as the instrument to connect different signatures of nonclassicality between those advanced in this introduction. Since we have introduced the pathologies in the common statistics as the very concept of nonclassicality, we show how this technique provides an excellent arena to analyze specific aspects related to the potential pathologies of the statistics. Our study goes from the attempt to explain the presence of pathologies in terms of classical-like models to analyzing the necessary conditions for obtaining them.

We start by analyzing the main component in the definition of nonclassicality, which is the complementarity between observables. We replicate Bell's theorem in this scenario and propose a classical-like model for complementarity. We follow this program and derive a set of inequalities that account for the presence of complementarity in the observed statistics. Finally, we apply the inversion procedure introduced to link the absence of a joint distribution for the observables involved with the violation of the inequalities and, accordingly, with the failure of the classical model.

Then, we scale the study to bipartite systems in a natural way. One of the main difficulties in the realization of Bell-like experiments is to ensure the same probability space for the outcomes of the whole system when incompatible observables must be measured. We demonstrated the legitimacy of this method to obtain the complete, potentially pathological statistics for all the observables involved in a Bell-type measurement in a single experiment. This approach allows us to recover Fine's theorem.

In the following section, we wonder which part of the retrieved pathologies of the statistics is caused by the measurement itself. This question arises because state and measurement contribute symmetrically to the computation of probabilities in quantum physics; however, the nonclassicality is usually fully ascribed to the state. First, we utilize the JMIO, but the inversion procedure is directly applied to the POVM representing the detector. This allows discovering negativities on the own representation

of the measurement. We show how these pathologies are necessary for obtaining any negativity in the final statistics.

Keeping the latter result in mind, several indirect signatures of nonclassicality are studied. The highly nonclassical measurements are replaced for their classical-like variants, without pathologies ascribed. Under these conditions, the result of the experiment is always a well-behaved probability distribution. We refer to these quantum signatures as *indirect*, since we utilize the P-representation to characterize the nonclassicality instead of the joint statistics.

In the last section, we report the study of two, in principle, different nonclassical behaviours. We found that $SU(2)$ coherent states can be expressed as the tensor product of identical photons. This equivalence unifies nonclassical polarization and photon entanglement.

## 1.2 Complementarity in quantumness

By definition, incompatibility is the key ingredient when talking about nonclassical signatures. It is, therefore, interesting trying to isolate to the maximum the contribution of complementarity to the pathologies of the statistics of the experiments without classical explanation. Two analyses of complementarity are reported, both of them based on the imperfect measurement of incompatible observables. First, a translation of Bell's hidden variables model is translated to a single subsystem scenario. The very same idea of separability as statistics independence is assumed. Secondly, we obtain the complete statistics of the experiment and analyze the conditions where pathologies appear. The results mimic the Fine's Theorem: when the classical-like model is not applicable, the complete probability distribution is not legitimate and vice versa.

### 1.2.1 A classical model for complementarity

The first test for complementarity was performed by designing a suitable classical model for the measurement process. By classical model we mean a structure for the joint probability distribution that would be accomplished if the process had no quantum characteristics. The model involves several assumptions, acceptable from a classical point of view. It leads to a set of inequalities that can be tested employing unsharp measurements [52].

#### 1.2.1.1 The experiment

In order to be presented, the experiment is divided into three parts, say the prepared state, the performed measurement and the obtained statistics. We consider an arbitrary

quantum two-level system (qubit) on a two-dimensional Hilbert space, whose more general state can be described as

$$\rho = \frac{1}{2}\left(\sigma_0 + \boldsymbol{s}\cdot\boldsymbol{\sigma}\right), \tag{1.13}$$

being $\boldsymbol{\sigma} = \{\sigma_X, \sigma_Y, \sigma_Z\}$ the Pauli matrices, $\sigma_0$ the identity matrix, and $\boldsymbol{s} = \{s_X, s_Y, s_Z\}$ a real vector fulfilling $|\boldsymbol{s}| \leq 1$. The qubit can be fully characterized in the density matrix formalism by the vector $|\boldsymbol{s}|$, which is equivalent to the Stokes parameters within a polarization context. It symbolizes the position of the state in the Bloch sphere: A null module, $|\boldsymbol{s}| = 0$, represents the maximally mixed state. On the contrary, the states on the surface of the Bloch sphere, $|\boldsymbol{s}| = 1$, are pure.

To measure two incompatible observables in the same experiment, we follow the standard method introduced in Sec. 1.1.1: The observed system is coupled to auxiliary degrees of freedom, and then, two compatible observables, the non-ideal versions, are measured in the combined system-auxiliary space. As the incompatible observables under study, we chose those described by the Pauli matrices $\sigma_X$ and $\sigma_Z$, whose eigenvalues are represented by $x'$ and $z'$. The nonideal observables measured are $X$ and $Z$, respectively, with $[X, Z] = 0$. Their outcomes are labelled by the variables $x$ and $z$. In accordance with the spectra of $\sigma_X$ and $\sigma_Z$, $x$ and $z$ are assumed dichotomic, with possible values $\pm 1$.

The most general structure for the observed statistics $\tilde{p}(x, z)$, without specifying any particular form for $X$ and $Z$, is

$$\tilde{p}(x, z) = \frac{1}{4}\left(1 + x\overline{x} + z\overline{z} + xz\overline{xz}\right), \tag{1.14}$$

where $\overline{x}$, $\overline{z}$, and $\overline{xz}$ are the measured mean values and correlations of $X$ and $Z$,

$$\overline{x} = \sum_{x,z=\pm 1} x\tilde{p}(x, z), \quad \overline{z} = \sum_{x,z=\pm 1} z\tilde{p}(x, z), \tag{1.15}$$

and

$$\overline{xz} = \sum_{x,z=\pm 1} xz\tilde{p}(x, z). \tag{1.16}$$

The exact expression in Eq. (1.14) can be straightly obtained by means of a Taylor series in powers of $x$ and $z$. The infinite sequence is reduced to these four terms as a consequence of the dichotomic behaviour of the outcomes: $x^{2n} = 1$ and $x^{(2n+1)} = x$ $\forall n \in \mathbb{N}$, and equivalently for $z$. It should be noted that $\tilde{p}(x, z)$ is a truly measurable statistic, meaning it has to be positive and normalizable for all $x$ and $z$. This constrains the values of $\overline{x}, \overline{z}$ and $\overline{xz}$.

To link the measured mean values $\overline{x}$ and $\overline{z}$ with observables under study, $\sigma_X$ and $\sigma_Z$, we assume a linear relation between analogous quantities

$$\overline{x} = \gamma_X \mathrm{tr}\left(\rho\sigma_X\right), \qquad \overline{z} = \gamma_Z \mathrm{tr}\left(\rho\sigma_Z\right), \tag{1.17}$$

where $\gamma_X$ and $\gamma_Z$ are two real factors, for definiteness and without loss of generality $\gamma_X, \gamma_Z \in (0, 1)$. We can see how they encompass the inaccurate character by computing variances: For dichotomic variables, the variance is determined by the mean value,

$$\Delta^2 x = 1 - \overline{x}^2, \tag{1.18}$$

and from Eq. (1.17) we know, $\overline{x}^2 \leq [\mathrm{tr}\,(\rho\sigma_X)]^2$. Thus, $\Delta^2 x$ is at least equal to $\Delta^2\sigma_X$ $\Delta^2 x \geq 1 - [\mathrm{tr}\,(\rho\sigma_X)]^2 = \Delta^2\sigma_X$,and the lesser $\gamma_X^2$, the larger the difference.

The link between the correlations $\overline{xz}$ and $\sigma_X$, $\sigma_Z$ is not so straightforward due to their non-commutativity. There is no ambiguity for the observed $\overline{xz}$, which is just the mean value of the commuting product $XZ$. We assume it related to a given observable of the system, $\sigma_n = \boldsymbol{\sigma} \cdot \boldsymbol{n}$ being $\boldsymbol{n}$ a real unit vector, that may differ depending on the experimental settings. Considering quantum linearity,

$$\overline{xz} = \gamma_{XZ}\mathrm{tr}\,(\rho\sigma_n)\,, \tag{1.19}$$

where again $1 \geq \gamma_{XZ} \geq 0$. Since the joint distribution $\tilde{p}(x, z)$ in Eq. (1.14) has to be nonnegative, the values of the three $\gamma$ parameters are not independent. The particular form of the constraint depends on the specific $\sigma_n$. For example, when $\sigma_n = \sigma_Y$ then $\gamma_X^2 + \gamma_Z^2 + \gamma_{XZ}^2 \leq 1$, which is actually the case of the Young example to be examined in detail below, while if $\sigma_n = \sigma_X$ we would have $(\gamma_X + \gamma_{XZ})^2 + \gamma_Z^2 \leq 1$.

#### 1.2.1.2 The classical model

Any classically consistent model must assume the existence of the joint probability distribution for the variables $x'$ and $z'$ on the system. In our model, it is labelled by $p_\Lambda(x', z')$.

A key assumption derived from a classically legitimate framework is the statistical independence or *separability*. This concept requires that the observed statistics of $X$ not depend on the observation of $Z$ and *vice versa*. This implies not depend on the specific observable chosen nor on the result of the measurement:

$$\tilde{p}(x, z) = \int dx' dz' p_X(x|x', z') p_Z(z|x', z') p_\Lambda(x', z'), \tag{1.20}$$

being $p_X(x|x', z')$ and $p_Z(z|x', z')$ conditional probabilities which along with $p_\Lambda(x', z')$ are assumed to be real, nonnegative, and normalized in $x$, $z$ $x'$ and $z'$. It is also implicit in the idea of separability that the values available for $\sigma_X$ and $\sigma_Z$, this is $x', z' = \pm 1$, and that the values of $x'$ do not condition the measure of $Z$. Therefore, in this context the separability condition is translated into the following definition: The probability distribution $\tilde{p}(x, z)$ is separable provided that

$$\tilde{p}(x, z) = \sum_{x', z' = \pm 1} p_X(x|x') p_Z(z|z') p_\Lambda(x', z'). \tag{1.21}$$

The following step is to propose a form for the conditional probabilities $p_X(x|x')$ and $p_Z(z|z')$ compatible with the observed marginals. By introducing the proportionality proposed in Eq. (1.17) in the general statistics, Eq. (1.14), the corresponding observed marginals result,

$$\tilde{p}_A(a) = \sum_{b=\pm 1} \tilde{p}(a,b) = \frac{1}{2}\left[1 + \gamma_A a \mathrm{tr}\left(\rho\sigma_A\right)\right], \tag{1.22}$$

for $A, B = X, Z$ and $a, b = x, z$. Compatible with those marginals, we consider the following conditional probabilities for the exact observables

$$p_X(x|x') = \frac{1}{2}\left(1 + \gamma_X x x'\right) \quad \text{and} \quad p_Z(z|z') = \frac{1}{2}\left(1 + \gamma_Z z z'\right). \tag{1.23}$$

These conditional probabilities also manifest the noisy role of $\gamma$ since the probability of obtaining the value $a$ known $a'$ is total, $p(a|a') = 1$, if and only if $\gamma_a = 1$, and there is no information when $\gamma_a \to 0$ being $p(a|a') \to 1/2$.

#### 1.2.1.3 Measurable inequalities

Now we have to derive the probability distribution of the state, $p_\Lambda(x', z')$, which links the measured statistics with the conditional probabilities. It is the key element to determine if the model is fulfilled. $p_\Lambda(x', z')$ has to satisfy the separability condition presented in Eq. (1.21) considering the conditional probability distributions in Eq. (1.23),

$$\frac{1}{4}\left(1 + x\overline{x} + z\overline{z} + xz\overline{xz}\right) = \sum_{x',z'=\pm 1} \frac{1}{2}\left(1 + \gamma_X x x'\right)\frac{1}{2}\left(1 + \gamma_Z z z'\right) p_\Lambda(x', z'). \tag{1.24}$$

In addition, it has no more than four terms, resorting again to a Taylor series on $x', z'$. Under these conditions there is only one solution for the probability distribution of the state,

$$p_\Lambda(x', z') = \frac{1}{4}\left(1 + x'\frac{\overline{x}}{\gamma_X} + z'\frac{\overline{z}}{\gamma_Z} + x'z'\frac{\overline{xz}}{\gamma_X\gamma_Z}\right). \tag{1.25}$$

This is the most general distribution compatible with the experimental data and the natural physical assumptions of a classical theory. The analysis is then reduced to the question of when is it a legitimate probability distribution.

Equation (1.25) is a *bona fide* probability distribution provided that $p_\Lambda(x', z') \geq 0$ for all $x', z'$ leading to the following family of four inequalities:

$$\begin{aligned} &1 + \tfrac{\overline{x}}{\gamma_X} + \tfrac{\overline{z}}{\gamma_Z} + \tfrac{\overline{xz}}{\gamma_X\gamma_Z} \geq 0, \quad 1 - \tfrac{\overline{x}}{\gamma_X} - \tfrac{\overline{z}}{\gamma_Z} + \tfrac{\overline{xz}}{\gamma_X\gamma_Z} \geq 0, \\ &1 + \tfrac{\overline{x}}{\gamma_X} - \tfrac{\overline{z}}{\gamma_Z} - \tfrac{\overline{xz}}{\gamma_X\gamma_Z} \geq 0, \quad 1 - \tfrac{\overline{x}}{\gamma_X} + \tfrac{\overline{z}}{\gamma_Z} - \tfrac{\overline{xz}}{\gamma_X\gamma_Z} \geq 0. \end{aligned} \tag{1.26}$$

They can be regarded as the conditions on the observed mean values $\overline{x}$, $\overline{z}$, and correlations $\overline{xz}$ to be consistent with the classical model. These four relations can be

summarized by looking for the most restrictive among them in each situation: For example, the second one is more restrictive than the first one when both $\overline{x}$ and $\overline{z}$ are positive numbers, and therefore, if the second inequality is fulfilled, also is the first one. Looking for the most restrictive condition in the general case, we use the formula for the minimum of two real numbers $a$, $b$,

$$\min(a,b) = \frac{a+b-|a-b|}{2}. \tag{1.27}$$

Then, we can encapsulate the first two as,

$$\min(1+\frac{\overline{x}}{\gamma_X}+\frac{\overline{z}}{\gamma_Z}+\frac{\overline{xz}}{\gamma_X\gamma_Z}, 1-\frac{\overline{x}}{\gamma_X}-\frac{\overline{z}}{\gamma_Z}+\frac{\overline{xz}}{\gamma_X\gamma_Z}) = 1-\left|\frac{\overline{x}}{\gamma_X}+\frac{\overline{z}}{\gamma_Z}\right|+\frac{\overline{xz}}{\gamma_X\gamma_Z} \geq 0, \tag{1.28}$$

and the second two as,

$$\min(1+\frac{\overline{x}}{\gamma_X}-\frac{\overline{z}}{\gamma_Z}-\frac{\overline{xz}}{\gamma_X\gamma_Z}, 1-\frac{\overline{x}}{\gamma_X}+\frac{\overline{z}}{\gamma_Z}-\frac{\overline{xz}}{\gamma_X\gamma_Z}) = 1-\left|\frac{\overline{x}}{\gamma_X}-\frac{\overline{z}}{\gamma_Z}\right|-\frac{\overline{xz}}{\gamma_X\gamma_Z} \geq 0. \tag{1.29}$$

Combining both results, we can finally rewrite our inequalities (1.26) as

$$1-\left|\frac{\overline{x}}{\gamma_X}-\frac{\overline{z}}{\gamma_Z}\right| \geq \frac{\overline{xz}}{\gamma_X\gamma_Z} \geq \left|\frac{\overline{x}}{\gamma_X}+\frac{\overline{z}}{\gamma_Z}\right|-1. \tag{1.30}$$

We can also express it in terms of the parameters of the density matrix $\rho$ in Eq. (1.13),

$$1-|s_X-s_Z| \geq \frac{\gamma_{XZ}}{\gamma_X\gamma_Z}s_n \geq |s_X+s_Z|-1, \tag{1.31}$$

being $s_j = \mathrm{tr}\,(\rho\sigma_j)$, $j = X, Z, n$. Consequently, the measured statistics could be explained through the classical model proposed in Eqs. (1.21) and (1.23) only when the state and measure parameters fulfill the inequality (1.31).

Noting that the system observables $\sigma_X$ and $\sigma_Z$ may always be chosen so that $s_X = s_Z = 0$ with $s_n = s_Y = |\boldsymbol{s}|$, complementarity inequalities are satisfied provided that

$$|\boldsymbol{s}| \leq \frac{\gamma_X\gamma_Z}{\gamma_{XZ}}. \tag{1.32}$$

Thus, for all states different from the maximally mixed state, $|\boldsymbol{s}| \neq 0$, we may always find values of $\gamma_{XZ}$, $\gamma_X$ and $\gamma_Z$ such that this inequality is violated. In conclusion, for every state different from the identity, it is possible to find a joint measurement so that the state violates the corresponding complementarity inequality, being therefore nonclassical regarding this classical model.

#### 1.2.1.4 Example: the Young interferometer

The paradigmatic example of complementarity appears in the Young interferometer as the inability to determine at the same time which slit was illuminated by the photon

and the interference pattern at the screen. This path-interference duality provided a nice illustration of the above formalism.

First, we introduce the observables under study. The slits of the interferometer are represented by the two orthogonal kets $|\pm\rangle$. Considering them as the eigenvectors of the Pauli matrix $\sigma_Z$, it becomes the path observable. In this manner, if the state only illuminates the upper slit, the mean value of $\sigma_Z$ becomes $\langle\sigma_Z\rangle = \mathrm{tr}(|+\rangle\langle+|\sigma_Z) = 1$, and equivalently $\langle\sigma_Z\rangle = \mathrm{tr}(|-\rangle\langle-|\sigma_Z) = -1$ for the lower slit. However, any interference on the screen only occurs provided by the coherent superposition of those states $|\pm\rangle$ so that we may represent interference by the observable $\sigma_X$. For $|\pm\rangle$, the expectation value of $\sigma_X$ is cancelled, $\langle\sigma_X\rangle = \mathrm{tr}(|\pm\rangle\langle\pm|\sigma_X) = 0$, and there is no interference. Nevertheless, in the case of the superposition state $|\psi\rangle = 1/\sqrt{2}(|+\rangle + |-\rangle)$ the expectation value reveals maximum interference $\langle\sigma_X\rangle = \mathrm{tr}(|\psi\rangle\langle\psi|\sigma_X) = 1$.

We consider that $\sigma_X$ is directly measured on the system space by projection on its eigenstates $|x\rangle = 1/\sqrt{2}(|+\rangle + x|-\rangle)$. Roughly speaking, those states physically correspond to detect maximum and minimum interference on the screen.

The path information will be transferred from the system space to an auxiliary space. Following a suggestive optical implementation of the interferometer, such auxiliary space may be the polarization of the light at each aperture. A different phase plate placed on each aperture can imprint the path information in the polarization states. We assume the apertures illuminated by right-handed circularly polarized light, represented by the vector $|\circlearrowright\rangle$ in the polarization space, so the phase plates produce the following aperture-dependent polarization transformation

$$|\pm\rangle|\circlearrowright\rangle \to |\pm\rangle|\pm\theta\rangle, \tag{1.33}$$

being

$$|\pm\theta\rangle = \cos\frac{\theta}{2}|\circlearrowright\rangle \pm \sin\frac{\theta}{2}|\circlearrowleft\rangle. \tag{1.34}$$

Then, the path information is retrieved by measuring any combination of the observables represented by the Pauli matrices $\Sigma_X$ and $\Sigma_Y$ in the auxiliary polarization space spanned by $|\circlearrowright\rangle$ and $|\circlearrowleft\rangle$ as eigenvectors of $\Sigma_Z$, say

$$\Sigma_\varphi = \cos\varphi\Sigma_X - \sin\varphi\Sigma_Y. \tag{1.35}$$

We denoted here the Pauli matrices by capital letters to emphasize that they are defined not in the system space, with basis $\{|+\rangle, |-\rangle\}$, but in the auxiliary polarization space, with basis $\{|\circlearrowright\rangle, |\circlearrowleft\rangle\}$. This polarization measurement can be easily achieved in practice with the help of a linear polarizer, where $\varphi$ represents the orientation of its axis.

We denote as $|z\rangle_\varphi$ the eigenvectors of $\Sigma_\varphi$, i. e., $\Sigma_\varphi|z\rangle_\varphi = z|z\rangle_\varphi$ with $z = \pm 1$. The photon passing through the polarizer is represented by the vector $|1\rangle_\varphi$ while the photon

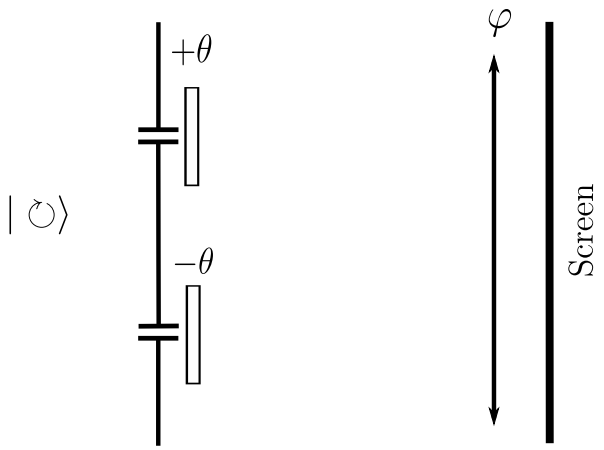


Figure 1.2: Young interferometer scheme with the polarization auxiliary space included [52]. Different phase plates, $\pm\theta$, are placed on each slit, and an analyzer with angle $\varphi$ is situated in front of the screen.

being stopped by the polarizer is represented by the vector $|-1\rangle_\varphi$. The statistics of such quantum measurement when the system state is $\rho$ in Eq. (1.13) leads to the following joint statistics by projection on the system-polarization states $|x\rangle|z\rangle_\varphi$ after the transformation (1.33)

$$\tilde{p}(x,z) = \frac{1}{4}\left(1 + x\gamma_X s_X + z\gamma_Z s_Z + xz\gamma_{XZ} s_y\right), \tag{1.36}$$

with

$$\gamma_X = \cos\theta, \quad \gamma_Z = \cos\varphi \sin\theta, \quad \gamma_{XZ} = \sin\varphi \sin\theta, \tag{1.37}$$

being in this case $\sigma_n = \sigma_Y$. As advanced, the $\gamma$ factors are actually points on the surface of a unit sphere,

$$\gamma_X^2 + \gamma_Z^2 + \gamma_{XZ}^2 = 1. \tag{1.38}$$

The path observation is more accurate, i. e. $\gamma_Z \to 1$, as $\varphi \to 0$ and $\theta \to \pi/2$. In that case, it tends to be no observation of interference $\gamma_X \to 0$. On the contrary, the interference is more noticeable $\gamma_X \to 1$ as $\theta \to 0$, in which case tends to be no path observation $\gamma_Z \to 0$.

The complementarity inequality Eq. (1.32) becomes

$$|\boldsymbol{s}| \leq \frac{\gamma_X \gamma_Z}{\gamma_{XZ}} = \frac{\cos\theta}{\tan\varphi}, \tag{1.39}$$

so that nonclassical results are more clearly revealed as $\theta \to \pi/2$ and $\varphi \to \pi/2$.

### 1.2.2 Joint probability distribution for complementarity

The second test for complementarity consists in applying the inversion procedure introduced in Sec. 1.1.1.2 to relate the legitimacy of the inferred distribution to the just retrieved inequalities.

#### 1.2.2.1 Inversion procedure

The path to obtaining the inversion matrices, $\mu$ in Eq. (1.7), is to impose that the complete statistics of the ideal observables $\sigma_X$ and $\sigma_Z$,

$$p_A(a) = \frac{1}{2}\left[1 + a\mathrm{tr}\left(\rho\sigma_A\right)\right], \tag{1.40}$$

is contained in the observed marginals $\tilde{p}_X(x)$ and $\tilde{p}_Z(z)$ in Eq. (1.52). Under these conditions, the inversion becomes

$$p_A(a) = \sum_{a'=\pm 1} \mu_A(a,a')\tilde{p}_A(a'), \tag{1.41}$$

more explicitly,

$$\frac{1}{2}\left[1 + a\mathrm{tr}\left(\rho\sigma_A\right)\right] = \mu_A(a,1)\frac{1}{2}\left[1 + \gamma_A\mathrm{tr}\left(\rho\sigma_A\right)\right] + \mu_A(a,-1)\frac{1}{2}\left[1 - \gamma_A\mathrm{tr}\left(\rho\sigma_A\right)\right], \tag{1.42}$$

from which the inversion matrices can be computed [35], resulting

$$\mu_A(a,a') = \frac{1}{2}\left(1 + \frac{aa'}{\gamma_A}\right), \quad a = x, z. \tag{1.43}$$

Now that we have the individual inversion matrices, the inversion procedure consists of applying both of them to the complete observed statistics $\tilde{p}(x,z)$ in Eq. (1.14) to infer the ideal joint distribution $p(x,z)$,

$$p(x,z) = \sum_{x',z'=\pm 1} \mu_X(x,x')\mu_Z(z,z')\tilde{p}(x',z'), \tag{1.44}$$

leading to

$$p(x,z) = \frac{1}{4}\left[1 + x\mathrm{tr}\left(\rho\sigma_X\right) + z\mathrm{tr}\left(\rho\sigma_Z\right) + xz\frac{\gamma_{XZ}}{\gamma_X\gamma_Z}\mathrm{tr}\left(\rho\sigma_n\right)\right]. \tag{1.45}$$

It can be seen that this distribution contains the ideal marginals for $\sigma_X$ and $\sigma_Z$, $\sum_z p(x,z) = \frac{1}{2}\left[1 + x\mathrm{tr}\left(\rho\sigma_X\right)\right]$.

The final step is to determine under which conditions is $p(x,z) > 0$. It arises that the inferred joint distribution $p(x,z)$ is exactly the same distribution as $p_\Lambda(x',z')$ in Eq. (1.25) as it can be readily seen using Eqs. (1.17) and (1.19). Thus, both distributions will be legitimate probability distributions under the same conditions in Eq. (1.31).

In conclusion, the classical-like model is valid when the joint probability distribution exists and is legitimate, which can be seen as a single-system version of Fine's theorem.

### 1.2.3 Concluding remarks

The classical-separable model in Eq.(1.20) formally adopts the standard structure of the hidden variables model from which Bell's inequalities are derived [53, 2]. In the case of Bell's theorem, statistical independence is required between the conditional probabilities of subsystems through separability. In the model for complementarity, this idea of statistical independence has been applied to the conditional probability of each individual observable. In this case, this condition does not reflect any locality hypothesis since there is only one subsystem and entanglement plays no role [54]. This is to say that the failure of a separable model in this single-system situation cannot be addressed to any non-local effect. On the contrary, it should be understood as a failure of the factorization condition by itself, pointing out the possible further implications that this condition may have.

The structure of the classical model, Eq. (1.20), and the structure of the inversion procedure, Eq. (1.44), share, to a certain level, the assumption of separability. This can be seen since the product of the inversion matrices of each observable is utilized to perform the total inversion. Moreover, by definition, the inversion matrices of each observable do not depend on the other observable (or outcome).

The joint nonideal measurement in the Young interferometer was reproduced in the classical domain [55]. The fundamental difference is the use of intensities instead of probabilities so that the inferred distribution is an intensity distribution. More specifically, as a suitable classical-like analog of $p(x, z)$, we obtain a joint distribution $I(\phi, z)$ compatible with the exact intensity distribution in the interference plane $I(\phi)$ and the intensity distribution in the apertures $I(z)$, which becomes potentially pathological, $I(\phi, z) \leq 0$. To clarify this non-intuitive result, it is remarkable that intensity distributions can replicate any probability distribution without carrying the same physical implications [56]. However, we consider that developing tools such as the inversion procedure, applicable on both sides of the classical-quantum borderline, might assist in this study as long as the differences and similarities remain clear.

## 1.3 Analysis of bipartite correlations

Bell's theorem establishes a series of bounds for the marginals of any legitimate statistics fulfilling his realistic, local, non-contextual model [39]. Clauser and Horn [38], derived an equivalent inequality for some combinations of statistical correlations. A mayor constraint in deriving and evaluating Bell/CH inequalities is that their experimental violation requires the measurement of incompatible observables. In addition,

the experimental procedures do not necessarily must share common joint statistics [48, 49, 57, 58, 59, 60, 61]. Both remarks obscure the certainties that we can obtain from the Bell inequalities.

In this context, the JMIO is a useful tool to overcome the contextuality difficulties in Bell-like experiments. In this manner, the statistics of all the observables involved are obtained from a single joint measurement of several non-ideal POVM in one and the same experimental arrangement [62].

The use of unsharp measurements in Bell scenarios has already been studied [63, 64]. However, the perspective was finding a realisable experimental arrangement to violate Bell's bounds. In this section, we go beyond the violations in terms of correlations and recover Fine's theorem [25]. We show that the statistics obtained after the data inversion violate Bell's inequalities if and only if it is pathological. We conclude that this joint-measurement approach is appropriate not only to evaluate Bell's inequalities but also to deeper investigate the pathologies in the statistics.

### 1.3.1 The joint measurement

The system is composed of two subsystems, $A$ and $B$, each one described in a two-dimensional Hilbert space, $\mathcal{H}_A$ and $\mathcal{H}_B$. As a physical example, we may consider two photons in two distinguishable field modes. The complete Hilbert space is the tensor product of both subspaces, $\mathcal{H}_A \otimes \mathcal{H}_B$, and the system state is described via the most general density matrix in the total space [65],

$$\rho = \frac{1}{4}(\sigma_0 \otimes \sigma_0 + \sum_{i=1}^{3} a_i \sigma_i \otimes \sigma_0 + \sum_{i=1}^{3} b_i \sigma_0 \otimes \sigma_i + \sum_{i=1}^{3} c_i \sigma_i \otimes \sigma_i), \tag{1.46}$$

for $i = 1, 2, 3$, where $\sigma_i$ are the Pauli matrices and $\boldsymbol{a} = \{a_i\}, \boldsymbol{b} = \{b_i\}, \boldsymbol{c} = \{c_i\}$ are real vectors with $|\boldsymbol{a}|, |\boldsymbol{b}| \leq 1$.

Next, we define the non-ideal measurement performed. First, two observables are considered on each subsystem, $X, Y$ in the subsystem $A$, and $U, V$ in the subsystem $B$. The exact, noiseless statistics of each observable is described by the corresponding POVM,

$$\Delta_W(w) = \frac{1}{2}\left(\sigma_0 + w\boldsymbol{S}_W \cdot \boldsymbol{\sigma}\right), \tag{1.47}$$

for $W = X, Y, U, V$ respectively. The spectrum of each observable is $w = x, y, u, v = \pm 1$. As usual, $\boldsymbol{\sigma}$ is the vector formed by the Pauli matrices. $\boldsymbol{S}_W$ are real vectors with $|\boldsymbol{S}_W| \leq 1$, ensuring $\Delta_W^\dagger(w) = \Delta_W(w)$ and $\Delta_W(w) > 0$. Therefore, $X, Y, U$ and $V$ are dichotomic observables that, in the proposed physical example, represent polarization measurements performed along a suitable spatial direction specified by the vector $\boldsymbol{S}_W$. Thus the observables may or may not commute depending on these vectors.

Now, to define the joint nonideal measurement on each subsystem we utilize the most general POVM for dichotomic observables in a two-dimensional space is considered

$$\tilde{\Delta}_A(x,y) = \frac{1}{4}\left[\sigma_0 + \tilde{\boldsymbol{S}}_A(x,y)\cdot\boldsymbol{\sigma}\right], \quad \tilde{\Delta}_B(u,v) = \frac{1}{4}\left[\sigma_0 + \tilde{\boldsymbol{S}}_B(u,v)\cdot\boldsymbol{\sigma}\right]. \tag{1.48}$$

Once again it is necessary to restrict the modulus of the vectors $|\tilde{\boldsymbol{S}}_A(x,y)| \leq 1$, $|\tilde{\boldsymbol{S}}_B(u,v)| \leq 1$ so that the joint measurement is a well defined POVM, $\tilde{\Delta}^{\dagger}_{A,B} = \tilde{\Delta}_{A,B}$ and $\tilde{\Delta}_{A,B} > 0$. The specific form of these vectors in our context is

$$\begin{aligned}\tilde{\boldsymbol{S}}_A(x,y) &= x\gamma_X\boldsymbol{S}_X + y\gamma_Y\boldsymbol{S}_Y + xy\gamma_{XY}\boldsymbol{S}_{XY},\\ \tilde{\boldsymbol{S}}_B(u,v) &= u\gamma_U\boldsymbol{S}_U + v\gamma_V\boldsymbol{S}_V + uv\gamma_{UV}\boldsymbol{S}_{UV},\end{aligned} \tag{1.49}$$

where $\gamma_{X,Y,U,V}$ are the real factors expressing the accuracy in the observation of each observable. In addition, in $\gamma_{XY,UV}$ it is included any information about the correlations between observables provided by the measurement.

Finally, the complete measurement is described by the tensor product of the POVMs of each subsystem,

$$\tilde{\Delta}_A(x,y) \otimes \tilde{\Delta}_B(u,v), \tag{1.50}$$

which is the POVM corresponding to the total joint non-ideal. The implementation of this POVM leads to observing a joint non-ideal statistics for the four outcomes,

$$\tilde{p}(x,y,u,v) = \mathrm{tr}\left[\rho\tilde{\Delta}_A(x,y)\otimes\tilde{\Delta}_B(u,v)\right], \tag{1.51}$$

where $\rho$ is the density matrix of the complete system in Eq. (1.46). These measurements are slightly more sophisticated than the Stern-Gerlach or polarization measurements, characterized by three spatial directions in stead of just one. Nevertheless, they still admit considerably simple experimental implementations, and, for example, the joint statistics (1.51) can be obtained in an eight-port homodyne detector [26, 66, 67].

### 1.3.2 Inversion procedure

In this bipartite context we need there are four inversion matrices to be founded. The concept is the same than in Sec. 1.2.2.1, however, in this scenario we link the ideal and non ideal POVMs instead of the probability distributions.

The POVMs $\tilde{\Delta}_A(x,y)$ and $\tilde{\Delta}_B(u,v)$ are assumed to provide complete information about the corresponding observables $X$, $Y$ and $U$, $V$, respectively. Therefore, the exact statistics of each $\Delta_W$ has to be contained in the corresponding marginal POVM,

$$\tilde{\Delta}_X(x) = \sum_{y=\pm1}\tilde{\Delta}_A(x,y) = \frac{1}{2}\left(\sigma_0 + x\gamma_X\boldsymbol{S}_X\cdot\boldsymbol{\sigma}\right), \tag{1.52}$$

and equivalently for $\tilde{\Delta}_Y(y)$, $\tilde{\Delta}_U(u)$ and $\tilde{\Delta}_V(v)$. Thus, we assume that for each $W$ there are state-independent functions $\mu_W(w,w')$ so that the exact $\Delta_W(w)$ in Eq. (1.47) related to the nonideal marginal $\tilde{\Delta}_W(w)$ in Eq. (1.52) as

$$\Delta_W(w) = \sum_{w'=\pm 1} \mu_W(w,w')\tilde{\Delta}_W(w'). \tag{1.53}$$

This equation allows computing the inversion matrices. Since each subsystem is essentially the system discussed in the complementarity case, these functions are the same as in Eq. (1.43),

$$\mu_W(w,w') = \frac{1}{2}\left(1 + \frac{ww'}{\gamma_W}\right). \tag{1.54}$$

Then, we can apply the inversion to the join POVM on each subsystem,

$$\begin{aligned}\Delta_A(x,y) &= \textstyle\sum_{x',y'=\pm 1} \mu_X(x,x')\mu_Y(y,y')\tilde{\Delta}_A(x',y'),\\ \Delta_B(u,v) &= \textstyle\sum_{u',v'=\pm 1} \mu_U(u,u')\mu_V(v,v')\tilde{\Delta}_B(u',v'),\end{aligned} \tag{1.55}$$

leading to the inferred operators

$$\begin{aligned}\Delta_A(x,y) &= \tfrac{1}{4}\left[\sigma_0 + \boldsymbol{S}_A(x,y)\cdot\boldsymbol{\sigma}\right],\\ \Delta_B(u,v) &= \tfrac{1}{4}\left[\sigma_0 + \boldsymbol{S}_B(u,v)\cdot\boldsymbol{\sigma}\right],\end{aligned} \tag{1.56}$$

with

$$\begin{aligned}\boldsymbol{S}_A(x,y) &= x\boldsymbol{S}_X + y\boldsymbol{S}_Y + xy\tfrac{\gamma_{XY}}{\gamma_X\gamma_Y}\boldsymbol{S}_{XY},\\ \boldsymbol{S}_B(u,v) &= u\boldsymbol{S}_U + v\boldsymbol{S}_V + uv\tfrac{\gamma_{UV}}{\gamma_U\gamma_V}\boldsymbol{S}_{UV}.\end{aligned} \tag{1.57}$$

The restrictions on the modulus of $\tilde{\boldsymbol{S}}_{A,B}$ and $\boldsymbol{S}_{X,Y,U,V}$ determine that the measured statistics and the true statistics of the corresponding observables are legitimate. However, there are no such restrictions of modulus for $\boldsymbol{S}_{A,B}$. Finally, the inferred joint distribution is obtained as

$$p(x,y,u,v) = \mathrm{tr}\left[\rho\Delta_A(x,y)\otimes\Delta_B(u,v)\right]. \tag{1.58}$$

Before analizing the possible pathologies, it has to be recalled that in classical physics this inversion always leads to a proper joint probability distribution [35, 26].

### 1.3.3 Retrieved statistics for an arbitrary state

Considering the general state in Eq.(1.46) the inferred distribution is,

$$p(x,y,u,v) = \frac{1}{16}\left[1 + \boldsymbol{a}\cdot\boldsymbol{S}_A(x,y) + \boldsymbol{b}\cdot\boldsymbol{S}_B(u,v) + \sum_{i=1}^{3} c_i S_{A_i} S_{B_i}\right], \tag{1.59}$$

where $\tilde{\boldsymbol{S}}_A$, $\tilde{\boldsymbol{S}}_B$, $\boldsymbol{S}_A$ and $\boldsymbol{S}_B$ are in Eqs. (1.49) and (1.57), while $S_{A_i}$ are the corresponding vector components. In order to better understand the potential negativities in the statistics, the different marginals of this joint distribution are examined.

The one-observable marginals are by construction the exact ones Eq. 1.47. The joint $A$ and $B$ marginals are:

$$p_{X,Y}(x,y) = \frac{1}{4}[1 + \boldsymbol{a}\cdot\boldsymbol{S_A}(x,y)], \qquad p_{U,V}(x,y) = \frac{1}{4}[1 + \boldsymbol{b}\cdot\boldsymbol{S_B}(u,v)]. \tag{1.60}$$

The lack of restrictions for $\boldsymbol{S}_{A,B}$ allows the appearance of negativities in these marginals, which represent the joint probability distribution for two incompatible observables on a two-level system. In agreement, the result is equivalent to the obtained in Sec. 1.2.2.1. Finally, the cross two-observable marginals:

$$p_{X,U}(x,u) = \frac{1}{4}\left(1 + u\boldsymbol{b}\cdot\boldsymbol{S}_U + x\boldsymbol{a}\cdot\boldsymbol{S}_x + xu\sum c_i S_{X_i} S_{U_i}\right), \tag{1.61}$$

and equivalently for $p_{X,V}$, $p_{Y,U}$, and $p_{Y,V}$. In difference with Eq. (1.60) this is the joint statistics of two commuting observables $X$ and $U$, so it has no problem being defined directly in terms of their common eigenvectors.

As further proof of the validity of our method, it is show how Eq. (1.61) is exactly the true joint distribution for $X$ and $U$. To this end, we recall that the POVM elements associated to $X$ and $U$ are, in their corresponding Hilbert spaces,

$$\Delta_X(x) = \frac{1}{2}(\sigma_0 + x\boldsymbol{S}_X\cdot\boldsymbol{\sigma}), \quad \Delta_U(u) = \frac{1}{2}(\sigma_0 + u\boldsymbol{S}_U\cdot\boldsymbol{\sigma}), \tag{1.62}$$

so that the joint statistics is

$$p_{X,U}(x,u) = \mathrm{tr}\left[\rho\Delta_X(x)\otimes\Delta_U(u)\right]. \tag{1.63}$$

For the state (1.46) and using the good properties of Pauli matrices under the trace, we readily get that this is the same as in Eq. (1.61).

Finally, we compute the three-observable marginals, which will be utilized in the next section,

$$p_{X,U,V}(x,u,v) = \frac{1}{8}\left[1 + \boldsymbol{b}\cdot\boldsymbol{S}_B + x\boldsymbol{a}\cdot\boldsymbol{S}_X + x\sum_{i=1}^{3} c_i S_{X_i} S_{B_i}(u,v)\right]. \tag{1.64}$$

Equivalent expressions hold for $p_{Y,U,V}$, $p_{X,Y,U}$, and $p_{X,Y,V}$. These are maybe the most interesting marginals regarding Bell's inequalities since the pathology of these distributions is responsible for the violation of Bell's inequalities. This is because they are the simplest distributions containing information about both subsystems and two complementary observables.

### 1.3.4 Recovering the Fine's theorem

This section explicitly shows how the violation of Bell inequalities implies that the retrieved joint distribution $p(x, y, u, v)$ takes negative values and *vice versa*.

To this end we consider Bell's inequalities expressed directly in terms of probabilities instead of mean values [25, 38]. The four double inequalities to be satisfied are of the form:

$$0 \geq p_{X,U}(x,u) - p_{X,V}(x,v) + p_{Y,U}(y,u) + p_{Y,V}(y,v) - p_Y(y) - p_U(u) \geq -1, \quad (1.65)$$

for $x, u = \pm 1$, and three other equivalent relations obtained by suitably permuting the observables. We define $C$ as the nucleus of the Bell double inequality in Eq. (1.65),

$$C = p_{X,U}(x,u) - p_{X,V}(x,v) + p_{Y,U}(y,u) + p_{Y,V}(y,v) - p_Y(y) - p_U(u), \quad (1.66)$$

so that the inequalities are

$$0 \geq C \geq -1. \quad (1.67)$$

Now, starting from the expressions for the two- and three-observable marginals in Eqs. (1.61) and (1.64), it can be proved that

$$\begin{aligned} \Sigma = p_{X,U,V}(x,u,-v) + p_{X,U,V}(-x,-u,v) + p_{Y,U,V}(y,u,v) + p_{Y,U,V}(-y,-u,-v) \\ = C + 1, \end{aligned} \quad (1.68)$$

which can also be derived using general properties of the probability distributions.

Now, both bounds for $\Sigma$ are analyzed. If the joint distribution $P(x, y, u, v)$ is legitimate, then the combination of marginals, $\Sigma$, is always such that $1 \geq \Sigma \geq 0$. This is because $\Sigma$ is a sum of probabilities, so it is nonnegative. Regarding the upper bound, for all $W = X, Y$ and $w = x, y = \pm 1$ we have

$$p_{W,U,V}(w,u,v) \leq p_{U,V}(u,v), \quad (1.69)$$

and therefore

$$\Sigma \leq p_{U,V}(u,-v) + p_{U,V}(-u,v) + p_{U,V}(u,v) + p_{U,V}(-u,-v) = 1. \quad (1.70)$$

In consequence, a violation of any of the bounds of Bell's inequalities (1.67) implies either $\Sigma < 0$ or $\Sigma > 1$, which are situations incompatible with a legitimate joint distribution for the observables involved in the experiment. Thus, Bell's inequalities can be expressed in terms of $\Sigma$, simply by replacing $C = \Sigma - 1$ in Eq. (1.67),

$$1 \geq \Sigma \geq 0. \quad (1.71)$$

### 1.3.5 Bell-CH inequality violation example

An example of bad-behaved inferred statistics is reported, together with the violation of Bell inequality (1.65). As the physical system, we consider the usual singlet state,

$$\rho = \frac{1}{4}\left(\sigma_0 \otimes \sigma_0 - \sum_{i=1}^{3} \sigma_i \otimes \sigma_i\right). \tag{1.72}$$

As the measurement to be performed, a remarkably simple scenario can be considered. We establish $\boldsymbol{S}_{XY} = \boldsymbol{S}_{UV} = \mathbf{0}$ as well choosing zero as all the third components of $\boldsymbol{S}_X$, $\boldsymbol{S}_Y$, $\boldsymbol{S}_U$ and $\boldsymbol{S}_V$. Therefore, the observables are measured along some plane $XY$, with directions specified by angles $\alpha$, $\alpha'$, $\xi$ and $\beta'$

$$\boldsymbol{S}_X = (\cos\alpha, \sin\alpha, 0)\,, \quad \boldsymbol{S}_Y = (\cos\alpha', \sin\alpha', 0)\,, \tag{1.73}$$

and

$$\boldsymbol{S}_U = (\cos\beta, \sin\beta, 0)\,, \quad \boldsymbol{S}_V = (\cos\beta', \sin\beta', 0)\,. \tag{1.74}$$

Under these conditions, the following angles can be chosen

$$\alpha = 0, \quad \alpha' = \frac{\pi}{2}, \quad \beta = \frac{3\pi}{4}, \quad \beta' = -\frac{3\pi}{4}, \tag{1.75}$$

and directly compute the corresponding probability distribution in Eq. (1.59),

$$p(1-1,-1,1) = -0.026, \tag{1.76}$$

meaning that $p(x,y,u,v)$ cannot be a legitimate probability distribution. Accordingly to the study presented in this section, this election of measurement violates the Bell-CH inequalities, being $C$ in Eq. (1.66)

$$C = -\frac{1}{2} - \frac{1}{\sqrt{2}} = -1.21 < -1. \tag{1.77}$$

### 1.3.6 Concluding remarks

From this study, we conclude that this procedure to measure incompatible observables is a useful tool to evaluate pathological behaviours directly on the statistical correlations. The examination of the marginals highlights the relevance of complementarity in the violation of Bell/CH's inequalities. The possibility of a joint probability distribution is bound to fail since two incompatible observables are involved, as observed in the corresponding marginals. This reinforces the legitimacy of the study of complementary through the same approach. However, the entanglement is necessary to violate the inequalities, which is clear if we examine the derivation of Fine's theorem, which relates the correlation in the inequalities to the three observable marginals. This

is, the state has to be such that it can reveal the pathologies. We elaborate on this idea in the next section.

As a step further, the union of both models, this is the classical model for complementarity and the Bell's model, which could be expressed as follows,

$$p(x,y,u,v) = \int d\lambda P(\lambda) P_X(x,|\lambda) P_Y(y|\lambda) P_U(u|\lambda) P_V(v|\lambda), \tag{1.78}$$

would be interesting in order to study quantum correlations in a unified way. This complete model would have the same assumptions as Bell's, but it would unify the analysis of entanglement and complementarity.

In addition to the mentioned hypotheses of locality, causality, and non-contextuality, it has been pointed out that the quantum linear relation between the probabilities and the field state, $p(x) = \mathrm{tr}[\rho\Delta(x)]$, may also be an implicit condition of the Bell's Hidden variables model [68]. To this end, a semiclassical violation of Bell inequalities for classical fields in terms of probabilities has been studied. The conversion between the classical-field intensities and probabilities utilizes the standard photon-counting equation. This equation is non-linear in these variables when more than one photon is present. This would indicate that Bell's inequalities are still a useful tool for learning about the origin and implications of quantum features and, moreover, about the quantum-classical borderline.

## 1.4 Detector contribution to nonclassical effects

When talking about quantum phenomena, we are used to refer to them as nonclassical features displayed by the states: squeezed states, entangled states... The nonclassical character is then attributed to the observed state[69] and it is called a nonclassical state.

As we have already introduced, all nonclassical effects are revealed in the pathologies of the observed statistics. In the simplest case of projector measurements, the probability of each outcome is, according to Born's rule, $p(m|\psi) = |\langle m|\psi\rangle|^2$, where $|m\rangle$ is the eigenstate of the measured observable When talking about generalized measurements, which involve positive operator-valued measures $\Delta(m)$, the probabilities of the outcomes are computed as $p(m|\psi) = \mathrm{tr}\left[|\psi\rangle\langle\psi|\Delta(m)\right]$. In both situations, the symmetry between the state and measurement can be appreciated. Moreover, the states participating in the typical measurements, such as projection onto number states for photo-counting statistics, are considered highly nonclassical by themselves. Thus, may the paradoxical experimental results be ascribed to the measurement states?

In this section, it is demonstrated that the nonclassicality of the detector is a necessary condition to obtain nonclassical statistics [70]. We report on the general analysis

and its particularization for some common signatures of nonclassicality: subPoissonian statistics, photon anti-correlations, quadrature squeezing, and Bell inequalities violations.

Due to the optical context, as the generalized nonclassicality signature we consider the lack of a *bona fide* Glauber-Surdashan $P(\alpha)$ distribution [12, 16, 18, 69]. As has been mentioned, it reveals the lack of joint statistics for field quadratures, so it is an indirect and limited signature of nonclassicality, but it is still useful. Moreover, the P-representation can be extended from density matrices to every quantum operator [71]. This makes it possible to establish, in the same way as for states, that the lack of a *bona fide* Glauber-Surdashan $P(\alpha)$ is a sign of the nonclassicality of the measurement. This can be applied alike to projective and generalized measurements.

Based on this, we address whether quantum experimental results are possible when the measurement performed admits a classical description. Specifically, whether pathologies in the recorded statistics remain when a measurement process with a legitimate $P(\alpha)$ is performed.

### 1.4.1 Nonclassical evidences

The same approach of indirect measurement presented in Sec. 1.1.1.2 is utilized. In the most general case, the measurement of two commeasurable observables, say $X$ and $Y$, can be properly represented in the system space by a positive operator-valued measure $\tilde{\Delta}(x, y)$, where $x, y$ are the outcomes of each observable. The corresponding statistics become $\tilde{p}(x, y|\rho) = \mathrm{tr}\left[\rho\tilde{\Delta}(x, y)\right]$, where $\rho$ is the density matrix of the system state again. The statistics marginals related to each observable are assumed to provide complete information about the ideal individual statistics, so the inversion exists. The link between ideal and non-ideal marginals reads

$$\Delta_A(a) = \int da' \mu_A(a, a')\tilde{\Delta}_A(a'), \tag{1.79}$$

for $a = x, y$ and $A = X, Y$. The inversion matrices, $\mu_A(a, a')$, are state-independent and completely determined by the measurement process, then we can invert the POVM itself instead of the statistics. The inversion (1.79) is extended from the marginals to the complete joint measurement, in order to obtain an operator-valued measure $\Delta(x, y)$ [26, 30, 72],

$$\Delta(x, y) = \int dx' dy' \mu_X(x, x')\mu_Y(y, y')\tilde{\Delta}(x', y'), \tag{1.80}$$

which is not a proper POVM since it can lead to negative values as signature of nonclassicality.

### 1.4.2 Apparatus contribution

As a density matrix, $\rho$ is always a well-behaved positive semidefinite matrix. Therefore, the potential pathologies in the inferred statistics $p(x, y)$ are likely to correspond to pathologies in the inferred operator-valued measure $\Delta(x, y)$ in Eq. (1.80). In this manner, if $p(x, y|\rho)$ does not exists, it is because $\Delta(x, y)$ does not exists, and if $p(x, y|\rho)$ takes negative values it is because $\Delta(x, y)$ is not positive definite. Then, the nonclassicality of the detector would be a necessary condition to observe nonclassicality in the state, and therefore their mutual contributions can hardly be split.

In order to demonstrate this affirmation, a complete characterization of the nonclassical detectors is developed fully equivalent to that of nonclassical states, the inferred operator measure (1.80) is expressed via the Glauber-Sudarshan $P(\alpha)$ representation as

$$\Delta(x, y) = \frac{1}{\pi} \int d^2\alpha P(x, y|\alpha)|\alpha\rangle\langle\alpha|, \tag{1.81}$$

where $|\alpha\rangle$ are the Glauber coherent states. This description is equally valid for one or multi-mode fields, $|\{\alpha\}\rangle = |\alpha_1, \ldots \alpha_n\rangle$. The $P(x, y|\alpha)$ function provides a practical characterization of a detection process, in agreement with the idea of detector tomography [73, 74, 75]. In our context, it serves as well to distinguish quantum from classical measurements: If $\Delta(x, y)$ is pathological, then $P(x, y|\alpha)$ cannot be a classical-like *bona fide* probability distribution and the measurement would be considered nonclassical.

First, we analyze what happens to the statistics if the measurement is classical so that $P(x, y|\alpha)$ is well-behaved. In that case, the inferred joint statistics becomes

$$p(x, y) = \mathrm{tr}\left[\rho \frac{1}{\pi} \int d^2\alpha P(x, y|\alpha)|\alpha\rangle\langle\alpha|\right] = \int d^2\alpha P(x, y|\alpha) Q(\alpha|\rho), \tag{1.82}$$

where $Q(\alpha|\rho)$ the Husimi Q-function [12] of $\rho$

$$Q(\alpha|\rho) = \frac{1}{\pi}\langle\alpha|\rho|\alpha\rangle. \tag{1.83}$$

The key point is that for every $\rho$ the function $Q(\alpha|\rho)$ exists and is nonnegative $Q(\alpha|\rho) \geq 0$. This demonstrates that for classical detectors, the statistics for the experiment is always classical and well-behaved. Consequently, there are nonclassical effects only provided that the measurement performed is itself nonclassical and that the system state $\rho$ has a significant projection in the negative spectrum region of the detection operator-valued measure.

### 1.4.3 Examples

After linking nonclassicality with pathological $P$-representation of the measurement $\Delta$ in a general enough framework, we can illustrate this scenario with some paradigmatic

examples of nonclassical effects.

#### 1.4.3.1 Bell tests

The most straightforward example that can be addressed is the violation of Bell inequalities pressented in Sec. 1.3. Here we show how any violation of Bell inequalities requires nonclassical detection. After the inversion procedure, the obtained joint distribution for the observables $X$, $Y$ and $U$, $V$, on their respective subsystems $A$ and $B$ in Eq. (1.58) is,

$$p(x,y,u,v) = \mathrm{tr}\left[\rho\Delta(x,y)\otimes\Delta(u,v),\right], \tag{1.84}$$

where the operator-valued measures after the inversion are in Eq. (1.56)

$$\Delta_A(x,y) = \frac{1}{4}(1+\boldsymbol{S}_A(x,y)\cdot\boldsymbol{\sigma}) \quad \text{and} \quad \Delta_B(u,v) = \frac{1}{4}(1+\boldsymbol{S}_B(u,v)\cdot\boldsymbol{\sigma}),$$

with $\boldsymbol{S}_A(x,y)$, $\boldsymbol{S}_B(u,v)$ in Eq. (1.57). We consider the simple situation utilized in Sec. 1.3.5 to violate Bell-CH inequalities, where $\boldsymbol{S}_{XY} = \boldsymbol{S}_{UV} = 0$, vectors $\boldsymbol{S}_A(x,y)$ and $\boldsymbol{S}_B(u,v)$ become $\boldsymbol{S}_A(x,y) = x\boldsymbol{S}_X + y\boldsymbol{S}_Y$ and $\boldsymbol{S}_B(u,v) = u\boldsymbol{S}_U + v\boldsymbol{S}_V$. In the case of the singlet maximally entangled state in Eq. (1.72) the statistics become

$$p(x,y,u,v) = \frac{1}{16}(1-\boldsymbol{S}_A(x,y)\cdot\boldsymbol{S}_B(u,v)), \tag{1.85}$$

which is pathological provided that $|\boldsymbol{S}_A(x,y)| > 1$, $|\boldsymbol{S}_B(u,v)| > 1$, or both, that imply $\Delta_A(x,y) < 0$ and $\Delta_B(u,v) < 0$ respectively, and therefore, do not admit a classical representation regarding its P-function. In the precedent example, $|\boldsymbol{S}_A(x,y)| = |\boldsymbol{S}_B(u,v)| = 2$.

This example shows how there is no room for pathologies in $p(x,y,u,v)$ and, therefore, for the corresponding violations of Bell-CH inequalities if the measurement performed admits a classical description even when the state at hand is the maximally entangled.

#### 1.4.3.2 SubPossonian statistics

A photon-number variance smaller than the mean number of photons is an emblematic test of nonclassicality. SubPossonian statistics, $\Delta^2 n < \langle\hat{n}\rangle$, is inconsistent with a well-behaved P-representation of the field state since the coherent states have Poissonian statistics and a convex combination of them cannot reduce the variance. The number statistics can be measured by projection onto number states $|n\rangle$ as

$$p(n) = \mathrm{tr}(\rho|n\rangle\langle n|). \tag{1.86}$$

The number projectors can be expressed as

$$|n\rangle\langle n| = \int d^2\alpha P_N(n|\alpha)|\alpha\rangle\langle\alpha|, \tag{1.87}$$

where $P_N(n|\alpha)$ is the Glauber-Sudarshan $P$-function of a number state [22]

$$P_N(n|\alpha) = \frac{n! e^{|\alpha|^2}}{2\pi|\alpha|(2n)!} \frac{\partial^{2n}}{\partial|\alpha|^{2n}} \delta\left(|\alpha|\right). \tag{1.88}$$

As it can be seen, the P-function of the number measurement is extremely singular, containing derivatives of the delta function. The objective then is to examine whether the subPoissonian behaviour of the statistics still holds when we replace the above highly nonclassical $P_N(n|\alpha)$ by closest POVM with a well-behaved $P$-representation.

To define the classical version of this measurement, we look for a POVM element $\Pi_n$ as close as possible to $|n\rangle\langle n|$ but with a well-defined, positive and normalized $P_{\Pi_n}(n|\alpha)$, i. e.,

$$\Pi_n = \int d^2\alpha P_{\Pi_n}(n|\alpha)|\alpha\rangle\langle\alpha|. \tag{1.89}$$

The criterion of closeness considered is the maximum overlap between the new elements of the POVM, $\Pi_n$, and the original $|n\rangle\langle n|$, by maximizing

$$\langle n|\Pi_n|n\rangle = \int d^2\alpha P_{\Pi_n}(n|\alpha) \left|\langle n|\alpha\rangle\right|^2. \tag{1.90}$$

Considering $|\langle n|\alpha\rangle|^2$ as a function of $\alpha$, it has a maximum for $|\alpha|^2 = n$. Therefore, the maximum overlap occurs when $P_{\Pi_n}(n|\alpha)$ is concentrated in such point. We follow Ref. [76] to utilize $n$ as a continuous variable so $P_{\Pi_n}(n|\alpha)$ can be defined as

$$P_{\Pi_n}\left(n|\alpha\right) = \delta\left(n - |\alpha|^2\right). \tag{1.91}$$

This switch to the continuum also ensures the completeness of $\Pi_n$, this is $\sum_n \Pi_n \propto I$.

In this situation, the corresponding measured statistics reads

$$p_\Pi(n) = \int d^2\alpha P_{\Pi_n}(n|\alpha) Q(\alpha|\rho) = \frac{1}{2}\int_{2\pi} d\phi Q\left(\alpha = \sqrt{n}e^{i\phi}|\rho\right), \tag{1.92}$$

where we have used that $d^2\alpha = (1/2)d|\alpha|^2 d\phi$ and $\phi$ is the phase of $\alpha$. By replacing the Q function in Eq. (1.83) and expressing the coherent states in the number basis, the statistics can be expressed in the form

$$p_\Pi(n) = \sum_{m=0}^{\infty} \frac{n^m e^{-n}}{m!} \langle m|\rho|m\rangle, \tag{1.93}$$

where $|m\rangle$ are number states.

To analyze if the subPoisonian statistics hold, we compute the variance on the statistics obtained by means of the classical detector, Eq. (1.93). The explicit forms of the moments $\langle n^k\rangle$ for any integer $k$ are,

$$\langle n^k\rangle = \int_0^\infty dn\, n^k p_\Pi(n) = \int_0^\infty dn \sum_{m=0}^{\infty} \frac{n^{m+k} e^{-n}}{m!} \langle m|\rho|m\rangle. \tag{1.94}$$

Taking into account the following expression,

$$\int_0^\infty dn\, n^{m+k} e^{-n} = (m+k)!, \tag{1.95}$$

the first and second moments become,

$$\langle n \rangle = \sum_{m=0}^{\infty} (m+1)\langle m|\rho|m\rangle, \qquad \langle n^2 \rangle = \sum_{m=0}^{\infty} (m+1)(m+2)\langle m|\rho|m\rangle. \tag{1.96}$$

Remembering the normalization of the state, $\sum_{m=0}^{\infty}\langle m|\rho|m\rangle = 1$, the variance of statistics in Eq. (1.93) results,

$$\Delta^2 n = \langle n^2 \rangle - \langle n \rangle^2 = \sum_{m=0}^{\infty} m^2 \langle m|\rho|m\rangle - \left( \sum_{m=0}^{\infty} m\langle m|\rho|m\rangle \right)^2 + \langle n \rangle \tag{1.97}$$

Note that $\langle m|\rho|m\rangle = \mathrm{tr}[\rho|m\rangle\langle m|] = p(m)$ is the original photon-number distribution and therefore $\langle \hat{n} \rangle = \sum_{m=0}^{\infty} m\langle m|\rho|m\rangle$ and $\langle \hat{n}^2 \rangle = \sum_{m=0}^{\infty} m^2\langle m|\rho|m\rangle$ are respectively the first and second moments of the quantum detection statistics. Thus, we can express Eq. (1.97) in terms of the variance of the quantum detection, $\Delta^2\hat{n}$, which is always nonnegative,

$$\Delta^2 n = \Delta^2 \hat{n} + \langle n \rangle \geq \langle n \rangle, \tag{1.98}$$

so that there is no possibility of subPoissonian statistics. Accordingly, if quantum measurements are replaced by classically-describable measurements all states are Poissonian or superPoissonian. Thus, we may safely say that subPoissonian statistics holds only if the measurement is subPoissonian itself, and so nonclassical.

#### 1.4.3.3 Anticoincidences

Next, we analyze the correlations of two photodetectors placed at the output ports of a beam splitter when it is iluminated with one or two photons as the flagship of quantum optics experiments.

In the first scenario, illustrated in Fig. 1.3a, a single photon impinges on a lossless beam splitter and two joint intensity measurements are performed at the output ports. Since the photon is indivisible, the detectors can never trigger both simultaneously, so that $\langle \hat{n}_1 \hat{n}_2 \rangle = 0$. This is maybe the clearest and simplest evidence of the quantum nature of light [77].

To analyze the closest classical scheme, a two-mode version of the single-mode number detection introduced in Eqs. (1.89) and (1.91) is considered,

$$\Pi_{n_1,n_2} = \int d^2\alpha P_{\Pi_n}(n_1, n_2|\alpha, \beta)|\alpha, \beta\rangle\langle\alpha, \beta|, \tag{1.99}$$

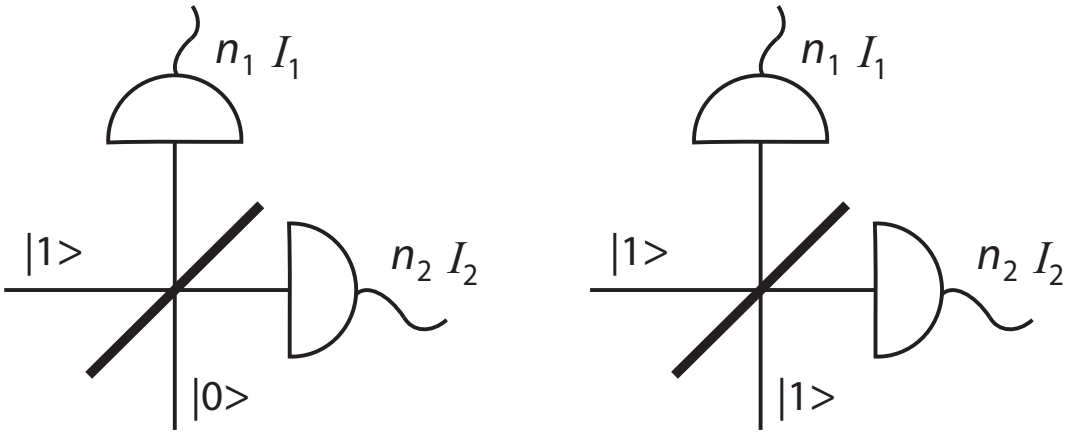


(a) Single-photon input sate illuminating a lossless beam splitter.

(b) Twin-photon input sate illuminating a balanced lossless beam splitter.

Figure 1.3: Experiment of anti-correlation of photo-counts [70].

with

$$P_{\Pi}\left(n_1, n_2|\alpha, \beta\right) = \delta\left(n_1 - |\alpha|^2\right)\delta\left(n_2 - |\beta|^2\right). \tag{1.100}$$

This classical-like measurement generates the following statistics

$$p_{\Pi}(n_1, n_2) = \sum_{m_1=0}^{\infty}\sum_{m_2=0}^{\infty}\frac{n_1^{m_1}e^{-n_1}}{m_1!}\frac{n_2^{m_2}e^{-n_2}}{m_2!}\langle m_1, m_2|\rho|m_1, m_2\rangle. \tag{1.101}$$

Considering a beam splitter with reflection coefficient $R$ and transmission coefficient $T$, with $|R|^2 + |T|^2 = 1$, the output state is,

$$\rho = (R|1,0\rangle + T|0,1\rangle)(R^*\langle 1,0| + T^*\langle 0,1|). \tag{1.102}$$

Then, the statistics in Eq. (1.101) results in this case of one-photon field,

$$p_{\Pi}(n_1, n_2) = \left(|R|^2 n_1 + |T|^2 n_2\right)e^{-n_1-n_2}. \tag{1.103}$$

The correlation under study leads $\langle n_1 n_2\rangle = 2$, so the alleged quantum effect would be never observed if the detectors were classical-like devices.

In these conditions, the case of one photon impinging simultaneously on each input port of a lossless 50 % beam splitter can be examined. This case, illustrated in Fig. 1.3b, corresponds to the Hong-Ou-Mandel effect. The quantum theory again predicts the result $\langle \hat{n}_1 \hat{n}_2\rangle = 0$ as evidence of the quantum nature of light.

The measurement performed is the same as in the previous case, therefore we utilize the same closest-classical measurement, described in Eqs. (1.99) and (1.100), leading to the statistics in Eq. (1.101). In the Hong-Ou-Mandel effect, the corresponding output state is

$$\rho = \frac{1}{2}(|2,0\rangle + |0,2\rangle)(\langle 2,0| + \langle 0,2|), \tag{1.104}$$

which makes the joint statistics in Eq. (1.101) become,

$$p(n_1, n_2) = \frac{1}{4}\left(n_1^2 + n_2^2\right) e^{-n_1-n_2}. \tag{1.105}$$

The latter statistics lead again to a not-null correlation, $\langle n_1 n_2\rangle = 3$, and therefore the nonclassical effect vanishes.

#### 1.4.3.4 Quadrature squeezing

The last nonclassical feature analyzed is the quadrature squeezing. It is characterized by a variance in a field quadrature, for example $x = \Re\{\alpha\}$, smaller than the variance of the coherent states, $\Delta^2 X < 1/4$, where we have chosen units so that $X = (a+a^\dagger)/2$. As in the case of Sub-Poissonian statistics, this variance cannot be produced by a convex combination of coherent states, so it is incompatible with a legitimate $P(\alpha)$.

The statistics of a quadrature measurement results by projection on the quadrature eigenstates, $|x\rangle$, which are highly nonclassical since they are infinitely squeezed. The closest classical measurement is built by replacing the strongly nonclassical $P_X(x|\alpha)$by

$$P_{\Pi_x}(x|\alpha) = \delta\left(x - \Re\{\alpha\}\right). \tag{1.106}$$

Taking into account that $d^2\alpha = dxdy$, the corresponding statistics reads

$$p_\Pi(x) = \int d^2\alpha P_{\Pi_x}(x|\alpha) Q(\alpha|\rho) = \int_{-\infty}^{\infty} dy Q\left(\alpha = x + iy\right), \tag{1.107}$$

this is

$$p_\Pi(x) = \sqrt{\frac{2}{\pi}} \int_{-\infty}^{\infty} dx' e^{-2(x-x')^2} \langle x|\rho|x\rangle. \tag{1.108}$$

We can proceed by computing the first two moments. Again, the classically measured moments can be related to the moments of the quantum measure, $\langle \hat{X}\rangle$, since $p(x) = \langle x|\rho|x\rangle$. Therefore it can be seen that

$$\langle x\rangle = \langle \hat{X}\rangle, \qquad \langle x^2\rangle = \langle \hat{X}^2\rangle + \frac{1}{4}, \tag{1.109}$$

and the corresponding variance results

$$\Delta^2 x = \Delta^2 \hat{X} + \frac{1}{4} \geq \frac{1}{4}. \tag{1.110}$$

Therefore we conclude that with classical quadrature measurements there is no possibility of no nonclassical behaviour regarding this physical variable.

Finally, the latter example is utilized to illustrate how these classical detectors can be created in a quantum world. A detector with a classical description emerges from a quantum one after a thermalization process. This is, by adding thermal noise to the quantum device, which is actually the same idea of combining a nonclassical state with thermal light to remove all its nonclassical properties [78]. To this end, we substitute

each highly nonclassical element of the quadrature measurement, $\Pi_x = |x\rangle\langle x|$, for a combination of them with thermal distribution:

$$\Pi_x^\tau = \int d^2\alpha \frac{e^{-|\alpha|^2/2\tau}}{2\pi\tau} D^\dagger(\alpha)|x\rangle\langle x|D(\alpha), \tag{1.111}$$

where $D(\alpha)$ is the displacement operator and $\tau$ is a measure of the amount of thermal fluctuations, leading to

$$\Pi_X^\tau = \int d^2\alpha \frac{e^{-|\alpha|^2/2\tau}}{2\pi\tau} |x + \frac{\Re(\alpha)}{2}\rangle\langle x + \frac{\Re(\alpha)}{2}|. \tag{1.112}$$

The probability distribution resulting from this measurement, $\mathrm{tr}[\rho\Pi_x^\tau]$, is identical to the obtained in Eq. (1.108) for $\tau = 1$. Alternatively, the same result is obtained by modeling a real detector as an ideal one preceded by a beam splitter of finite transmittance, where $\tau$ would be proportional to the inverse of the quantum efficiency [79].

### 1.4.4 Concluding remarks

The link between the lack of classical description for detectors and for the recorded statistics has been described, demonstrating that there is no quantum light without quantum detectors. We have explicitly shown that this is the case for the most typical signatures of nonclassical behaviour. However, this cannot mean that the state plays no role. The state must be such that it can reveal these pathologies. This is especially clear in the violations of Bell's inequalities, where a separable state $\rho = \rho_A \otimes \rho_B$ will never be able to violate them, even if the measurement performed is nonclassical.

To further develop this idea we remark on the possibility of expressing Eq. (1.82) in the opposite way, this is, with the state being described as usual by its P-representation $P(\rho|\alpha)$ and the measurement by its always positive Q-function, $Q(\alpha|\Pi(x,y))$. Under these circumstances, the pathologies in the P-representation of the state would be needed together with an appropriate measurement capable of revealing these pathologies. Therefore, we conclude that the nonclassicality of the detector is a necessary but not sufficient condition to obtain nonclassical statistics.

The same questions about the influence of the detector can be approached using the analysis of complementarity proposed in Sec. 1.2.1. This can be done by emulating Eq. (1.25), where the state is described by a well-behaved quasiprobability distribution $Q(\rho|\alpha)$ and the potential pathologies of the detector are the cause of the measured pathologies. In the same spirit, it may be investigated a model for complementarity similar to Eq. (1.20) assuming a nonpathological description of the state $p_\Lambda(x', z')$ and without previous assumptions on the conditional probabilities relating variables $\tilde{q}(x, z|x', z')$. In this situation, the classical model for the measured joint statistics of

$X$ and $Z$ may read as

$$\tilde{p}(x,z) = \sum_{x',z'=\pm} \tilde{q}(x,z|x',z')p_\Lambda(x',z'), \tag{1.113}$$

where $\tilde{q}(x,z|x',z')$ is the conditional probability describing the complete measurement. Not even the factorization condition $\tilde{q}_x(x|x',z')\tilde{q}_z(z|x',z')$ assumed. As previously established, $p_\Lambda(x',z')$ describes the probability distribution for the variables $x',z'$, that also will be a pair of dichotomic variables, $x',z' = \pm 1$. In line with the precedent examples, the purpose would be to describe the state, $p_\Lambda(x',z')$, in such a way that there is no room for pathologies on its description. As the most classical-like distribution compatible with quantum mechanics, a discrete $Q$-like distribution may be considered, which is always positive and well-behaved. This $Q$-like function or $Q$-Symbol [80, 81], is given by projection of the system density-matrix on the four pure states described by $\boldsymbol{s} = \frac{1}{\sqrt{3}}(x',z',x'z')$ in Eq. (1.13) with $x',z' = \pm 1$. Then, the analysis may consist in analyzing under what conditions of $\tilde{q}(x,z|x',z')$ any pathological behaviour of the inferred statistics disappear.

## 1.5 Unification of nonclassical polarization and photon entanglement

This chapter has already discussed several manifestations of the quantum nature of light. In recent years, efforts have been made to clarify what is truly common and what are the inevitable differences between the wide variety of nonclassical evidence and criteria, especially when talking about the consequences of the superposition principle [82, 83, 84, 85, 86]. This attempt is compelling not only from a theoretical point of view, by allowing a better understanding of the engaging phenomena behind the quantum theory, but also from the perspective of its applications. A common description of different quantum features may permit to exchange or even optimize their use as resources for quantum technologies.

In this context, we demonstrate that nonclassical polarization is equivalent to the entanglement between indistinguishable photons. As an example of applicability, the measurement of both magnitudes within the same experiment is reported in Chapter 2.

### 1.5.1 Quasiprobability quantum coherence

We have seen how nonclassicality in quantum optics has been historically defined as the lack of a well-behaved Glauber-Sudarshan P-representation [19]. This absence of a legitimate $P(\alpha)$ corresponds to the impossibility of expressing the state at hand as

a convex combination of the states considered classical in this context, the Glauber coherent states $\{|\alpha\rangle\}$. This idea of nonclassicality can be generalized to different scenarios by modifying the set of states considered as the classical reference. Thus any convex combination of the elements of this new classical set can be considered classical, including classical statistical mixtures of pure reference states.

This is the case of the quasiprobability representation of quantum coherence (QPQC) introduced in [87]. It arises from the decomposition of a state in terms of a finite number of states among the set of classical ones $\{|c\rangle\}$,

$$\hat{\rho} = \sum_i P_i |c_i\rangle\langle c_i| + \rho_{res}, \tag{1.114}$$

where $\rho_{res}$ is a residual component that does not lie in the linear span of classical states. The decomposition of the state presented in Eq. (1.114) is optimal since the quasiprobability $P_i$ corresponding to any classical state is always non-negative. On the contrary, a negative $P_i$ or a $\rho_{res} \neq 0$ revelates the nonclassicality of the state.

The states defined as classical, $|c\rangle$, depend on the quantum feature being investigated. For example, the set of factorizable states $\{|\psi_1\rangle \otimes \cdots \otimes |\psi_N\rangle\}$ is considered as the classical reference for entanglement [88]. Regarding polarization, the angular-momentum coherent states [89], also known as SU(2) coherent states, have been historically considered classical-like states. This is due to their minimum uncertainty in the phase space, their invariance under SU(2) transformations, and their straightforward relation to Glauber coherent states [90, 91, 92]. Thus, if the set of classical states were the same for several quantum features, these characteristics would be unified, and their characterization in terms of QPQC would be equivalent to all intents.

### 1.5.2 Factorization of angular momentum coherent states

In this section it is shown how the angular momentum coherent states, $|\vec{s}\rangle$, can be expanded as the tensor product of indistinguishable photons, $|q\rangle$. This is to say, they are factorizable states:

$$|\vec{s}\rangle \leftrightarrow |q\rangle^{\otimes N}. \tag{1.115}$$

Note that, as long as we focus on indistinguishable photons, $|\psi_1\rangle = \cdots = |\psi_N\rangle$, factorizable states of $N$ total number of photons can be written as $|\psi_1\rangle \otimes \cdots \otimes |\psi_N\rangle = |\psi\rangle^{\otimes N}$.

To demonstrate the equivalence in Eq. (1.115), we start with the usual parametrization for the angular momentum coherent states,

$$|\vec{s}\rangle = \sum_{m=0}^{N} \binom{N}{m}^{1/2} \left(\cos\frac{\theta}{2}\right)^m \left(\sin\frac{\theta}{2}\right)^{N-m} e^{-i(N-m)\phi} |m\rangle_H |N-m\rangle_V, \tag{1.116}$$

where $\{|m\rangle_H\}$ and $\{|N-m\rangle_V\}$ are the photon-number basis of each one of the orthogonal polarization modes that define the polarization space. In this case, we consider

horizontal and vertical linear polarization. The notation $|\vec{s}\rangle$ instead of the more usual one $|\theta,\phi\rangle$ is just a matter of simplicity, since we are not interested in the specific value of each angle. For the same reason, we condense the terminology via $\left(\cos\frac{\theta}{2}\right)^m = \chi^{n_H}$, $\left(e^{-i\phi}\sin\frac{\theta}{2}\right)^{N-m} = \xi^{n_V}$ and $|m\rangle_H \otimes |N-m\rangle_V = |n_H\rangle \otimes |n_V\rangle$, so we can rewrite Eq. (1.116) as

$$|\vec{s}\rangle = \sum_{\substack{n_H,n_V=0 \\ n_H+n_V=N}}^{N} \binom{N}{n_H}^{1/2} \chi^{n_H}\xi^{n_V}|n_H,n_V\rangle, \tag{1.117}$$

in the mentioned two-mode Fock basis $\{|n_H,n_V\rangle\}$, with the usual tensor product notation, $|n_H,n_V\rangle = |n_H\rangle \otimes |n_V\rangle$.

On the other hand, the description of the polarization state of a single photon is formally equivalent to the description of a 1/2-spin particle. One possible basis of the two-dimensional Hilbert is formed by the horizontal and vertical polarization states $\{|H\rangle,|V\rangle\}$,

$$|H\rangle = \begin{pmatrix} 1 \\ 0 \end{pmatrix}, \quad |V\rangle = \begin{pmatrix} 0 \\ 1 \end{pmatrix}. \tag{1.118}$$

Therefore, any pure state, or qubit, becomes

$$|q\rangle = \alpha_H|H\rangle + \alpha_V|V\rangle, \tag{1.119}$$

with $|\alpha_H|^2 + |\alpha_V|^2 = 1$. Then, the tensor product of $N$ indistinguishable photons reads as follows,

$$|q\rangle^{\otimes N} = \tag{1.120}$$
$$\alpha_V^N|V\rangle^{\otimes N} + \tbinom{N}{1}\alpha_H\alpha_V^{N-1}|H\rangle|V\rangle^{\otimes N-1} + \cdots + \tbinom{N}{N-1}\alpha_H^{N-1}\alpha_V|H\rangle^{\otimes N-1}|V\rangle + \alpha_H^N|H\rangle^{\otimes N}$$
$$= \sum_{m=0}^{N}\binom{N}{m}\alpha_H^m\alpha_V^{N-m}|H\rangle^{\otimes m}|V\rangle^{\otimes N-m},$$

which belongs to a $2N$-dimensional Hilbert space, $\mathcal{H}^{\otimes N}$, whose basis can be defined by the tensor product of the basis of $N$ two-dimensional Hilbert-spaces $\{|k_1\rangle \otimes \cdots \otimes |k_N\rangle\}$ for $k_1,...,k_n = H,V$.

The key point of this derivation is the connection that can be made between the elements of both bases. Specifically, the states composing the two-mode Fock basis utilized in Eq. (1.117), $|n_H,n_V\rangle$, can be expressed in the single-photon basis, $\{|H\rangle,|V\rangle\}$,

as

$$\begin{aligned} |n_H, 0\rangle &= |H\rangle^{\otimes n_H} \\ |1,1\rangle &= \frac{|H,V\rangle + |V,H\rangle}{\sqrt{2}} \\ &\cdots \\ |n_H, n_V\rangle &= \frac{|H\rangle^{\otimes n_H}|V\rangle^{\otimes n_V} + \text{permutations}}{\binom{N}{n_H}^{1/2}}. \end{aligned} \tag{1.121}$$

These equivalences allow us to express the symmetric tensor product of qubits in the Fock basis, Eq. (1.120), showing the total correspondence with the angular momentum coherent state, Eq. (1.117),

$$\begin{aligned} |q\rangle^{\otimes N} &= \sum_{m=0}^{N} \binom{N}{m} \alpha_H^m \alpha_V^{N-m} |H\rangle^{\otimes m} |V\rangle^{\otimes N-m} \\ &= \sum_{n_H=0}^{N} \binom{N}{m}^{1/2} \alpha_H^m \alpha_V^{N-m} |m, N-m\rangle = |\vec{s}\rangle. \end{aligned} \tag{1.122}$$

Following Ref. [93], the first line would be the angular momentum coherent state in the particle description whereas the second line would be the mode description. We utilize this treatment to find that two nonclassical properties are equivalent via the QPQC.

Eq. (1.122) determines that the set of states utilized as the classical reference for computing entanglement, factorizable states, and the classical set for nonclassical polarization, angular-momentum coherent states, are actually identical even though those states are usually expressed in different bases. This makes entanglement quasiprobability distribution and polarization quasiprobability distribution exactly the same property with the same potential pathologies. We take advantage of this feature in the following chapter to detect both polarization nonclassicality and entanglement in a certain state by means of a single experiment.

### 1.5.3 Concluding remarks

The strict equivalence between non-classical polarization and photon entanglement has been shown. Remarkably, strong relationships between polarization squeezing and quantum correlations between the individual components have been established since the very definition of spin-squeezing [94, 95, 96, 97]. However, the proposed unification goes further in this direction for several reasons. Firstly, we found the equivalence with particle entanglement: neither modes nor continuous variable entanglement. These notions of entanglement have recently been confirmed as independent quantum resources [98]. Secondly, this analysis includes all polarization nonclassical features, beyond the

signature of squeezing. Finally, the presence of one phenomenon is found as a necessary and sufficient condition for the presence of the other. Moreover, if we consider the quasiprobability quantum coherence as the quantifier of polarization nonclassicality and entanglement, both quantities become identical.

In this section, the difference between the two main definitions of nonclassicality present in this work becomes evident. One is based on choosing a set of states with some required characteristics and considering them the classical reference. This is the case of the historical concept of nonclassicality in quantum optics in terms of quasiprobabilities in the phase space, but it is also the concept of the recently introduced QPQC presented in this section. On the other hand, nonclassicality regarded as the lack of common statistics for incompatible observables [35, 99].

As we have already said, the latter definition implies the former since a lack of a well-behaved P-representation is related to a lack of a joint distribution for complimentary quadratures. However, these interpretations are clearly different, as we can see from the nonclassical behavior of $SU(2)$ coherent states, or even Glauber-coherent states, regarding its lack of a joint distribution for certain incompatible observables [26].

What makes the latter definition more general is the possibility of looking for any pair of incompatible observables giving rise to a pathological distribution instead of restricting ourselves to the corresponding defined by the classical states. This seems compelling from a conceptual point of view, even if this definition leads to just one classical-like state, the maximally mixed state, proportional to the identity operator at least in finite-dimensional spaces. In that sense, recalling the nonclassicality given by the different quasiprobabilities, one is also always allowed to choose a different nonclassical feature for which the state might not be a convex combination of the new classical set. Therefore, any state could show any nonclassicality if the feature is wisely chosen.

# Quantum Coherence

*Anytime my life flashes in front of me*
*I see a child there, as if on a screen.*
*Standing in the shadows, flickering,*
*for a moment I know what it means*

*Secrets of the Stars. The Milk Carton Kids*

## 2.1 Introduction to coherence

Coherence is a deeply-rooted concept in physics theory. Historically, it arose in a classical optical context as the perfect tool to deal with the statistical properties of light. Nowadays, its quantum version accounts for the statistical properties of quantum nature and it is on the spot regarding the technological applications of quantum theory.

### 2.1.1 Classical background

The statistical behaviour of light is inherited from the very statistical nature of its emission, i.e. from the matter itself. The lack of knowledge due to the high number of emitters and the extremely small time scale of these phenomena situates the electric field as a random variable [100]. By contrast, the large resolving time of the light detectors provoked for a long time that all light measurements were a time average of the intensity, so randomness and statistics are present in light from generation to detection.

Classical coherence appears as the relationship between electromagnetic fields in two space-time points, with interference and diffraction as its primordial workspaces. In order to introduce the basic concepts, we consider two ergodic fields interfering at some point of space, for example in a Young interferometer. The intensity $I(z)$ at the

point of observation of the interference, $z$, becomes

$$\langle|E(z)|^2\rangle = \langle|\vec{E}(\mathbf{x}_1,t_1)|^2\rangle + \langle|\vec{E}(\mathbf{x}_2,t_2)|^2\rangle + \langle\vec{E}(\mathbf{x}_1,t_1)^*\vec{E}(\mathbf{x}_2,t_2)\rangle + \langle\vec{E}(\mathbf{x}_1,t_1)\vec{E}(\mathbf{x}_2,t_2)^*\rangle, \tag{2.1}$$

where $\langle\dots\rangle = \lim_{t\to\infty}\frac{1}{2T}\int_{-T}^{T}dt$ represents the time average carried out by the detector. The function governing the interference is called mutual coherence function,

$$\Gamma(\mathbf{x}_1,t_1;\mathbf{x}_2,t_2) = \langle\vec{E}(\mathbf{x}_1,t_1)\vec{E}(\mathbf{x}_2,t_2)^*\rangle \text{ and } g^{(2)} = \frac{\langle\vec{E}(\mathbf{x}_1,t_1)\vec{E}(\mathbf{x}_2,t_2)^*\rangle}{\sqrt{\langle|\vec{E}(\mathbf{x}_1,t_1)|^2\rangle\langle|\vec{E}(\mathbf{x}_2,t_2)|^2\rangle}}, \tag{2.2}$$

is its normalized version, the second-order degree of coherence. Since the fields at hand are stationary, the mutual coherence function depends only on the time difference, $\tau = t_2 - t_1$. One of the main results in classical coherence theory is the Wiener-Khintchin theorem, which gives the relation between the mutual coherence function of a stationary field and the cross-spectral density, $I(\nu)$,

$$\Gamma(\mathbf{x}_1,\mathbf{x}_2,\tau) = \int_0^\infty I(\mathbf{x}_1,\mathbf{x}_2,\nu)e^{-i2\pi\nu\tau}d\nu, \tag{2.3}$$

where $\nu$ is the light frequency.

The mutual coherence function can be extended to describe the statistical relation between more than two electric fields, thus the average of all the fields considered defines the correlation function,

$$\Gamma^{(m,n)}(\mathbf{x}_1,t_1;\dots;\mathbf{x}_{n+m},t_{n+m}) = \langle\prod_{j=1}^{m}\vec{E}(\mathbf{x}_j,t_j)\prod_{k=m+1}^{m+n}\vec{E}(\mathbf{x}_k,t_k)^*\rangle. \tag{2.4}$$

From this function, infinite degrees of coherence can be defined as

$$g^{(n)} = \frac{\Gamma^{(n,n)}(\mathbf{x}_1,\dots,\mathbf{x}_{2n})}{\left[\prod_{j=1}^{2n}\Gamma^{(n,n)}(\mathbf{x}_j,\dots,\mathbf{x}_j)\right]^{\frac{1}{2n}}}. \tag{2.5}$$

In classic interferometers, the second-order degree of coherence can be directly related to visibility,

$$V = \frac{I_{\max}-I_{\min}}{I_{\max}+I_{\min}} \propto |g^{(2)}| \tag{2.6}$$

so, for a long time, it was considered the more coherence, the more resolution. However, this connection between resolution and coherence is substantiated in the direct observation of the interference by the human eye (or by a same-operation better-performance element as the cameras) implicit in the concept of visibility. This behaviour defined the role of coherence until the 20$^{\text{th}}$ century, when different types of *interference* were measured [101] and new light states arose, some of which were able to generate higher resolution measures without second order of optical coherence [102]. The light sources

utilized until that moment had been thermal, for which the probability distribution of the electric field is Gaussian. This is why the definition of coherence based on the second momentum of these distributions had been enough to describe the phenomena until then [100]. However, the mentioned discoveries stimulated a new description of light, accounting for the complete statistical distribution of fields $P(E, E^*)$. In this manner, higher orders of coherence started to play a part in the description and use of light,

$$\langle f(E, E^*) \rangle = \int_0^\infty dE dE^* f(E, E^*) P(E, E^*). \tag{2.7}$$

### 2.1.2 Quantum-optical coherence

A direct translation of the previous theory into the quantum domain, this is by exchanging the random variables by their corresponding operators and averages by expectation values, implicates an ordering problem when the operators involved do not commute. As an example, considering one mode fields, we can compute the n-order degree of coherence as,

$$g^{(n,n)} = \frac{\mathrm{tr}(\rho a^{\dagger n} a^n)}{\mathrm{tr}(\rho a^\dagger a)^n} \neq \frac{\mathrm{tr}(\rho a^n a^{\dagger n})}{\mathrm{tr}(\rho a a^\dagger)^n}. \tag{2.8}$$

This problem is extensible to the whole statistics, so there can be built multiple quantum-optical coherence approaches corresponding to the different ordering of operators. In addition, the functions $P(E, E^*)$ that play the role of probability distribution may be non legitimates taking for example negative values, as it has been seen in Chapter 1.

The well-established quantum-optical theory of coherence was developed by Glauber and Surdashan [20, 21, 22]. It is a direct translation of the classical theory by choosing one particular order for the operators. This is the normal ordering, where the creation operators are always to the left of the annihilation operators. This selection is actually grounded in the operating way of the most commonly used detectors, the photoelectric detectors. The action of those elements is described as the absorption of photons and emission of electrons due to the photoelectric effect. This ordering allows the quantum correlation functions to agree with the classical ones by exchanging variables with the corresponding operators.

### 2.1.3 Quantum-mechanical coherence

The later theory of quantum-optical coherence is specifically designed for electromagnetic fields, as was its classical predecessor. However, the superposition principle allows the formulation of an equivalent concept of quantum coherence accounting for the statistical relationship between different state elements. The superposition principle

establishes that the normalized linear combination of states is also a state

$$|\psi\rangle = \beta_1|\phi_1\rangle + \beta_2|\phi_2\rangle + ... \qquad \text{with} \quad \sum_i |\beta_i|^2 = 1. \tag{2.9}$$

In classical optics, coherence describes the statistical relationship between the amplitudes of the electric field components in which the total field state can be decomposed. In quantum mechanics, quantum coherence describes the statistical relationship between the probability amplitude of the states, $\beta_i$, that compose the total state,

$$\langle\phi_1|\psi\rangle\langle\psi|\phi_2\rangle = \beta_1\beta_2^*. \tag{2.10}$$

It is therefore clear the dependence on the basis, which gives the states the opportunity to be both coherent and incoherent depending on the choice. This dependence is already present in classical optics, as it can be seen for example in the case where the field components are orthogonal polarization modes. Also to this dependence can be related the possibility of transforming quantum coherence into more specific types of correlations such as entanglement or steering [104, 105, 106].

Quantum coherence leads to fascinating implications at a fundamental level, such as the classical-quantum borderline itself [107, 108, 109], along with prospering practical applications [110, 111, 112]. Among them, quantum computing is maybe the most eye-catching application of quantumness nowadays. Along with quantum information processing, both entail an immense increase in computational speed. This may allow an incredible development in calculus with a huge computational time cost, which is one of the main problems in many areas of research such as material science, atmospheric optics or chemistry [113, 114, 115]. However, quantum technologies go beyond these promising advantages and concentrate at this point plenty of results, so they can only be described as an ongoing revolution[116]. We can remark on quantum communication protocols for long-term security [117], programmable quantum systems providing a practical advantage in simulations [118], or quantum sensing [119], which will be discussed in more depth in the following.

#### 2.1.3.1 Resource theories

This interest in manipulating quantum correlations generated a complete field of study, the quantum resource theory. The aim was to give a protocol to manipulate and quantify the amount of resources in order to optimize their performance. Initially proposed for entanglement, [120], the main structure of these theories has been extended to a wide variety of resources such as coherence [103], purity [121], nonclassicality [122], etcetera. To the point of multi-resource theories for systems handling with different conservation laws [123]. As the last example, we include the resource of superposition [124]. This is considered a generalization of quantum coherence. Its particularity is that it is defined in systems where the states of the bases are not orthogonal but only

linearly independent. This is a great example of the sometimes extreme subdivision in studying quantum correlations. This escalation of theories is due to the effective support to take advantage of quantum features demonstrated by resource theories, for instance, in quantum information processing [125] or in metrology [127].

Initially defined for finite-dimensional spaces and discrete orthonormal basis, the elements and mathematical structure underlying these theories are common. The set of free states, lacking the resource under study. In contrast, the resource states contain a certain amount of resource distillable, this is likely to be utilized. The set of free operations, which enclose the physical transformations over the states that do not generate resource when applied to free states. Finally, it is necessary to define a quantifier, which gives account for the amount of resource. Given certain resource, the definition of these elements can be more or less evident. For example, regarding coherence, the set of free states is composed of diagonal states. However, recalling the basis dependence, the diagonal states are not univocally defined [128]. Still, there are several definitions of incoherent operations [126], each one of them giving rise to slightly different legitimate quantifiers.

The quantifiers utilized in this work are distance-based, this is, the amount of coherence corresponds to the distance between the state and the nearest incoherent one. Different distances produce different quantifiers. Among those used, only the relative entropy of coherence is considered a true measure of coherence accomplishing all the mathematical conditions set in Ref. [129] to properly reflect the presence and evolution of the resource. The remaining quantifiers do not fulfill all these mathematical conditions so they are understood as monotones: nonnegative, convex quantifiers that do not increase under incoherent operations but that are not unique for pure states, not additive under tensor products, or that can increase under incoherent operations if there is the possibility of post-selecting the outcomes of the measurement. In the following, the concept *measure* is utilized in a more flexible way than in Ref. [129], being in this particular case synonym of *monotone*.

#### 2.1.3.2 Previous connections between coherence and nonclassicality

Quantumness has been historically related to the capacity to produce unexpected interference (by electrons[130], single photons[77], molecules [131], or even cats [132]). In this regard, coherence would be what quantumness is all about, and decoherence the way to recover the classical world. However, this concept is also usually distinguished from entanglement, steering, and Bell-like correlations [133, 134]. And also distinguished from more sophisticated definitions of quantumness, such as those for Markov processes [135], in which the connection to coherence disappears for non-Markovian statistics.

As we have seen in the previous chapter, in quantum optics the concept of quantumness was related to quantum mechanical coherence by definition: all the non-diagonal

states on the basis of classical-like states were nonclassical. Therefore, coherence and nonclassicality were one and the same thing -as well as incoherence and classicality-. For this relationship to be sustained, the basis for computing the coherence is restricted to the basis of classical states. Curiously, the classical (incoherent) states are the Glauber-coherent states and they are highly coherent regarding the photon number basis.

In definitions such as the quasiprobability representation of quantum coherence [87], nondiagonal states (states with coherence) are nonclassical concerning that specific feature. Even if this still implies a preferred set of states, this may be more reasonable since the classical-like states are not universally valid but really explainable by classical theories regarding the feature we want to study or exploit.

In both scenarios, coherence is the signature of nonclassicality by definition. This connection is, however, not so immediate if we consider the definition of nonclassicality as the absence of joint distribution for incompatible observables since this surely forces us to abandon the comfortable classical-like diagonal state.

### 2.1.4 Chapter outline

This chapter considers several of the most important aspects of quantum-mechanical coherence among the just presented in this introduction. Each section deals with one angle of this multifaceted element in quantum theory, trying to obtain a comprehensive scope that allows for a better understanding of the concept at the present time.

The exposition of the study starts from its most pragmatic component, the experimental measuring of a remarkably versatile definition of coherence, the quasiprobability representation of quantum coherence. The experiment that enables this reconstruction is evidence of the astonishing precision achievable in the production and detection of quantum states. It also illustrates how quantum correlations can be realistically handled in practice. We report the reconstruction of the quasiprobability quantum coherence of a two polarization-mode squeezed vacuum and its polarization basis independence.

We continue considering the role of coherence in quantum metrology. As it has been said, the first scenario in which coherence arose was the study of interference. Interferometry has been the main tool of metrology for decades, and it continues to play a central role in extremely accurate detections [136]. This is why the development of coherence was soon promoted to characterize and improve the resolution of interferometers. Nevertheless, there was no clear relation between quantum coherence and resolution estimators. We describe a new definition of coherence specially designed for a signal detection process and its straightforward connection to the resolution of the measurement.

In the subsequent two sections, we work from the perspective of the resource theories. Firstly, we present a quantitative research about quantum coherence as a resource.

The last aspect of coherence discussed is perhaps the main one from a conceptual perspective: the role of coherence as the main quantum feature. From this consideration, it seems reasonable to define a measurement of nonclassicality for which coherence is the necessary and sufficient condition. In this spirit, we introduce a definition of nonclassicality based on quantum coherence.

To conclude, we demonstrate that this definition of nonclassicality equals the absence of joint probability distribution for two incompatible observables introduced in Chapter 1.

## 2.2 Experimental characterization of quantum coherence

In addition to its fundamental role in the understanding of quantum theory mechanisms, quantum coherence is an empirically exploitable property of nature [106, 104]. Its relevance in quantum computer science is especially remarkable, from the hardware itself [137] to the quantum algorithms [138]. Correcting errors that generate decoherence is a principal task in this context, to the extent that a whole field such as Quantum Error Correction emerges [139]. In consequence, the several quantifiers introduced from a theoretical point of view have to be measurable in practice with the appropriate experimental setup [140, 141]. The possibility of performing such measurements has an intrinsic value as proof of the usefulness of the quantum theory of coherence for practical purposes. Moreover, finding results compatible with the ideal cases shows the extreme accuracy achievable by this kind of experiments [142].

In this section, we report an analysis of the coherence of a two-mode squeezed vacuum (TMSV),

$$|\xi\rangle = \sqrt{1-|\xi|^2}\sum_{n=0}^{\infty}\xi^n|n,n\rangle, \tag{2.11}$$

where the modes are orthogonal polarization directions. Talking specifically about the quantifiers of coherence presented in this thesis, they are all calculated, one way or another, from the density matrix of the state. Therefore, the experimental determination of the density matrix in the first place allows indirect measurement of the quantifiers under study. The corresponding quantifiers were the Hibert-Schmidt (HS) coherence [103] and the quasiprobability representation of quantum coherence (QPQC) [87] introduced in Sec. 1.5. Then, we compared their performances regarding the dependence with the polarization basis.

### 2.2.1 Polarization tomography

In the examination of quantum features, polarization is a widely employed degree of freedom since it is easy to handle but still capable of presenting several nonclassical behaviours. This is why it is a useful encoder of quantum information. Besides, quantum tomography allows the indirect determination of a state when many identical copies are available [143]. In the following, the polarization tomography performed on the TMSV is presented[144]. This characterization allowed the reconstruction of the two-photon polarization sector of the state [90, 91]. The setup which generated the data under study belongs to the Integrated Quantum Optics Group at Paderborn University led by Prof. Dr. Christine Silberhorn. Avoiding technical details, the system can be described by dividing it into three parts (see Fig. 2.1). The production of the state consists of a pump laser imprinting a spontaneous parametric down-conversion source which generates two-mode squeezed states [145]. These modes are orthogonal polarization modes, say horizontal (H) and vertical (V). The analyzer is a conventional polarization tomography experiment: a half-wave plate (HWP) and a quarter-wave plate (QWP) followed by a polarized beam splitter (PBS) that separates horizontal and vertical polarized photons. Finally, the detection process is carried out by two click counter detectors (CC) which give the number of photons arriving at each detector on each realization. These are composed of superconducting nanowire single-photon detectors with $\approx 82\%$ efficiencies, preceded by a multiplexing system that allows for a resolution of up to eight photons [146, 147].

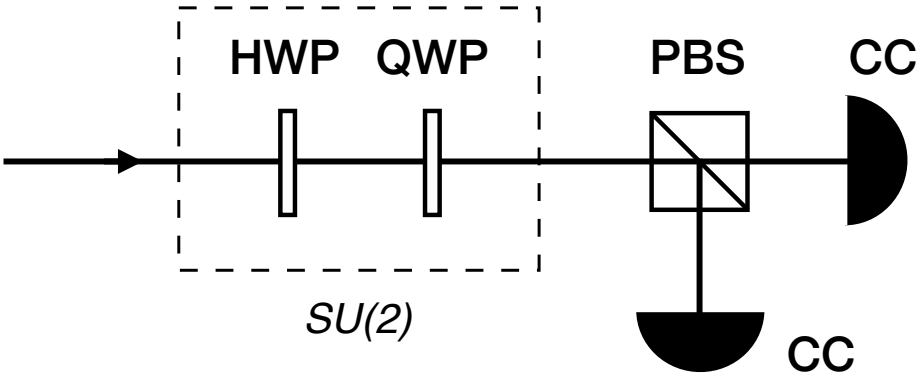


Figure 2.1: Scheme of the setup for the polarization tomography. The SU(2) transformation is performed by means of a combination of a half-wave plate (HWP) and a quarter-wave plate (QWP). The polarization beam splitter(PBS) sends each polarization to one click counter detector (CC).

As mentioned, on each repetition one detector measures the number of photons arriving with horizontal polarization $n_H$, and the other the number of photons with vertical polarization, $n_V$. The amount of times that each combination $(n_H, n_V)$ is detected is collected in a coincidences matrix $C_{n_H,n_V}$. One example of coincidences

matrix is presented in Fig. 2.2. As we can see, during the experiment there where two realizations in which 2 horizontal and 0 vertical photons were detected.

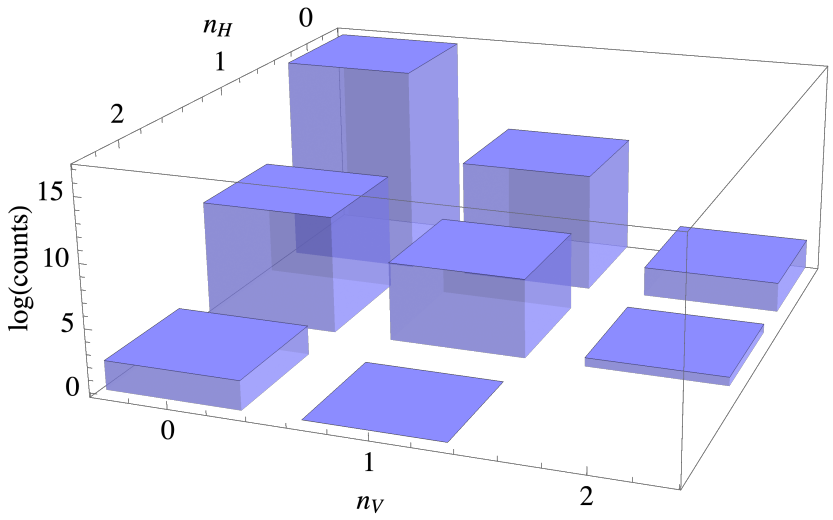


Figure 2.2: Example of recorded coincidence matrix for polarization setting with $\theta_{HWP} = \theta_{QWP} = 0°$.

The combination of wave plates generates a SU(2) transformation of the initial polarization modes. The polarized beam splitter decomposes the H/V components after the rotation performed by the wave plates. The combinations of the wave-plates angles were

$$\begin{aligned} 2\theta_{\mathrm{HWP}} &\in \{0°, 15°, \ldots, 165°\} \quad \text{and} \\ 2\theta_{\mathrm{QWP}} &\in \{-90°, -75°, \ldots, +90°\}. \end{aligned} \tag{2.12}$$

Each one of these polarization settings corresponds to one direction on the Poincaré sphere, which is represented as

$$\vec{\Omega} = \begin{bmatrix} \cos(2\theta_{\mathrm{QWP}})\sin(4\theta_{\mathrm{HWP}} - 2\theta_{\mathrm{QWP}}) \\ \sin(2\theta_{\mathrm{QWP}}) \\ \cos(2\theta_{\mathrm{QWP}})\cos(4\theta_{\mathrm{HWP}} - 2\theta_{\mathrm{QWP}}) \end{bmatrix}. \tag{2.13}$$

As shown in Fig. 2.3, the 156 configurations cover the Poincaré sphere relatively densely and generate an overcomplete tomographic measurement provided we will restrict ourselves to a finite number of photons.

### 2.2.2 Density operator reconstruction

The data generated by the previously presented measurement approach allow us to reconstruct the density operator of the incoming state. The basis at hand is the two-mode Fock basis,

$$\{|n_H, n_V\rangle\} \quad \text{with} \quad |n_H, n_V\rangle = |n_H\rangle_H \otimes |n_V\rangle_V \quad \text{and} \quad n_H, n_V \in \{0, 1, ...\infty\}. \tag{2.14}$$

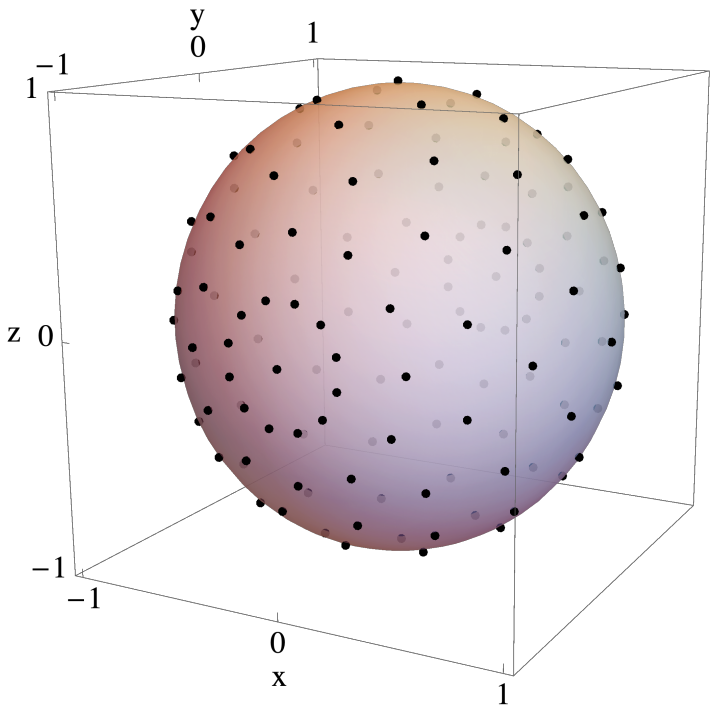


Figure 2.3: Directions on the Poincaré sphere of the 156 polarization measurements performed.

When there is no wave-plate transformation, $\vec{\Omega} = (0, 0, 1)^T$, the POVM representing the measurement performed is $|k, N-k\rangle\langle k, N-k|$ where $N$ defines the subspace of constant total number of photons so $N = n_H + n_V$, $N \in \{0, 1, ..., 16\}$ and $0 \leq k \leq N$.

On the contrary, when there is a nontrivial SU(2) transformation involved, $\vec{\Omega} \neq (0, 0, 1)^T$, the *modus operandi* utilized is to obtain the corresponding rotated POVM. To this end, a beam-splitter-type transformation is applied to the polarization modes,

$$\begin{bmatrix} \hat{a}_+ \\ \hat{a}_- \end{bmatrix} \mapsto \begin{bmatrix} t & r \\ -r^* & t^* \end{bmatrix} \begin{bmatrix} \hat{a}_H \\ \hat{a}_V \end{bmatrix}, \tag{2.15}$$

where $\hat{a}_+$ and $\hat{a}_-$ are the annihilation operators after the transformation and $|r|^2 + |t|^2 = 1$. This transformation can be related to the Poincaré vector as $t = \cos(\theta/2)$, $r = \sin(\theta/2)$, $\arg r - \arg t = \phi$ and $\vec{\Omega} = (\sin\theta\cos\phi, \sin\theta\sin\phi, \cos\theta)^T$. This conduces to the following photon-number state transformation,

$$\begin{aligned} |(k, N-k)_{\vec{\Omega}}\rangle =& \frac{(|t|\hat{a}_H + |r|\hat{a}_V)^{\dagger k}}{\sqrt{k!}} \frac{(-|r|\hat{a}_H + |t|\hat{a}_V)^{\dagger(N-k)}}{\sqrt{(N-k)!}} |\text{vac}\rangle \\ =& \sum_{l=0}^{N} e^{i\phi l} q_{l,k}(\theta) |n_H = l, n_V = N-l\rangle, \end{aligned} \tag{2.16}$$

using the abbreviation

$$q_{l,k}(\theta) = \sum_{u=\max\{0,l-k\}}^{\min\{l,N-k\}} \frac{(-1)^u \sqrt{k!(N-k)!l!(N-l)!}}{(l-u)!(k-l+u)!u!(N-k-u)!} t^{N-k+l-2u} r^{k-l+2u}. \tag{2.17}$$

Therefore the elements of the POVM result

$$\hat{\Pi}_k(\vec{\Omega}) = |(k, N-k)_{\vec{\Omega}}\rangle\langle(k, N-k)_{\vec{\Omega}}|. \tag{2.18}$$

The density operator of the state, fixed a $N$-photon subspace, can be expanded in the computational H-V Fock basis, Eq. (2.14), as

$$\hat{\rho}^{(N)} = \sum_{l_1,l_2}^{N} \rho_{l_1,l_2} |l_1, N-l_1\rangle\langle l_2, N-l_2|. \tag{2.19}$$

In the following, the subscript $j \in \{1, 2, ..., 156\}$ is utilized to denote the different measurement directions, $\vec{\Omega}_j$. On each measurement, the probability of finding $k$ photons in the first detector and $N-k$ photons in the second is

$$p_k(\vec{\Omega}_j) = \mathrm{tr}[\rho^{(N)} \hat{\Pi}_k(\vec{\Omega}_j)] = \sum_{l_1,l_2=0}^{N} e^{i(l_2-l_1)\phi_j} q_{l_1,k}(\theta_j) q_{l_2,k}(\theta_j) \rho_{l_1,l_2}. \tag{2.20}$$

These probabilities can be obtained from the measured coincidences matrices. Since we restrict ourselves to a given $N$-photon subspace, we are interested in the matrix elements $C_{k,N-k}$, and the probabilities are

$$p_k(\vec{\Omega}_j) = \frac{C_{k,N-k}}{\sum_{k=0}^{N} C_{k,N-k}}. \tag{2.21}$$

We combine the probabilities $p_k(\vec{\Omega}_j)$ of all the measurements in one vector with double index, $\vec{p} = [p_k(\vec{\Omega}_j)]_{(k,j)}$. In the same way we can express $\hat{\rho}$ as a vector with double index, $\vec{\rho} = [\rho_{l_1,l_2}]_{(l_1,l_2)}$. Finally, the vectors $q_{k,l}(\theta)$ can be grouped in the matrix,

$$Q = [e^{i(l_2-l_1)} q_{l_1,k}(\theta_j) q_{l_2,k}(\theta_j)]_{(k,j),(l_1,l_2)}. \tag{2.22}$$

The relation (2.20) between the probabilities and the matrix elements can be expressed now as

$$\vec{p} = Q\vec{\rho}. \tag{2.23}$$

The inverse of this relation allows obtaining the elements of the density matrix. Since $Q$ is a rectangular matrix, the needed inverse is numerically computed as the Moore-Penrose pseudoinverse $Q^+$, [149].

$$\vec{\rho} = Q^+\vec{p}. \tag{2.24}$$

Due to the accessible data, the reconstruction and the consequent coherence analysis were centered on the two-photon subspace. Higher pump power would make appear more frequently states with a higher number of photons, allowing the reconstruction of subspaces of larger dimension. In consequence, we reconstruct the density operator corresponding to Eq. (2.19) with $N = 2$ using Eq. (2.24), finding (see Fig. 2.4)

$$\hat{\rho} = \begin{pmatrix} 0.07 & 0.07 - 0.04i & 0.04 \\ 0.07 + 0.04i & 0.866 & -0.05 + 0.04i \\ 0.04 & -0.051 - 0.04i & 0.06 \end{pmatrix}, \tag{2.25}$$

with standard deviation

$$\sigma(\hat{\rho}) = \begin{pmatrix} 0.04 & 0.04 & 0.08 \\ 0.04 & 0.004 & 0.06 \\ 0.08 & 0.06 & 0.04 \end{pmatrix}. \tag{2.26}$$

The error estimation of the elements of the density matrices is computed by following a quadratic propagation,

$$\sigma(\rho_{i,j}) = \sqrt{\sum_k \left(\frac{\partial \rho_{i,j}}{\partial p_k}\right)^2 \sigma(p_k)^2}, \tag{2.27}$$

where an error margin is assigned to each probability $p_k$,

$$\sigma(p_k) = \sqrt{\frac{p_k\,(1 - p_k)}{\left(\sum_k^N C_k\right) - 1}}. \tag{2.28}$$

The imaginary parts of the reconstructed density operator elements, Eq.(2.25), are comparable to the obtained standard deviation, Eq.(2.26). This allows us to neglect these components of the reconstruction as they are consistent with a zero contribution within the error margin.

Finally, we address the ideal case of the two-mode squeezed vacuum introduced in Eq. (2.104), which on each $N$-photon subspace (with $N$ even) becomes

$$\rho_\xi^N = |N/2, N/2\rangle\langle N/2, N/2|. \tag{2.29}$$

Due to experimental imperfections, other elements different from $\rho_{1,1}$ are not canceled in this reconstruction. At this point, it is worth remarking that there was no correction for detection losses or any other statistical treatment during the data process. Hence, this analysis considers all the experiment's impurities while still exhibiting quantum properties.

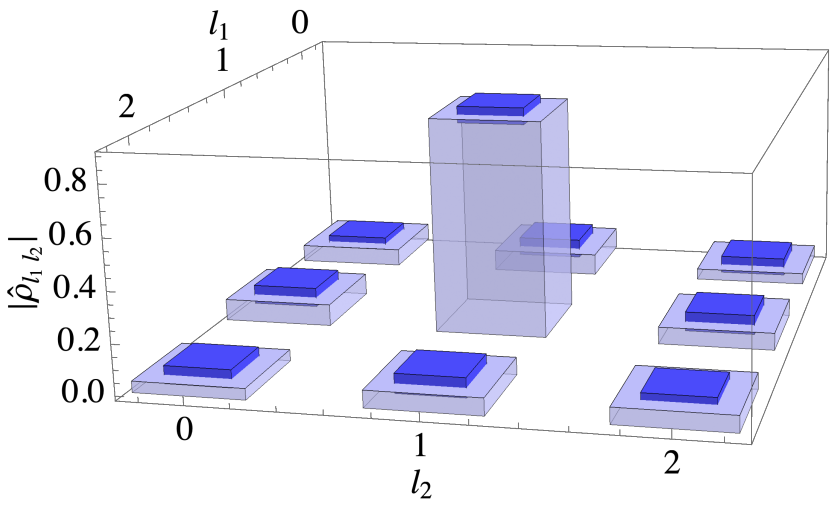


Figure 2.4: Reconstructed density matrix in the 2-photon subspace. Darker blue bars represent the estimated error ($\pm 10\sigma$).

### 2.2.3 Computation of the Hilbert-Schmidt coherence

Once the density operator is reconstructed, it is possible to compute any quantifier of coherence. As a representative example of the distance-based quantifiers [129], we focus on the coherence based on the HS-norm,

$$\mathcal{C}_{HS}\left(\hat{\rho}\right) = \sum_{k \neq k'} |\rho_{k,k'}|^2. \tag{2.30}$$

This measure of coherence goes from $\mathcal{C}_{HS} = 0$, for incoherent states, to $\mathcal{C}_{HS} = 1 - \frac{1}{N}$ for pure states with constant probability $\rho_{ii} = 1/N$, which is deeply discussed in Sec. 2.4.

In the Fock basis, $\{|n_H, n_V\rangle\}$, the analyzed state is almost incoherent since it is almost diagonal, and the coherence reads

$$\mathcal{C}_{HS}(\hat{\rho}) = 0.028 \pm 0.001, \tag{2.31}$$

where the error was estimated again through a standard quadratic error propagation.

One of the main characteristics of quantum coherence is its basis dependence, with the exception of some measures specially designed to try to avoid this connection [148]. The HS-coherence of the reconstructed density operator is computed as a function of the polarization basis orientation, this is, $\mathcal{C}_{HS}\left(\hat{\rho}'\right)$ where $\hat{\rho}' = U(\vec{\Theta})\hat{\rho}U^{\dagger}(\vec{\Theta})$ with the unitary transformation corresponding to the SU(2) rotation

$$U(\vec{\Theta}) = \left[e^{i\phi l} q_{l,k}\left(\theta\right)\right]_{(l,k)} \tag{2.32}$$

where $q_{l,k}\left(\theta\right)$ is the same as in Eq. (2.16). In Fig. (2.5), the HS-coherence for the rest of the orientations of the basis is shown. Therefore, it can be seen how the state almost

reaches both bounds by varying the basis, going from an incoherent to a maximally coherent state. It also can be seen how the minimum of coherence does not coincide with the case $\theta = 0°$ and there is a small angular translation of 3°. This means that the modes of the produced state are not exactly horizontal and vertical polarization modes but are slightly rotated.

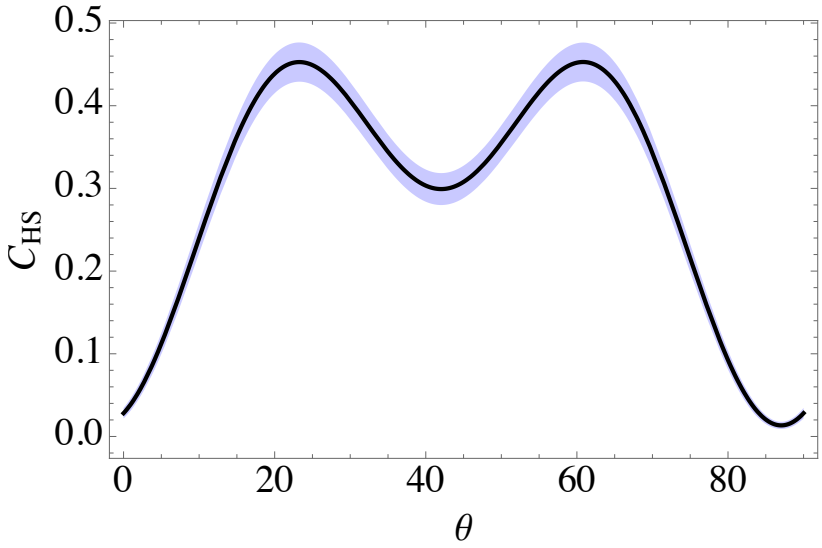


Figure 2.5: Coherence based on the Hilbert Schmidt distance for the TMSV reconstructed state in Eq. (2.25) as a function of the polarization basis orientation. The blue band shows an error margin of $\pm 5\sigma$.

### 2.2.4 Quasiprobability quantum coherence computation

The second measure of coherence computed for the reconstructed state is the quasiprobability representation of quantum coherence introduced in [87], which has been previously presented in Sec. 1.5. Remarkably, the current report refers to the first experimental reconstruction of this kind of coherence measurement.

The elements of the incoherent set are the angular-momentum coherent states [89]. Since we are restricting ourselves to the two-photon subspace, we can explicitly express the $N = 2$ case in Eq. (1.117),

$$|\vec{s}\rangle = \xi^2|0,2\rangle + \sqrt{2}\chi\xi|1,1\rangle + \chi^2|2,0\rangle, \tag{2.33}$$

assuming $|\chi|^2 + |\xi|^2 = 1$. The QPQC is given by the quasiprobabilities $\vec{P} = [P(s_i)]_i$ from the optimum decomposition of the state, see Eq. (1.114),

$$\hat{\rho} = \sum_i P(s_i)|s_i\rangle\langle s_i| + \rho_{res}, \tag{2.34}$$

where stationary elements of the incoherent set $|s_i\rangle$ are those satisfying [87]

$$\frac{\partial\langle s|\hat{\rho}|s\rangle}{\partial\chi^*} = 0 \text{ and } \frac{\partial\langle s|\hat{\rho}|s\rangle}{\partial\xi^*} = 0. \tag{2.35}$$

As demonstrated in Chapter 1, we can express $|\vec{s}\rangle$ in the basis $\{|H\rangle\otimes|H\rangle, |H\rangle\otimes|V\rangle, |V\rangle\otimes|H\rangle, |V\rangle\otimes|V\rangle\}$, and it becomes equivalent to the tensor product of two qubits $|q\rangle$. Therefore, the stationary elements become

$$|\vec{s_i}\rangle = |q_i, q_i\rangle. \tag{2.36}$$

To find them, the separability eigenvalue equations [88] can be utilized,

$$\hat{\rho}_q|q\rangle = \lambda|q\rangle, \tag{2.37}$$

where $\hat{\rho}_q = (\langle q|\otimes\mathbb{1})\,\hat{\rho}\,(|q\rangle\otimes\mathbb{1})$ with $\hat{\rho}$ expressed likewise in the basis $\{|H\rangle\otimes|H\rangle, |H\rangle\otimes|V\rangle, |V\rangle\otimes|H\rangle, |V\rangle\otimes|V\rangle\}$. Accordingly, the quasiprobabilities corresponding to the stationary qubit states, $P(q_i)$, are equivalent to the $P(q_i)$ in Eq. (2.34) $\forall i$.

We follow the latter procedure and resolve Eq. (2.37). The obtained states $|q_i\rangle$ are represented in the Bloch sphere on the left side of Fig. 2.6. In the right section of this figure are represented the stationary states for the ideal TMSV state. It can be seen how those for the experimental state are slightly biased with respect to those for the ideal one.

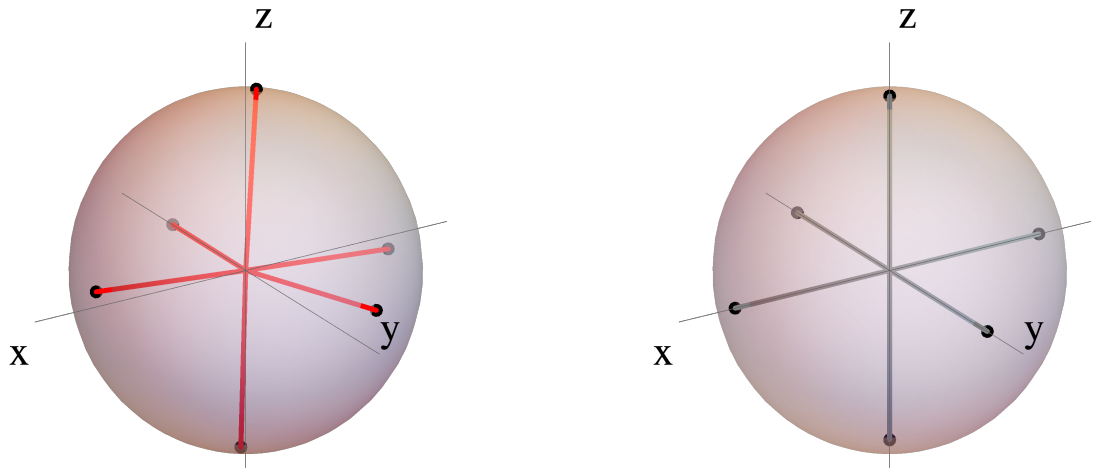


Figure 2.6: Representation on the Bloch sphere of the stationary qubit states $|q_i\rangle$ for the reconstructed state (left) and for the ideal TMSV state (right).

Once we have the stationary points, the QPQC is computed as follows [87],

$$\vec{P} = \mathbf{G}^{-1}\vec{g}, \tag{2.38}$$

where $g_i = \mathrm{tr}\,(\hat{\rho}\,|q_i, q_i\rangle\langle q_i, q_i|)$, and $\mathbf{G}^{-1}$ is the inverse of the Gram-Schmidt matrix, $G_{i,j} = \mathrm{tr}\,(|q_i, q_i\rangle\langle q_i, q_i \mid q_j, q_j\rangle\langle q_j, q_j|)$. The quasiprobability distribution obtained for the reconstructed state is represented in Fig. 2.7.

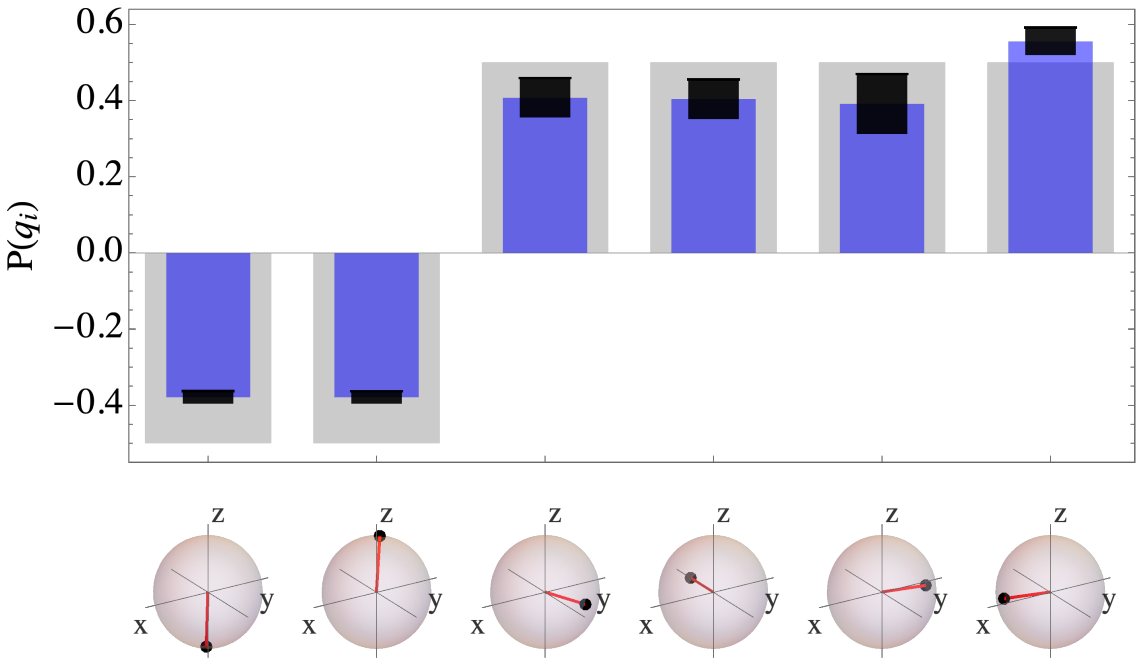


Figure 2.7: Quasiprobabilities for the reconstructed state (blue) as a function of the corresponding stationary qubit states. The black bars represent the estimated error ($\pm 5\sigma$). In grey, the quasiprobabilities corresponding to the ideal case.

As expected, we find negativities accounting for the nonclassical behaviour of the experimentally produced state. The negative values, $P_1 = P_2 = -0.380 \pm 0.003$, are considerably similar to the ideal case, for which $P_1 = P_2 = -0.5$. We can contrast this result with previous realizations of the experiment. For example, for lower pump power and distinguishable photons, the negativities decay to $P_1 = -0.012 \pm 0.002$ and $P_2 = -0.014 \pm 0.02$.

The error estimation for the quasiprobability distribution has been computed following a Monte Carlo approach. We randomly generated 25.000 matrices with Gaussian distribution of standard deviation 2.26 around the reconstructed density operator Eq. (2.25). From each matrix, the quasiprobabilities were produced, obtaining 11.171 valid quasiprobability distributions. Finally, the resulting distribution of each element $P_i$ has the standard deviation represented in Fig. (2.7).

As a final step to complete the reconstruction of the state, we compute the component orthogonal to the plane formed by the classical states,

$$\hat{\rho}_{\text{res}} = \hat{\rho} - \sum P\left(q_i\right) |q_i, q_i\rangle\langle q_i, q_i| = 6 \times 10^{-10}, \tag{2.39}$$

which is virtually zero if we consider a typical simple machine precision of $10^{-7}$, in agreement with [87].

#### 2.2.4.1 Polarization basis rotation independence

The elements of the incoherent set are invariant under polarization basis transformation. This quality is transferred to the QPQC as we can see from both theoretical and experimental points of view, as we are about to demonstrate.

To this end, we start by noting that the stationary elements solving Eq. (2.35) are different. For $\eta = \chi, \xi$ and $U(\vec{\Theta})$ in Eq. (2.32), we find,

$$\frac{\partial \langle s|\hat{\rho}'|s\rangle}{\partial \eta^*} = \frac{\partial \langle s|U(\vec{\Theta})\hat{\rho}U^\dagger(\vec{\Theta})|s\rangle}{\partial \eta^*} = 0 \rightarrow |s_i'\rangle \tag{2.40}$$

connected to the non-rotated solutions $|s_i\rangle$ through

$$|s_i'\rangle = U(\vec{\Theta})|s_i\rangle. \tag{2.41}$$

This difference is shown in Fig. 2.8 where we display the stationary states corresponding to the reconstructed state expressed in different polarization basis.

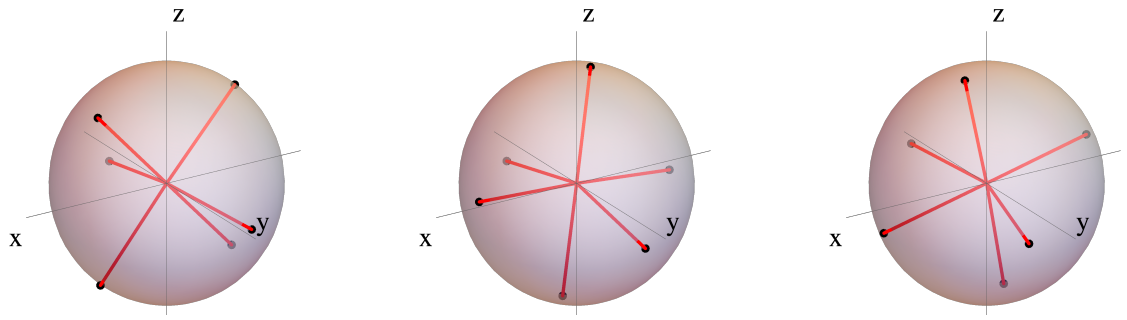


Figure 2.8: Stationary qubit states for the reconstructed state expressed in different polarization basis. The applied basis transformations correspond to $\phi = 0°$ and $\theta = 20°$ left, $\theta = 45°$ center, and $\theta = 80°$ right.

However, the relation between solutions in Eq. (2.41) allows the Gram-Schmidt matrix as well as the vector $\vec{g}$ to remain invariant,

$$\begin{aligned} \boldsymbol{G}' &= [|\langle s_i'|s_j'\rangle|^2]_{i,j} = [|\langle s_i|U^\dagger(\vec{\Theta})U(\vec{\Theta})|s_j\rangle|^2]_{i,j} = \boldsymbol{G} \\ \vec{g}' &= [\langle s_i'|\rho'|s_i'\rangle]_i = [\langle s_i|U^\dagger(\vec{\Theta})U(\vec{\Theta})\rho U^\dagger(\vec{\Theta})U(\vec{\Theta})|s_i\rangle]_i = \vec{g}, \end{aligned} \tag{2.42}$$

and therefore the values of the quasiprobability distribution do not alter

$$\vec{P}' = \boldsymbol{G}'^{-1}\vec{g}' = \boldsymbol{G}^{-1}\vec{g} = \vec{P}. \tag{2.43}$$

#### 2.2.4.2 Distinguishable case

Finally, we show the performance of this method in detecting nonclassicality without falsifying the results. To this end, we reproduced the analysis for data of a state composed by distinguishable photons. This distinction is performed by the time delay between photons on each mode caused by the high birrefringence of the source. For

the data utilized in the preceding sections, this delay was compensated in the setup itself. However, we considered interesting to utilize this states to test the reliability of the method.

The negativities in the quasiprobabilities disappear in this case, as it can be seen in Fig. 2.9. This behavior accounts for the classical nature of the state, which results in an statistical mixture of just two stationary states, $\hat{\rho} \approx \frac{1}{2}(|q_5, q_5\rangle\langle q_5, q_5| + |q_6, q_6\rangle\langle q_6, q_6|)$. Thus, we conclude that this method does not falsify signatures of photon entanglement and polarization nonclassicality.

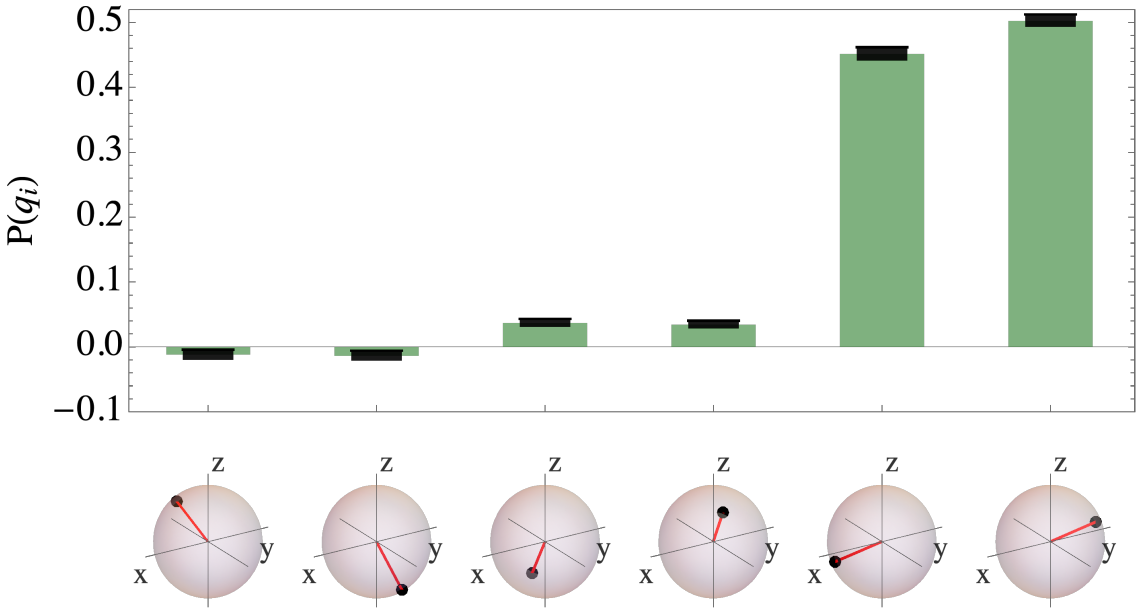


Figure 2.9: Quasiprobabilities for the distinguishable state (green bars) as a function of the corresponding stationary qubit states. The black bars represent the estimated error ($\pm 5\sigma$).

### 2.2.5 Concluding remarks

The first experimental characterization of QPQC has been reported in this section. The outcome is in strong agreement with the theoretical values. Moreover, the basis-independence shown by the experiment coincides exactly with the theoretical conclusions.

This invariance under polarization basis transformations is a highly desirable but also reasonable characteristic of the QPQC if we recall its character as nonclassicality marker. Since the SU(2) transformation does not alter the polarization structure of the state, it should not modify its classical or quantum character.

## 2.3 Coherence for signal estimation

Among the areas of application of coherence we can include quantum metrology as one of the most fruitful. The effort to perform the most careful observation of physical phenomena, from temperatures [150], to gravitational waves [151], meets the limits imposed by the bizarre consequences of quantum physics, involving basic issues such as state reduction and uncertainty relations [153, 154].

In the usual framework of quantum metrology, the value of a parameter is encoded on a probe state by means of a unitary transformation. Then, a measure is performed to estimate the parameter with a certain sensitivity. The central point of quantum metrology is to choose the best combination of these elements in order to obtain the highest accuracy possible. For example, certain quantum correlations of the probe state enhance this sensitivity [156, 157], as well as nonlinear transformations [158]. In this context, the resource theories consider the practical scenario in which there are clear practical limits to the amount of energy, entanglement or coherence available, and try to optimize the performance of the experiment taking this restriction into account [159, 160].

Despite this direct application, there is not a clear theory regarding the relationship between the concept of coherence and the accuracy of the measurement process [161, 162], being sometimes even contradictory [163, 164]. We elaborate on this relation without assuming previous definitions of resolution or coherence. This leads to a new definition of quantum coherence specifically defined in the measuring context. The corresponding quantifier of coherence is related to resolution by a rather simple equality that fills the gap between the resource of coherence and the accuracy of the signal estimation process.

### 2.3.1 Estimation process

The concept of measurement can be attributed to uncountable very different processes that humans do to obtain knowledge about several magnitudes. From measures of reflectance [165] to trans-Neptunian objects [166], the process behind the information acquisition is quite universal: a known state is modified as a function of the property that we want to measure and then the variation is compared to the original state.

This is the paradigmatic signal detection process and it defines our metrological scheme. Specifically, the signal to be detected, $\lambda$, shifts the pointer $\rho_0$ against a "ticked ruler" in which the ticks or references are actually repeated shifts of a basic mark [167, 168]. The pointer is a quantum state with density matrix $\rho_0$, which is transformed by a signal-dependent unitary transformation $D(\lambda) = \exp(-i\lambda G)$ to

$$\rho(\lambda) = D(\lambda)\rho_0 D^\dagger(\lambda), \tag{2.44}$$

where $G$ is the infinitesimal generator of the transformation, satisfying $D^\dagger(\lambda) = D(-\lambda)$. $G$ also defines the basis of the space by means of its eigenvectors.

The ticked ruler is the measurement performed, to be called $M$, described by a POVM $\Pi(m)$, where the outcomes $m$ represent the ticks of the ruler. We consider that the ticks are spaced by the effect of the same transformation that shifts the probe, this is

$$\Pi(m) = D(m)\Pi_0 D^\dagger(m), \quad \Pi_0 = \Pi(0), \tag{2.45}$$

for the same unitary transformation $D(m)$ above, and $\Pi_0$ is the origin for the ticks. In consequence, $M$ becomes a covariant measurement [93]. For definiteness and without loss of generality, we will assume that $m$ is a continuous variable extending from $-\infty$ to $\infty$. Thus, the measurement is actually the ordered collection of all the effects caused by the range of values of interest for the signal. Detection then consists on inferring the signal from the observation of the effect. This is how meters, clocks, thermometers, voltmeters, etcetera, are actually constructed.

This structure guarantees that we can derive general conclusions about the performance of the detection process independent both of the signal value $\lambda$ and of the outcome $m$ obtained. This is clearly manifest by computing the statistics of the measurement $p(m|\lambda)$ conditioned to the signal value $\lambda$,

$$p(m|\lambda) = \mathrm{tr}\left[\rho(\lambda)\Pi(m)\right], \tag{2.46}$$

which explicitly in terms of the value of $\rho_0$ and $\Pi_0$ leads to

$$p(m|\lambda) = \mathrm{tr}\left[\rho_0 D(m-\lambda)\Pi_0 D^\dagger(m-\lambda)\right] = p(m-\lambda). \tag{2.47}$$

This conditional probability, along with the prior information we might have about $\lambda$ if any, are the building blocks of a complete signal-estimation process, for example within a Bayesian formulation [93, 169, 170].

As a result, the conditional probability depends on $\lambda$ and $m$ just through the combination $m-\lambda$, this is $p(m|\lambda) = p(\mu)$, where $\mu = m - \lambda$. We can refer to this property as shift invariance [200, 201]. The performance of the whole detection process is fixed by the coherence properties of $\rho_0$ and $\Pi_0$ with respect to $G$, as we shall see clearly below.

There are some conditions that $\Pi_0$ must satisfy so that the shift-invariant ruler $\Pi(m) = D(m)\Pi_0 D^\dagger(m)$ provides a legitimate measurement. Given the form of $\Pi(m)$, the necessary and sufficient conditions for the reality, nonnegativity, and normalization of $p(\mu)$ are $\Pi_0^\dagger = \Pi_0$, $\Pi_0 \geq 0$ and

$$\int dm \Pi(m) = I. \tag{2.48}$$

The consequences of the latter condition are particularly interesting talking about coherence. To see this, we twice insert in the first relation in Eq. (2.45) the resolution of the identity in terms of the eigenvectors of $G$, $G|g\rangle = g|g\rangle$, assumed to be continuous and nondegenerate without loss of generality. Then, using $D(m)|g\rangle = \exp(-igm)|g\rangle$ we get

$$I = \int dm \int dg \int dg' e^{im(g-g')} |g\rangle\langle g|\Pi_0|g'\rangle\langle g'| = 2\pi \int dg |g\rangle\langle g|\Pi_0|g\rangle\langle g|, \tag{2.49}$$

which implies

$$\langle g|\Pi_0|g\rangle = \frac{1}{2\pi}, \tag{2.50}$$

which further implies

$$\langle g|\Pi(m)|g\rangle = \frac{1}{2\pi}. \tag{2.51}$$

Consequently, the only elements of $\Pi(m)$ with non-trivial meaning are its non-diagonal components in the basis of the generator of the transformation, which can be regarded as the physical origin of coherence [202, 203, 204].

### 2.3.2 Mutual coherence function

A new definition of coherence arises quite naturally after some algebra in the statistics of the measurement outcomes in Eq. (2.47). The statistics $p(\mu)$ can be related to $\rho_0$, $\Pi_0$, and $G$ by a suitable choice of the $|g\rangle$ basis for the trace, together with another use of the resolution of the identity

$$p(\mu) = \int dg \int dg' \langle g|\rho_0|g'\rangle\langle g'|\Pi_0|g\rangle e^{i(g-g')\mu}. \tag{2.52}$$

By means of the change of variables $g' = g + \tau$, it can also be expressed as

$$p(\mu) = \int d\tau \Gamma(\tau) e^{-i\tau\mu}, \tag{2.53}$$

where $\Gamma(\tau)$ is the *quantum mutual coherence function*, introduced as [205]

$$\Gamma(\tau) = \int' dg \langle g|\rho_0|g+\tau\rangle\langle g+\tau|\Pi_0|g\rangle. \tag{2.54}$$

The prime on the integral denotes the fact that the range of integration over $g$ may depend on $\tau$. It is remarkable how $\Gamma(\tau)$ merges, in a symmetrical way, the quantum coherences in the $|g\rangle$ basis of both elements involved in the measurement process: the detection apparatus, $\langle g+\tau|\Pi_0|g\rangle$, and the probe state, $\langle g|\rho_0|g+\tau\rangle$. This is why it is also labeled as *process coherence function*.

This definition allows interpreting Eqs. (2.53) and (2.54) as a quantum version of a celebrated theorem of classical coherence optics, the Wiener-Kintchine theorem [19, 206], already recalled in Sec. 2.1.1, which establishes that the spectral density and

the coherence function are a Fourier transform pair. In the current case, the statistics $p(\mu)$ plays the role of the spectral density $I(\nu)$ while $\Gamma(\tau)$ plays the role of the coherence function with the same name. This analysis can be extended to the discrete variable domain since Eqs. (2.53) and (2.54) also holds in the case in which $m$ and/or $g$ are discrete variables, which can be seen by replacing where necessary integrals by sums in the process from Eq. (2.47) to Eq. (2.52). In that context, the conditions for $\Pi(m)$ being a POVM are still positivity and resolution of the identity, however, in the discrete case, the latter does not translate into Eq. (2.51) and the equivalent will depend on the ranges of $m$ and $g$.

The next objective is to establish a link between the width of the spectral-like function, $p(\mu)$, and the width of the coherence-like function, $\Gamma(\tau)$. To this end, we follow the approach presented in Ref. [100] as particularly simple and insightful. Thus, regarding the measure of coherence, we utilize the coherence time introduced by Mandel [207, 208]

$$\tau_c = \int d\tau |\gamma(\tau)|^2, \tag{2.55}$$

where $\gamma(\tau)$ is the corresponding degree of coherence as the properly normalized coherence function $\gamma(\tau) = \Gamma(\tau)/\Gamma(0) = 2\pi\Gamma(\tau)$. Along, concerning resolution, we define the signal uncertainty $\Delta\lambda$ as

$$\Delta\lambda = \frac{1}{2\sqrt{\pi}\int d\mu p^2(\mu)}, \tag{2.56}$$

which takes account of the fluctuations of the measurement statistics, $p(\mu) = p(m|\lambda)$. This is a measure of uncertainty in terms of Rényi entropy [209, 210, 211]. By applying the Parseval's relation to Eq. (2.53), the resolution-coherence relation is obtained,

$$\tau_c \Delta\lambda = \sqrt{\pi}. \tag{2.57}$$

Therefore, the signal uncertainty is inversely proportional to the coherence time as a rather clear and meaningful relation between signal resolution and coherence. This relation does not establish a bound but an exact value of the resolution, determined once and for all when we choose the measurement and the probe, depending just on their coherence properties with respect to the generator of the transformation and independent of the signal value.

### 2.3.3 Gaussian model

Computing this relation in the particular case of Gaussian form for probe and ruler allows a fruitful connection with other metrological quantifiers, such as the Cramér-Rao bound [212, 213]. In addition, Gaussian elements are easily implementable in practice, so it is considered a suitable test of relation in Eq. (2.57).

The probe is assumed to be in a pure state $\rho_0 = |\psi_0\rangle\langle\psi_0|$ so that

$$\psi_0(g) = \langle g|\psi_0\rangle = \frac{1}{\sqrt{\Delta G\sqrt{2\pi}}} e^{-(g-g_0)^2\Delta^2\Phi_S} e^{ik_0 g}, \tag{2.58}$$

being $\Phi$ the observable conjugate to $G$ and its variance

$$\Delta^2\Phi_l = 1/(4\Delta^2 G), \tag{2.59}$$

where $l = S, M$ represents the evaluation of the variances in the probe or ruler states respectively. Likewise, the ruler elements are of the form

$$\langle g|\Pi_0|g'\rangle = \frac{1}{2\pi} e^{-\Delta^2\Phi_M (g-g')^2/2}. \tag{2.60}$$

$\Delta^2\Phi_M$ and $\Delta^2\Phi_S$ are parameters characterizing the measurement and probe, respectively, that essentially represent the uncertainty in the observable $\Phi$ conjugate to the generator $G$ that imprints the signal value on the probe. In these terms, they actually encode the coherence of the probe and measurement in the basis corresponding to the degree of freedom expressed by $G$. Taking this into account, the mutual coherence function becomes

$$\Gamma(\tau) = \frac{1}{2\pi} e^{-(\Delta^2\Phi_M + \Delta^2\Phi_S)\tau^2/2}, \tag{2.61}$$

leading to a coherence time

$$\tau_c^2 = \frac{\pi}{\Delta^2\Phi_M + \Delta^2\Phi_S}, \tag{2.62}$$

and, finally, a resolution

$$\Delta^2\lambda = \Delta^2\Phi_M + \Delta^2\Phi_S. \tag{2.63}$$

This value can be compared with the Cramér–Rao bound, which establishes the maximum resolution achievable as the inverse of the Fisher information. Both coincide exactly in the case of the Gaussian model (2.63),

$$\Delta^2_{CR}\lambda = \frac{1}{F} = \Delta^2\lambda, \tag{2.64}$$

where $F$ is the Fisher information,

$$F = \int_{-\infty}^{\infty} dm \left[\frac{\partial p(m|\lambda)}{\partial\lambda}\right]^2 \frac{1}{p(m|\lambda)}, \tag{2.65}$$

being $p(m|\lambda)$ the statistics of the measure in Eq. (2.47).

#### 2.3.3.1 Examples: position and phase shifts

This general analysis is made concrete for specific transformations, *i.e.* for specific generators, $G$. It fits perfectly well to signal detection based on the Heisenberg-Weyl

group of transformations. As the physical system at hand, we can consider the one-dimensional motion of a particle with position- and momentum-like operators satisfying the commutation relation $[X, P] = i$. This is equally valid for a one-mode field where $X$ and $P$ are the field quadratures. Let it be $G = P$ so we are detecting position shifts leading to a signal uncertainty

$$\Delta^2\lambda = \Delta^2 X_M + \Delta^2 X_S. \tag{2.66}$$

We can see that the larger the squeezing, the larger the coherence and the larger the resolution. This is a natural and intuitive relation, that nevertheless is not satisfied by other approaches to coherence where larger squeezing means lesser coherence as shown for example in Ref. [161].

The second example considered, $G = N$, is one of the most useful and studied generators in quantum metrology which includes as the prime physical example time delays emerging from free evolution of single mode fields [214]. The phase shift generated by $N$ is the fundamental basis of interference, which is the most powerful signal detector as demonstrated in the detection of gravitational waves [215].

As it can be inferred from the Cramér-Rao bound, in order to be metrologically useful the probe states experiencing phase shifts must have a very large mean number of photons. This requirement allows the useful approximation of the discrete spectrum of $N$ by a continuous one, extending its domain to the entire real axis as a good simplifying assumption. Similarly regarding the domain of variation for the phase.

There is a readily physical picture of the observable $\Phi$ conjugate to $G$, this is the quantum-optical phase observable [216, 217]. For a single-mode field, $\Phi$ can be well described by the positive operator valued measure

$$\Pi(\phi) = |\phi\rangle\langle\phi|, \quad |\phi\rangle = \frac{1}{\sqrt{2\pi}} \sum_{n=0}^{\infty} e^{-i\phi n}|n\rangle, \tag{2.67}$$

where $|\phi\rangle$ are the nonorthogonal, unnormalized Susskind-Glogower phase states being $|n\rangle$ the photon-number states as the eigenstates of the number operator $N$, this is $N|n\rangle = n|n\rangle$. This represents the case of an ideal phase measurement. To deal with a more realistic one we just replace $\Pi_0$ by

$$\Pi_0 = \frac{1}{\sqrt{2\pi}\Delta\Phi_M} \int d\phi e^{-\phi^2/(2\Delta^2\Phi_M)}|\phi\rangle\langle\phi|, \tag{2.68}$$

leading, in the number representation, to

$$\langle n|\Pi|n'\rangle = \frac{1}{2\pi} e^{-\Delta^2\Phi_M(n-n')^2/2}, \tag{2.69}$$

with the above-mentioned approximation for the variable $n$. Furthermore, the probe

considered is a Gaussian in the number basis described as

$$\psi_0(n) \simeq \frac{1}{\sqrt{\Delta N\sqrt{2\pi}}} e^{-(n-\bar{n})^2/(4\Delta N^2)}. \tag{2.70}$$

All these elements together exactly reproduce the results of the general analysis in Eq. (2.63) being $\Delta^2\Phi_S = 1/(4\Delta^2 N)$.

### 2.3.4 Non-Gaussian scenario

Finally, the performance of the quantum Wiener-Kintchine theorem was examined outside the Gaussian scenario by applying it to a non-Gaussian probe state together with a ruler with non-Gaussian elements. To this end, the measurement considered was an ideal phase measurement (2.67) over a normalizable version of the Susskind-Glogower phase states as the probe,

$$|\xi\rangle = \sqrt{1-|\xi|^2}\sum_{n=0}^{\infty}\xi^n|n\rangle, \tag{2.71}$$

specially interesting when $|\xi| \to 1$. The signal uncertainty obtained by computing (2.56) is

$$\Delta^2\lambda = \pi\left(\frac{1-|\xi|^2}{1+|\xi|^2}\right)^2. \tag{2.72}$$

We compare this result with that arising from calculating the Fisher information, which conduces to

$$\Delta^2_{CR}\lambda = \frac{(1-|\xi|^2)^2}{2|\xi|^2}. \tag{2.73}$$

It is worth noting the similarity between the findings of both methods, regarding that we are working with $|\xi| \to 1$. In this limit, the quantum Wiener–Kintchine theorem gives a resolution of $\pi(1-|\xi|^2)^2$ and the Cramér–Rao bound of $2(1-|\xi|^2)^2$. This example shows the generality of the theorem introduced beyond the more developed Gaussian model.

Moreover, this example provides a case where the introduced theory is not compatible with previous approaches. This is when $|\xi| \to 0$ where we have $\Delta^2_{CR}\lambda \to \infty$ while $\Delta^2\lambda \to \pi$, being this last limit more physically sound as far as for $G = N$ we have that $\lambda$ is a phase and therefore bound to a $2\pi$ interval. This constraint is not respected by the Cramér–Rao bound because of its local nature.

### 2.3.5 Concluding remarks

Despite the clear classical parallels, this coherence-resolution theory is of quantum nature by construction, and so it embraces the classical-limit scenario, where the probe is a convex combination of Glauber coherent states with resolution bounded by the standard quantum limit, as well as situations where quantumness allows to improve

resolution beyond the classical limit via a Heisenberg-limit scaling. These different scenarios, from classical to fully quantum, are actually implicit in the choices of $\Pi_0$, $\rho_0$, and $G$, which will manifest for example in Eq. (2.64) through the scaling of the Fisher information with the mean energy.

The developed formalism of quantum coherence focused on quantum metrology shows compelling evidence that coherence is the true resource behind the resolution. The relation between both magnitudes involves all the elements of the estimation process, with the apparatus and probe contributing equally to the detection performance. This is a valuable result that acknowledges that the system and detector are inextricably mingled to produce the observed statistics, as required by basic quantum postulates such as the very Born's rule. This also agrees with the results on nonclassicality reported in Chapter 1. In addition, the value of the resolution does not depend on the value of the signal and its accuracy has been confirmed by the more common Fisher information analysis. This approach can be extended to transformations with two parameters by studying the transformations represented by phase-space displacements [218].

## 2.4 Study of coherence based on the Hellinger-like distance

In this section we analyze the performance of coherence regarding the principal transformations in quantum optics, say, displacement, squeezing and beam splitters.

The central quantifier of coherence utilized is the quantifier based on the *l1-norm*, which is a well-established coherence monotone in spaces of finite dimension, [103, 129]. The first objective is to express this quantifier as a distance-based quantifier, within the spirit of the equivalence between the *l2-norm* and the Hilbert-Schmidt distance [129]. To this end, we introduce a Hellinger-like distance, differing from the proper Hellinger distance in the definition of the square root. It is utilized to redefine the quantifier and compute it for the examples considered more relevant. In the following section, the need for this definition becomes clear.

### 2.4.1 The definition

The usual workspace regarding coherence analyses is an abstract Hilbert space of finite dimension, $N$. Due to the dependence on the basis, we also set an abstract basis, $\{|j\rangle\}_{j=1,\ldots,N}$, assuming it orthogonal and representing some physical variable or observable $J$ [219].

To determine the distance between two density matrices, a suitable version of the Hellinger distance [220] was introduced [221]. Therefore, given two matrices $\rho_1$ and $\rho_2$,

the Hellinger-like distance between them is defined as

$$d_H(\rho_1, \rho_2) = \sqrt{\mathrm{tr}[(\sqrt{\rho_1} - \sqrt{\rho_2})^2]}, \tag{2.74}$$

where the square root represents, in this case, the square root of the individual elements,

$$\langle i|\sqrt{\rho}|j\rangle = \sqrt{\langle i|\rho|j\rangle}. \tag{2.75}$$

where $\rho_{i,j} = \langle i|\rho|j\rangle$ are the matrix elements of $\rho$ in the basis $\{|j\rangle\}$. In accordance with the usual definition of coherence in this context, we set the quantifier as the distance to the closest incoherent state, $\rho_d$, meaning by incoherent the states diagonal in the reference basis. In such a way $\rho_d$ turns out to be the diagonal part of $\rho$ in the same basis [219],

$$\rho_d = \sum_{j=1}^{N} \rho_{j,j}|j\rangle\langle j|, \tag{2.76}$$

Thus, the quantifier of coherence based on the Hellinger-like distance is defined as [221]

$$\mathcal{C}_H = [d_H(\rho, \rho_d)]^2 = \mathrm{tr}\left[(\sqrt{\rho} - \sqrt{\rho_d})^2\right], \tag{2.77}$$

reproducing the definition of coherence established in Ref. [202] based on the genuine Hellinger distance. As it has been introduced, $\mathcal{C}_H$ can be reduced to the quantifier of coherence based on the *l1-norm* [103],

$$\mathcal{C}_H = \mathcal{C}_{l_1} = \sum_{j\neq k}^{N} |\rho_{j,k}|. \tag{2.78}$$

This formulation highlights the role of the nondiagonal terms as the essential elements determining the coherence of a state in a basis. The latter expression can be disclosed in terms of the *purity* of the square root density matrix

$$\mathcal{C}_H = \mathrm{tr}\left(\sqrt{\rho}^2\right) - 1. \tag{2.79}$$

When $\rho$ is a pure state, it becomes

$$\mathcal{C}_H = \left(\sum_{j=1}^{N} \sqrt{p_j}\right)^2 - 1, \tag{2.80}$$

being $p_j = \rho_{j,j}$ the statistics of the basis variable $J$, which makes it specially advantageous.

Finally, it is necessary to remark that the *l1-norm* of coherence in Eq. (2.78) can be applied to Hilbert spaces of infinite dimension [221, 222]. As long as the basis we chose is a numerable, orthonormal one, say $\{|n\rangle\}_{n=0,1,\ldots\infty}$, so Eqs. (2.78) and (2.80) are equivalent by replacing $N$ by $\infty$ in the summations.

### 2.4.2 Computing coherence

In the following, the coherence of some representative states is reported with the purpose of analyzing its performance regarding the fundamental elements of each state.

#### 2.4.2.1 Phase-like states

By optimizing Eq. (2.80) it can be seen that the states making $\mathcal{C}_H$ maximum are those with constant distribution in $p_j$, this is $\rho_{ii} = 1/N$. In that case, the maximum value obtained for pure states is

$$\mathcal{C}_{H_{\max}} = N - 1, \tag{2.81}$$

which is actually the maximum value that any state, pure or mixed, may display [223, 224]. The pure states with this probability distribution are

$$|\Phi\rangle = \frac{1}{\sqrt{N}} \sum_{j=1}^{N} e^{i\phi_j} |j\rangle, \tag{2.82}$$

where $\phi_j$ are arbitrary phases, so these states can be regarded as finite-dimensional phase states after a suitable phase adjustment [225]. Note that this measure of coherence is not bounded when $N$ is allowed to vary, this is, it is possible to enhance the coherence by adding photons. This is quite counterintuitive regarding classical optics where the degree of coherence does not depend on the intensity.

#### 2.4.2.2 Rotated number states

Looking for a finite-dimensional space where implementing this measure of coherence we focus on the Hilbert space of a two-mode field,

$$\mathcal{H}_1 \otimes \mathcal{H}_2 = \bigoplus_{NT=0}^{\infty} \mathcal{H}_{NT}. \tag{2.83}$$

Each subspace of a fixed total number of photons, $\mathcal{H}_{NT}$, is a subspace of finite dimension $NT + 1$, isomorphic to a spin space with $S = NT/2$. $\mathcal{H}_{NT}$ can be expanded by the basis $\{|j\rangle\}$ with

$$|j\rangle = |j, NT - j\rangle, \quad j \in 0, ..., NT. \tag{2.84}$$

These two modes represent in our analysis the two output modes of a lossless beam splitter (BS). As a brief reminder, the BS can be parameterized by a $2 \times 2$ matrix linking the input $a_{1,2}$ and output $b_{1,2}$ complex-amplitude operators

$$\begin{pmatrix} b_1 \\ b_2 \end{pmatrix} = \begin{pmatrix} \tau_1 & \rho_2 \\ \rho_1 & \tau_2 \end{pmatrix} \begin{pmatrix} a_1 \\ a_2 \end{pmatrix}, \tag{2.85}$$

where $\tau_{1,2}$, $\rho_{1,2}$ are the corresponding complex transmission and reflection coefficients, see Fig. 2.10. Since we are working with a lossless beam splitter the transformation

matrix is unitary [179], implying

$$|\tau_1| = |\tau_2| = \cos\theta, \quad |\rho_1| = |\rho_2| = \sin\theta, \tag{2.86}$$

where $\theta \in [0, \pi/2]$ express the balance between transmission and reflection, and

$$\delta_{\rho_1} - \delta_{\tau_2} + \delta_{\rho_2} - \delta_{\tau_1} = \pi, \tag{2.87}$$

where $\delta$ are the phases of the corresponding coefficients.

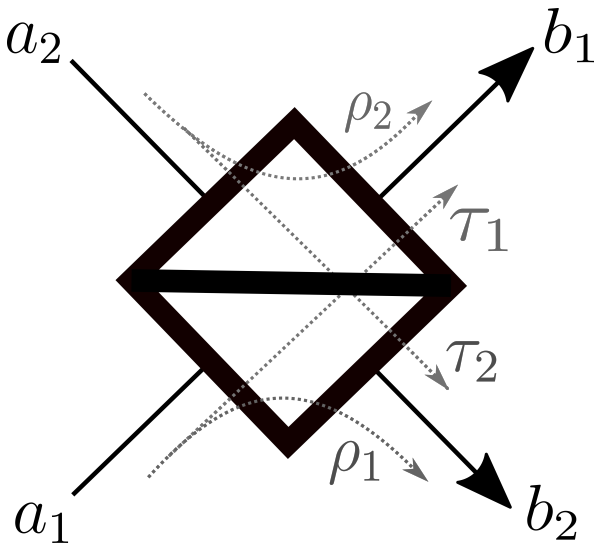


Figure 2.10: Scheme of a beam splitter specifying the transmission and reflection coefficients $\tau_{1,2}$, $\rho_{1,2}$.

Regarding the quantum resource theories of coherence, beam splitters are not free operations since these elements are able to enhance the coherence previously present in the system [178, 221] as long as we are on the number basis. In this context, we study how much $\mathcal{C}_H$ is able to generate a beam splitter when we consider input incoherent pure states, this is when a different number state illuminates each one of the BS input ports

$$|n_1\rangle_{a_1} \otimes |n_2\rangle_{a_2} = |n_1, n_2\rangle = \frac{1}{\sqrt{n_1! n_2!}} a_1^{\dagger n_1} a_2^{\dagger n_2} |0, 0\rangle. \tag{2.88}$$

The output state can be readily obtained in the number basis by inverting the input-output relation (2.85) to express the input modes $a_{1,2}$ in terms of the output modes $b_{1,2}$, and translating the result to Eq. (2.88) to get

$$|\text{out}\rangle_{n_1,n_2} = \frac{1}{\sqrt{n_1! n_2!}} \left(e^{i\delta_{\tau_1}} \cos\theta b_1^\dagger + e^{i\delta_{\rho_2}} \sin\theta b_2^\dagger\right)^{n_1} \left(e^{i\delta_{\rho_2}} \sin\theta b_1^\dagger + e^{i\delta_{\tau_2}} \cos\theta b_2^\dagger\right)^{n_2} |0, 0\rangle. \tag{2.89}$$

The subscripts $n_1$ and $n_2$ express the initial distribution of the total number of photons between the input modes. These states include as particular cases the $SU(2)$ coherent states, for $n_1 = 0$ or $n_2 = 0$ [89], and the Holland-Burnett states of maximum $SU(2)$

squeezing and maximum interferometric resolution, the twin photon states, for $n_1 = n_2$ [180].

Another description of the output state can be performed by using the decomposition formulas for the $SU(2)$ Lie algebras [181]. After some simple algebra, and using relation (2.87), we get that the output state (2.89) in the basis $\{|j\rangle\}$ in Eq. (2.84) becomes

$$|\text{out}\rangle_{n_1,n_2} = \sum_{j=0}^{n_1+n_2} c_j |j\rangle, \tag{2.90}$$

where

$$c_j = \sqrt{n_1! n_2! j! (n_1+n_2-j)!}\, e^{ij(\delta_{\tau_1}-\delta_{\rho_2})} \times \sum_{k=\max(0,j-n_2)}^{n_1} \frac{(-1)^k \cos^{n_2+2k-j}\theta \sin^{n_1-2k+j}\theta}{(n_1-k)!k!(n_2+k-j)!(j-k)!}.$$

The aim is to analyze the coherence of the output states in Eqs. (2.90) and (2.91) as a function of the three variables involved say, the BS transmitance/reflectance ratio, $\theta$; the relation between the number of photons on each input mode, $n_1/n_2$; and the total number of photons involved, $NT = n_1 + n_2$. $\mathcal{C}_H$ was computedd by using Eq. (2.80) with $p_j = |c_j|^2$.

We started by setting the total energy of the subspace and studying the $\mathcal{C}_H$ dependence on $\theta$ and the different input configuratons. The result can be express analytically for one and two photons cases:

When $n_1 + n_2 = 1$, the qubit example, there is just a single configuration of $n_1/n_2$, the input number state $|1,0\rangle$. The corresponding output state, omitting irrelevant relative phases, is the split photon $|\text{out}\rangle_{1,0} = \cos\theta|1,0\rangle + \sin\theta|0,1\rangle$. The maximum value of coherence, $\mathcal{C}_H = 1$, occurs for a 50 % beam splitter, $\theta = \pi/4$. In this situation the output state becomes a phase-like state $|\phi\rangle$ in Eq. (2.82).

For $n_1 + n_2 = 2$ there are only two meaningful output states,

$$|\text{out}\rangle_{2,0} = \cos^2\theta|2,0\rangle + \sqrt{2}\sin\theta\cos\theta|1,1\rangle + \sin^2\theta|0,2\rangle \tag{2.91}$$

and

$$|\text{out}\rangle_{1,1} = \sqrt{2}\sin\theta\cos\theta|2,0\rangle + \left(\cos^2\theta - \sin^2\theta\right)|1,1\rangle - \sqrt{2}\sin\theta\cos\theta|0,2\rangle. \tag{2.92}$$

It is noticeable that the SU(2) squeezed state $|\text{out}\rangle_{1,1}$ can paradoxically get larger coherence than the SU(2) coherent state $|\text{out}\rangle_{2,0}$, see Fig. 2.11, which betrays its name a bit. Moreover, this maximum value, $\mathcal{C}_H = 2$, holds for an unbalanced BS, with $\theta$

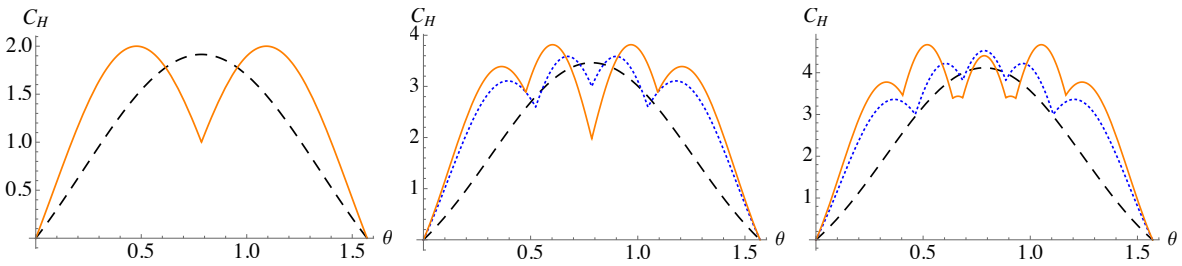


(a) $|\text{out}\rangle_{2,0}$ black- dashed line and $|\text{out}\rangle_{1,1}$ orange-solid line.

(b) $|\text{out}\rangle_{4,0}$ black-dashed line, $|\text{out}\rangle_{3,1}$ blue-dotted line and $|\text{out}\rangle_{2,2}$ orange-solid line.

(c) $|\text{out}\rangle_{5,0}$ black-dashed line, $|\text{out}\rangle_{4,1}$ blue-dotted line, and $|\text{out}\rangle_{3,2}$ orange-solid line.

Figure 2.11: $\mathcal{C}_H$ for different rotated number states as a function of the beam splitter's parameter $\theta$.

satisfying $\tan(2\theta) = \pm\sqrt{2}$. For these optimum beam splitters we have that the output states are once more phase-like states (2.82),

$$|\text{out}\rangle_{1,1} = \frac{1}{\sqrt{3}}\left(\pm|2,0\rangle + |1,1\rangle \mp |0,2\rangle\right). \tag{2.93}$$

A numerical computation is presented for a larger number of photons, confirming the main results already presented. For the case of an even number of photons, that is $n_1 + n_2 = 2k$ for integer $k$, we focused on $NT = 4$. The twin-photon states obtain the larger coherence $|\text{out}\rangle_{2,2}$ emerging from an unbalanced beam splitter, as shown in Fig. 2.11b. Such states $|\text{out}\rangle_{2,2}$ are no longer phase-like states, so the absolute maximum coherence $\mathcal{C}_{H_{max}} = n_1 + n_2$ is not reached. Nevertheless, for the optimum case, there is a symmetric split of the photons between the output modes, this is

$$|\langle n_1, n_2|\text{out}\rangle_{2,2}| = |\langle n_2, n_1|\text{out}\rangle_{2,2}|, \tag{2.94}$$

which results specially useful in relation to the sensitivity of two-path interferometers [185].

Regarding an odd number of photons, the situation is quite similar, with maximum coherence obtained for input states closer to the equal splitting of the photons between input modes, say $|k+1, k\rangle$, and unbalanced beam splitter $\theta \neq \pi/4$, as shown in Fig. 2.11c for five photons.

The maximum value of coherence in Eq. (2.81) is not always achievable, regardless of the beam splitter parameters. This is because the outcome states become more and more distant to the phase-like states (2.82). This idea led us to an alternative expression for the coherence as a function of the maximum overlap between the system state $|\psi\rangle$, assumed pure, and the phase-like states $|\boldsymbol{\phi}\rangle$ when $\boldsymbol{\phi}$ is varied

$$\mathcal{C}_H = (\sqrt{n_1 + n_2 + 1}\,\max_{\boldsymbol{\phi}}\langle\boldsymbol{\phi}|\psi\rangle)^2 - 1. \tag{2.95}$$

In Fig. 2.12, it is represented the maximum coherence achievable on each subspace along with the maximum available $\mathcal{C}_H = n_1 + n_2$.

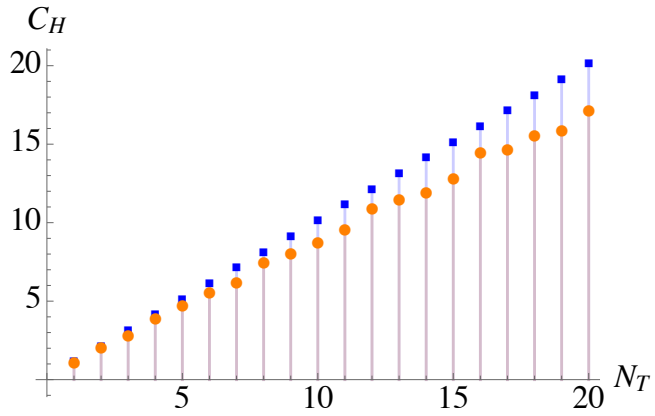


Figure 2.12: Maximum coherence achieved for incoming two mode number states on each subspace as a function of the total number of photons involved $N_T$ (orange circles). In blue squares maximum coherence available on each subspace, $\mathcal{C}_{H_{\max}} = n_1 + n_2$.

#### 2.4.2.3 Phase states

As we have remarked, the definition of coherence introduced in Eq. (2.77) can be extended to Hilbert spaces of infinite dimension [221]. As the basis we chose a numerable one, say $\{|n\rangle\}_{n=0,1,\ldots\infty}$, so Eqs. (2.78) and (2.80) are equivalent by replacing $N$ by $\infty$ in the summations.

To begin with the examples of states in infinite dimensional spaces, we consider the normalizable Susskind-Glogower phase states [226]

$$|\xi\rangle = \sqrt{1-|\xi|^2}\sum_{n=0}^{\infty}\xi^n|n\rangle. \tag{2.96}$$

The coherence becomes

$$\mathcal{C}_H = \frac{2|\xi|}{1-|\xi|}, \tag{2.97}$$

which, in terms of the mean number of photons

$$|\xi|^2 = \frac{\bar{n}}{1+\bar{n}}, \tag{2.98}$$

results

$$\mathcal{C}_H = 2\left(\bar{n} + \sqrt{\bar{n}+\bar{n}^2}\right). \tag{2.99}$$

Therefore $\mathcal{C}_H \to \infty$ as $|\bar{n}| \to \infty$, becoming proportional to the mean number of photons when it is large enough, $\bar{n} \gg 1$.

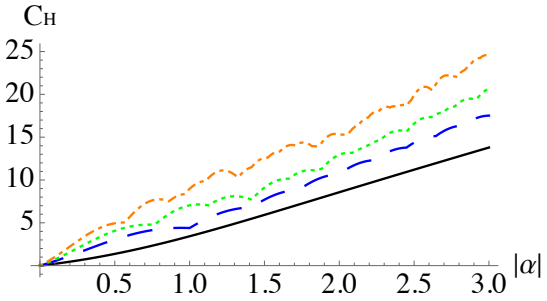


(a) Solid-black line for $n_0 = 0$, this is a coherent state, $n_0 = 1$ in dashed-blue line, $n_0 = 2$ in dotted-green line, and $n_0 = 4$ in dash-dotted orange line.

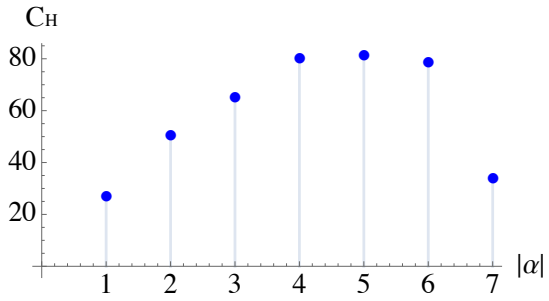


(b) Fixed mean number of photons, $\bar{n} = 49$.

Figure 2.13: Coherence for displaced number states $D(\alpha)|n_0\rangle$ as a function of the displacement $|\alpha|$.

#### 2.4.2.4 Displaced-number states

We study the coherence generated by the displacement operator $D(\alpha) = \exp(\alpha a^\dagger - \alpha^* a)$ in the case of displaced number states, $D(\alpha)|n_0\rangle$. These include the coherent states as the displacement of the vacuum state, $n = 0$. The general trend of $\mathcal{C}_H$ in the number basis is to grow with the displacement $|\alpha|$. More specifically, in Fig. 2.13a it is shown how this growth is quite irregular and softer for the coherent state, $n_0 = 0$. This trend implies, again, the more energetic, the more coherent. However we can see that the grown in coherence is higher for high number states, so, we can ask which is the optimum distribution of energy between $n_0$ and $|\alpha|$. As it can be seen In Fig. 2.13b, actually exist such optimum distribution of enegy between the initial number state and the displacement. It is shown the case of $\bar{n} = 49$, but the behaviour is reproduced by all the cases studied.

#### 2.4.2.5 Squeezed coherent states

We analyzed the coherence generated by the displacement operator and by the squeeze operator, $S(\xi) = \exp[\frac{1}{2}(\xi^* a^2 - \xi a^{\dagger 2})]$, in pure displaced squeezed vacuum states,

$$D(\alpha)S(\xi)|0\rangle, \tag{2.100}$$

where the coherent amplitude is $R = |\alpha|$, and the squeezing parameter $r = |\xi|$. As in the previous cases, coherence increases with the energy, in this particular case it turns out that both relevant parameters, the displacement $R$ and the compression $r$ make $\mathcal{C}_H$ increase. This implies that squeezed coherent states are more coherent than coherent states. For low energetic states, say low compression and low displacement, the squeezed state almost remain incoherent, see Fig. 2.14. In that regime, $\mathcal{C}_H$ is almost

linear. It is when both parameters are relatively high that the growth in coherence is significant.

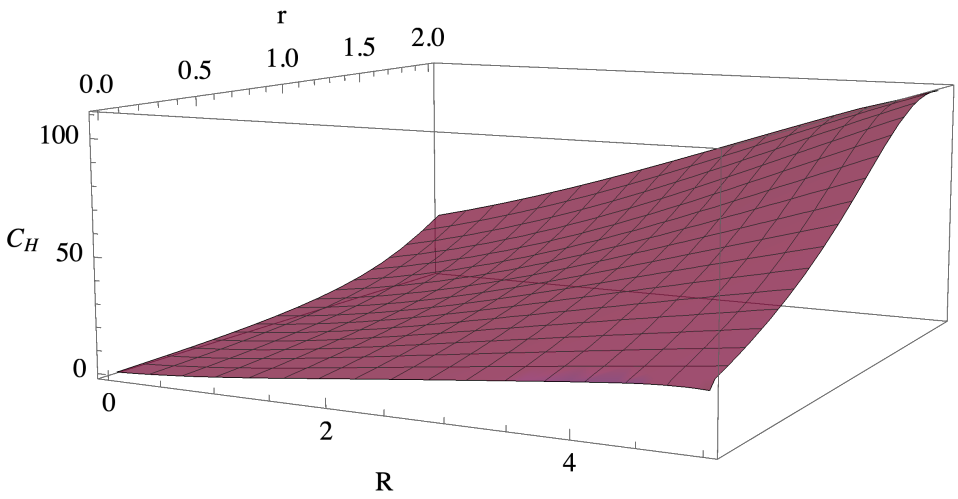


Figure 2.14: $\mathcal{C}_H$ of squeezed coherent states as a function of displacement, R, and compression, r.

We proceed to fix the total energy of the state, the mean photon number of photons, looking for the optimum distribution of energy between squeezing and displacement. In Fig. 2.15 is shown an optimum configuration when around 30% of the energy is utilized to squeeze the state. This case implies a huge improvement in the total amount of coherence. Such optimum distribution corresponds to the limit in which squeezed coherent states become suitable approximations of normalized phase states, as states that tend to be optimum regarding metrology [227].

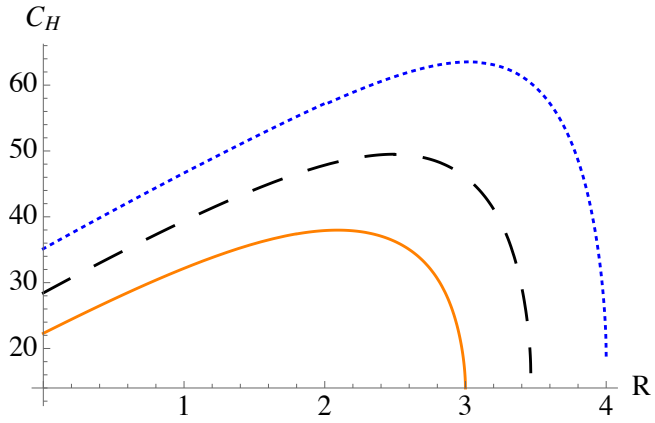


Figure 2.15: $\mathcal{C}_H$ of squeezed coherent states as a function of displacement, $R$, for a given mean number of photons, $\bar{n} = 9$ orange solid line, $\bar{n} = 12$ black dashed line and $\bar{n} = 16$ blue dotted line.

#### 2.4.2.6 Coherent state throughout a beam splitter

As in the case of incoherent incoming states, we can analyze the coherence gained by the coherent states when passing thought a beam splitter. The BS considered is the one introduced in Eqs. (2.85)-(2.87). The input in terms of the vacuum state is

$$|\alpha_1, \alpha_2\rangle = e^{\alpha_1 a_1^\dagger - \alpha_1^* a_1} e^{\alpha_2 a_2^\dagger - \alpha_2^* a_2} |0,0\rangle, \tag{2.101}$$

and the output becomes

$$|\text{out}\rangle_{\alpha_1\alpha_2} = |e^{i\tau_1}\alpha_1 \cos\theta + e^{i\rho_1}\alpha_2 \sin\theta, e^{i\tau_2}\alpha_2 \cos\theta + e^{i\rho_2}\alpha_1 \sin\theta\rangle, \tag{2.102}$$

where the kets represent the product of Glauber coherent states.

In Fig. 2.16, it can be seen how the optimum beam splitter configuration is the one that allows a symmetrical output, with the same mean number of photons on each mode. The minimum coherence corresponds to the single-mode coherent state $\mathcal{C}_{H_{min}} = \mathcal{C}_H(|\alpha = \sqrt{\bar{N}}\rangle)$, and it appears when the output state is of the form $|\alpha = \sqrt{\bar{N}}, 0\rangle$.

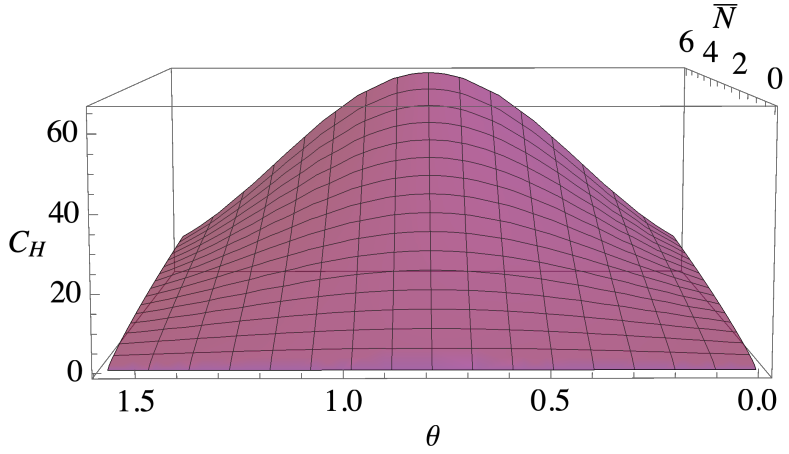


Figure 2.16: $\mathcal{C}_H$ for the state $|\text{out}\rangle_{\sqrt{\bar{N}},0}$ as a function of the parameter $\theta$.

Since the coherence of the initial state is not zero, we can compute the $\mathcal{C}_H$ gained when it goes through the beam splitter as a function of the incoming amount of coherence. To this end we define the gain in coherence as the following percentage

$$\mathcal{G} = \frac{\mathcal{C}_{H_{\max}}}{\mathcal{C}_{H_{\text{input}}}} \times 100. \tag{2.103}$$

for an input state of the form of a single-mode coherent state $|\alpha = \sqrt{\bar{N}}, 0\rangle$.
Different definitions of this concept have been developed [186]. In Fig. 2.17, it can be seen how $\mathcal{G}$ increases with the initial coherence of the single-mode state but the growth ratio is smaller for high $\bar{N}$.

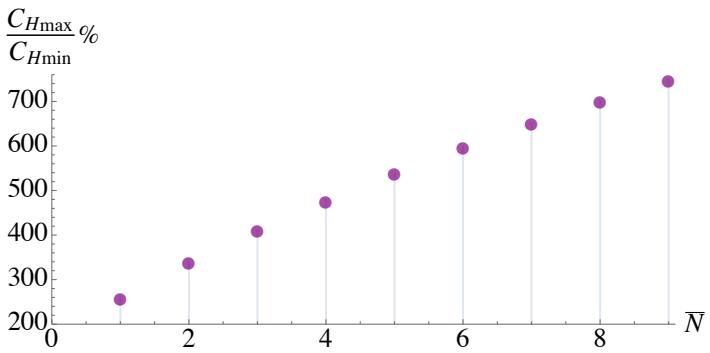


Figure 2.17: Percentage of coherence gained as a function of the mean number of photons in the coherent input case.

#### 2.4.2.7 Two-mode squeezed vacuum throughout a beam splitter

As a particular application of the previously presented twin photons state, $|n,n\rangle$, we consider the situation when each port of the BS is illuminated by one mode of the two-mode squeezed vacuum state (TMSV),

$$|\xi\rangle = \sqrt{1-\xi^2}\sum_{n=0}^{\infty}\xi^n|n,n\rangle, \tag{2.104}$$

where $\xi$ is the squeezing parameter, considered real without loss of generality. Therefore, we can calculate its coherence as

$$\mathcal{C}_H = \left[\sum_{n=0}^{\infty}\left(\sqrt{1-\xi^2}\xi^n\sum_{j=0}^{n}|c_j|\right)\right]^2 - 1, \tag{2.105}$$

where $c_j$ is in Eq. (2.91). The minimum coherence, at $\theta = 0$, becomes [221]

$$\mathcal{C}_H = \frac{2\xi}{1-\xi} \tag{2.106}$$

and the optimum transformation regarding coherence is not a balanced beam splitter, reasonable if we recall the performance of each element of the state $|n,n\rangle$ (figures 2.11a and 2.11b).

To compare the performance of the beam splitter when illuminated by the coherent state and by the TMSV, we consider two different situations: a) both presenting the identical incoming amount of coherence, $\mathcal{C}_{H_{input}}$, and b) both having the same mean number of photons, $\bar{n}$.

When the two states have the same incoming coherence, e. g. $C_{H_{min}} = 3.0$, the corresponding coherent state before the beam splitter is $|\alpha_1 = \sqrt{0.83}, 0\rangle$. The coherence gain caused by the coherent state transformation is $\mathcal{G}_\alpha \approx 245\%$. However, the gain produced by the beam splitter considering a TMSV is remarkably higher, $\mathcal{G}_\xi \approx 364\%$.

Regarding states with the same energy, the mean number of photons of the TMSV

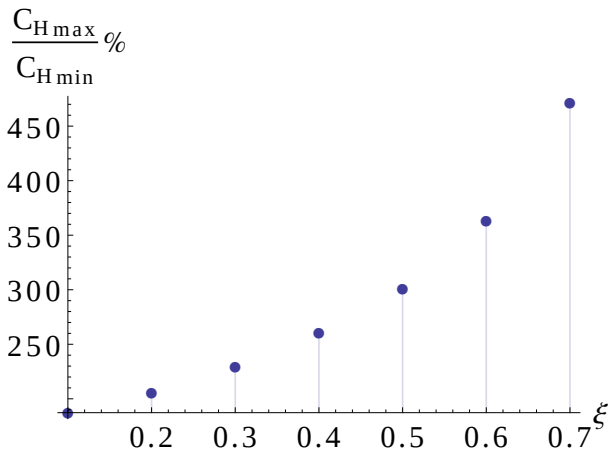


Figure 2.18: Gain in coherence for the TMSV as a function of the squeezing parameter $\xi$ [189].

is $\bar{n} = \frac{\xi^2}{1-\xi^2}$, thus, for $\bar{n} = 1$ the gain in coherence caused by the beam splitter is $\mathcal{G}_\xi \approx 470\%$ whereas for a coherent state with $|\alpha|^2 = 1$ it is $\mathcal{G}_\alpha \approx 260\%$. Therefore, the TMSV is able to obtain more coherence since the squeezing allows it to resemble the constant statistics of phase-like states better.

### 2.4.3 Concluding remarks

Along the process, a detailed study of the role of beam splitters as quantum coherence makers was performed. The optimum configuration of the reflectance-transmittance parameters was obtained for several incoming states. In all cases, the best combination is such that the outcoming state is as similar as possible to the phase-like states. This is also the conclusion in infinite dimensional spaces. For instance, talking about the optimum relation between squeezing and displacement in squeezed coherent states, the more coherent states are closer to the normalized phase states.

The intuition given by classical optics of using balanced beam splitters to generate maximum coherence is just a particular case, of course, valid for incoming coherent states. Nevertheless, we have seen this is not universal and shown a general description of the optimum configuration. This asymmetry has been recently evidenced in the metrological domain [187, 188], where unbalanced beam splitters make optimal the phase sensitivity of a Mach-Zehnder interferometer.

The results on beam splitters can be qualitatively reproduced by using the relative entropy of coherence [189], whose form adapted to pure states is

$$\mathcal{C}_S = -\sum_j |c_j|^2 \ln |c_j|^2. \tag{2.107}$$

To illustrate this resemblance we reproduced in the finite-dimensional space the rotated number states cases shown in Fig. 2.11. The relative entropy of coherence

shows the same trend, as can be seen in Fig. 2.19. Nevertheless, the behaviour around the symmetrical beam splitter is considerably smoother.

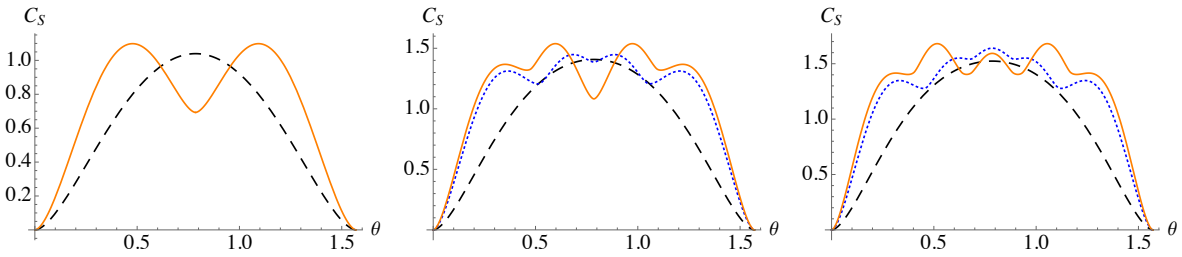


(a) $|\text{out}\rangle_{2,0}$ (black, dashed line) and $|\text{out}\rangle_{1,1}$ (orange, solid line) as functions of the beam splitter's parameter $\theta$.

(b) $|\text{out}\rangle_{4,0}$ (black, dashed line), $|\text{out}\rangle_{3,1}$ (blue, dotted line), and $|\text{out}\rangle_{2,2}$ (orange, solid line)

(c) $|\text{out}\rangle_{5,0}$ (black,dashed line), $|\text{out}\rangle_{4,1}$ (blue, dotted line), and $|\text{out}\rangle_{3,2}$ (orange, solid line).

Figure 2.19: $\mathcal{C}_S$ for different rotated number states.

The maximum value $C_S^{\max} = -\ln\left[(n_1 + n_2 + 1)^{-1}\right]$ is again achieved by the phase-like states in Eq. (2.82) and the difference with the maximum coherence achievable for the rotated number states also increases as the dimension does.

## 2.5 Approach to nonclassicality based on coherence

As it has been presented in the introduction of this chapter, the concept of coherence is understood as the distinctive quantum feature. Therefore, it seems consistent to assume it as the basis of any approach to understanding and quantifying nonclassical behavior.

In this spirit, we establish a measure of nonclassicality arising as the maximum coherence that a field state can display by varying the basis [221], in the same understanding that the degree of polarization is the maximum coherence between two filed modes that can be reached under unitary transformations [190, 191, 192]. The quantitative relation between quantum coherence and nonclassicality ensures that nonzero coherence concerning at least one basis is a necessary and sufficient condition for finding some nonclassicality in any basis, which agrees with previous reports of nonclassicality in the absence of coherence [128]. As a result, the new measure does not hide nonclassical features due to an unsuitable choice of the basis at hand.

### 2.5.1 Quantifier of nonclassicality based on Hellinger-like distance

We introduced a distance-based quantifier of nonclassicality, in line with previous measures of quantumness of this kind present in quantum resource theories [159, 122]. The

distance employed is the Hellinger-like distance introduced in Eqs. (2.74) and (2.75). We utilized the same abstract Hilbert space of finite dimension $N$, and the same orthogonal basis $\{|j\rangle\}_{j=1,\ldots,N}$. As the state of reference, the *classical state*, we considered the maximally mixed state, $I/N$. It has been shown how the normalized identity is actually the only classical state under very generic conditions, [26, 228]. Supporting this concept emerges the approach to nonclassicality in Ref. [229]. These two ideas merge, recalling that the identity is the only matrix that is diagonal in all bases, so the classical state will always remain classical.

The resulting quantifier of nonclassicality is

$$\mathcal{NC}_H = [d_H(\rho, I/N)]^2 = \mathrm{tr}\left[\left(\sqrt{\rho} - I/\sqrt{N}\right)^2\right]. \tag{2.108}$$

The minimum $\mathcal{NC}_{H_{min}} = 0$ clearly holds if and only if $\rho = I/N$ as the only classical state. On the contrary, the maximum value $\mathcal{NC}_{H_{max}} = N - 1$ occurs again for pure phase-like states for which $\rho_{ii} = 1/N$.

#### 2.5.1.1 Pythagorean equation

In order to establish the relation between $\mathcal{C}_H$ and $\mathcal{NC}_H$ it was necessary to quantify the fluctuations on the statistics of the observable defined by the basis, $J$. The probabilities for the potential outcomes are the diagonal terms of the density matrix, $p_j = \rho_{j,j}$. We refer to the quantity accounting for the fluctuations on this statistics as *certainty* [230], in contrast to the concept of uncertainty. This name reflects the relationship between this magnitude and the insight we have about the value of the observable. Accordingly, it has to be maximum when the probability distribution has only one therm, $p_j = \delta_{j,j_0}$, so the value of the observable is known. On the other hand, the certainty has to be minimum when the probabilities are equally distributed, this is $p_j = 1/N$, so that all the possible values are equally probable. Since these fluctuations are absolutely independent of the coherence terms of $\rho$, we define the certainty quantifier as the Hellinger-like distance between $\rho_d$ and $I/N$:

$$\mathcal{S}_H(\rho) = [d_H(\rho_d, I/N)]^2 = \mathrm{tr}\left[\left(\sqrt{\rho_d} - I/\sqrt{N}\right)^2\right] = 2\left(1 - \frac{1}{\sqrt{N}}\sum_{j=1}^{N}\sqrt{\rho_{jj}}\right). \tag{2.109}$$

This implies that $I/N$ is the incoherent state with larger indetermination on the statistics of $J$ in the coherence basis $\{|j\rangle\}$. Therefore, the larger the distance between $\rho_d$ and $I/N$, the lesser the fluctuations. As it was required, the maximum $\mathcal{S}_H(\rho) = 2(1 - 1/\sqrt{N})$ holds for the elements of the coherence basis $\{|j\rangle\}$ while the minimum $\mathcal{S}_{H_{min}} = 0$ occurs when $\rho_{ii} = 1/N$. After the last equality in Eq. (2.109), $\mathcal{S}_H$ can be

related to the Rènyi entropy of order 1/2 [231]

$$H_{1/2} = 2\ln\left(\sum_{k=1}^{n} p_k^{1/2}\right), \tag{2.110}$$

reinforcing its interpretation of certainty.

Given the previous definitions of coherence (2.77), nonclassicality (2.108), and certainty (2.109), we can establish the following relation between these magnitudes

$$\mathcal{NC}_H = \mathcal{C}_H + \mathcal{S}_H. \tag{2.111}$$

One way of proving this statement is by inserting the closest incoherent state $\rho_d$ in the definition of the quantifier of nonclassicality in Eq. (2.108),

$$\mathcal{NC}_H = \mathrm{tr}\left[\left(\sqrt{\rho} - \sqrt{\rho_d} + \sqrt{\rho_d} - I/\sqrt{N}\right)^2\right] = \tag{2.112}$$

$$\mathrm{tr}\left[\left(\sqrt{\rho} - \sqrt{\rho_d}\right)^2\right] + \mathrm{tr}\left[\left(\sqrt{\rho_d} - I/\sqrt{N}\right)^2\right] + 2\mathrm{tr}\left[\left(\sqrt{\rho} - \sqrt{\rho_d}\right)\left(\sqrt{\rho_d} - I/\sqrt{N}\right)\right].$$

As long as $\mathrm{tr}\left(\sqrt{\rho}\sqrt{\rho_d}\right) = \mathrm{tr}\left(\sqrt{\rho_d}^2\right)$, it can be readily shown that

$$\mathrm{tr}\left[\left(\sqrt{\rho} - \sqrt{\rho_d}\right)\left(\sqrt{\rho_d} - I/\sqrt{N}\right)\right] = 0. \tag{2.113}$$

Therefore, we obtain the following Pythagoras-like equation in a finite-dimensional space:

$$\mathrm{tr}\left[\left(\sqrt{\rho} - I/\sqrt{N}\right)^2\right] = \mathrm{tr}\left[\left(\sqrt{\rho} - \sqrt{\rho_d}\right)^2\right] + \mathrm{tr}\left[\left(\sqrt{\rho_d} - I/\sqrt{N}\right)^2\right]. \blacksquare \tag{2.114}$$

The central point of this version of the Pythagorean theorem is the interpretation that we can make of each term in the underlying right-triangle structure. This may be illustrated with the aid of Fig. 2.20, where $\rho_d$ is the orthogonal projection of $\rho$ into the incoherent hyperplane. The hypotenuse represents nonclassicality while coherence and certainty are the cathetus since both are orthogonal as shown in (2.113). Arbitrary Pythagorean theorems may be obtained by replacing $I/N$ with any incoherent state so that the orthogonality (2.113) will still hold. However, the choice $I/N$ is clearly the one where hypotenuse and cathetus have the clearest physical meaning. As already studied in Refs. [232], Eqs (2.111) and (2.114) can be regarded as a duality relation between coherence and certainty in the coherence basis.

Accordingly to this relation any difference between coherence and nonclassicality relies on the properties of the basis, represented by $\mathcal{S}_H$. In particular, the maximum value achievable for $\mathcal{C}_H$ by varying the basis is bounded by $\mathcal{NC}_H$, in agreement with [233]. It is worth remembering here the dependence of $\mathcal{NC}_H$ on the basis. This seems to disagree with a more classical-like perspective where the distance to $I/N$ has been

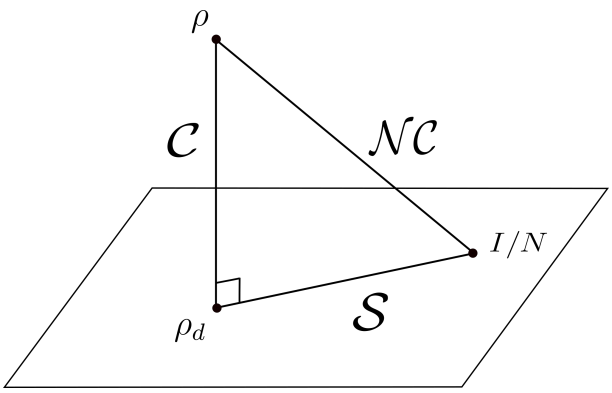


Figure 2.20: Right-triangle formed by $\rho$, $\rho_d$ and $I/N$ in finite dimensional spaces. Image from [221].

proposed as an intrinsic or absolute form of coherence, independent of any reference observable [148, 222, 234, 235]. However, even if the value of $\mathcal{NC}_H$ may change, we can consider this measure of nonclassicality as an on/off the detector in the following sense: Recalling that the normalized identity is invariant under basis transformations, $\mathcal{NC}_H$ is zero if and only if the state is $I/N$, and therefore any state presenting some nonclassicality in one basis will present certain nonclasicality in all bases. The maximum $\mathcal{NC}_H$ by varying the basis is $\mathcal{NC}_{H_{\max}} = N - 1$, coincides with the maximum coherence (2.81), as it can be seen in the following example for the qubit state.

These implications are connected to draw the following conclusion of Eq. (2.111): Nonzero coherence in at least one basis is a necessary and sufficient condition for nonzero nonclassicality in all bases. In consequence, $\mathcal{C}_H = 0$ in one basis does not imply $\mathcal{NC}_H = 0$ since the state may have coherence in a different basis in agreement with [128].

#### 2.5.1.2 The qubit

As an example, we computed the coherence, nonclassicality, and certainty of an element in a two-dimensional Hilbert space, $N = 2$. In quantum optics the most famous qubit is a single photon split into two field modes, representing typically two orthogonal polarization states or the two inner paths in a two-beam interferometer. A qubit can be fully characterized in the density matrix formalism by a three-dimensional real vector $\boldsymbol{s} = \{s_x, s_y, s_z\}$, which represents the position of the state in the Bloch sphere, Eq. (1.13). Recalling that the elements of $\boldsymbol{\sigma}$ are the Pauli matrices, the qubit density matrix becomes

$$\rho = \frac{1}{2}\left(1 + \boldsymbol{s}\cdot\boldsymbol{\sigma}\right). \tag{2.115}$$

Choosing the basis $\{|j\rangle\}_{j=-1,1}$ as the eigenvectors of the $\sigma_z$ matrix we arrive to

$$\mathcal{C}_H = \sqrt{s_x^2 + s_y^2}, \quad \mathcal{S}_H = 2 - \sqrt{1+s_z} - \sqrt{1-s_z}, \tag{2.116}$$

and naturally $\mathcal{NC}_H = \mathcal{C}_H + \mathcal{S}_H$.

Next, we vary the basis in order to obtain both maximum and minimum values of the coherence and see what happens to the nonclassicality. For fixed $|\boldsymbol{s}|$, this is for fixed purity, the maximum of both magnitudes $\mathcal{C}_H$ and $\mathcal{NC}_H$ holds when the projection of the Bloch vector along the direction of the basis vanishes, this is $s_z = 0$, giving

$$\mathcal{C}_{H_{\max}} = \mathcal{NC}_H = |\boldsymbol{s}|. \tag{2.117}$$

This example shows again the deep equivalence between maximum coherence, nonclassicality, and purity that has been already put forward in works such as [236], [237], and also in Ref. [233] identifying purity as the maximal coherence which is achievable by unitary operations, purity being the most elementary resource for quantum information processing.

Now we compute those quantities in the basis in which $\rho$ is diagonal where the corresponding Bloch vector reads $s'_z = |\boldsymbol{s}|$, $s'_x = s'_y = 0$. In this basis null coherence is found

$$\mathcal{C}_{H_{min}} = 0, \tag{2.118}$$

and yet nonclassicality is not canceled for any state different from the maximally mixed

$$\mathcal{NC}_H = 2 - \sqrt{1 + |\boldsymbol{s}|} - \sqrt{1 - |\boldsymbol{s}|}. \tag{2.119}$$

### 2.5.2 Infinite dimension: numerable basis

We have already seen that the *l1-norm* of coherence can be extended to infinite-dimensional Hilbert spaces with a numerable basis in Sec. 2.4. Now we seek to extend the whole analysis, including the definition of nonclassicality and the Pythagorean relation between magnitudes.

The major difficulty of this translation is the lack of a physical state proportional to the identity in infinite dimensional spaces. This would imply the absence of classical states in such spaces. As an alternative, we replace the identity with an incoherent physical state $\rho_T$ as close as desired to having a uniform distribution in the coherence basis, once more we choose a numerable, orthonormal basis, $\{|n\rangle\}_{n=0,1,\ldots\infty}$. Such a state approaches to be a maximally mixed state, which can be the case of a thermal-like state in the limit when the analog of the temperature, $T$, tends to infinity

$$\rho_T = (1 - \xi) \sum_{n=0}^{\infty} \xi^n |n\rangle\langle n| \quad \text{with } \xi \to 1. \tag{2.120}$$

Thus, the definition of $\mathcal{NC}_H$ in Eq. (2.108) translates into the corresponding limit of $\mathrm{tr}\left[\left(\sqrt{\rho} - \sqrt{\rho_T}\right)^2\right]$.

The key point to transcribe the Pythagorean theorem in Eq. (2.111) is to prove the orthogonality condition,

$$\mathrm{tr}\left[\left(\sqrt{\rho}-\sqrt{\rho_d}\right)\left(\sqrt{\rho_d}-\sqrt{\rho_T}\right)\right]=0, \tag{2.121}$$

where $\rho_d$ has the same meaning as the diagonal part of $\rho$. The above relation holds for any $\rho_T$ diagonal in the number basis since it ensures $\mathrm{tr}\left(\sqrt{\rho}\sqrt{\rho_T}\right)=\mathrm{tr}\left(\sqrt{\rho_T}\sqrt{\rho_d}\right)$, and by construction $\mathrm{tr}\left(\sqrt{\rho}\sqrt{\rho_d}\right)=\mathrm{tr}\left(\sqrt{\rho_d}\sqrt{\rho_d}\right)$. Therefore, we readily get this new version of the Pythagorean theorem in an infinite-dimension Hilbert space:

$$\mathrm{tr}\left[\left(\sqrt{\rho}-\sqrt{\rho_T}\right)^2\right]=\mathrm{tr}\left[\left(\sqrt{\rho}-\sqrt{\rho_d}\right)^2\right]+\mathrm{tr}\left[\left(\sqrt{\rho_d}-\sqrt{\rho_T}\right)^2\right], \tag{2.122}$$

which has the same interpretation as in the finite-dimension scenario as far as we consider the above-mentioned limit $\xi\to 1$ for $\rho_T$. A particular consequence of this limit can be seen by computing the certainty

$$\mathcal{S}_H=\mathrm{tr}\left(\sqrt{\rho_d}^2\right)+\mathrm{tr}\left(\sqrt{\rho_T}^2\right)-2\mathrm{tr}\left(\sqrt{\rho_d}\sqrt{\rho}_T\right)=2-2\sqrt{1-\xi}\sum_{n=0}^{\infty}\xi^{n/2}\sqrt{p_n}, \tag{2.123}$$

where $p_n=\langle n|\rho|n\rangle$. In order to proceed with the $\xi\to 1$ limit we shall consider that the following quantity is finite, which is the key ingredient of coherence as shown in Eq. (2.80),

$$\sum_{n=0}^{\infty}\sqrt{p_n}<\infty, \tag{2.124}$$

which is actually satisfied by all the cases to be considered in this work. In such a case, $\lim_{\xi\to 1}\left[\mathrm{tr}\left(\sqrt{\rho_d}\sqrt{\rho_T}\right)\right]=0$, so that

$$\mathcal{NC}_H=C_H+2. \tag{2.125}$$

Roughly speaking, $\mathcal{S}_H=2$ means that as $\xi\to 1$ the distance between the *physical* state $\rho_d$ and $\rho_T$ tends to be maximum. Therefore, in this infinite-dimensional case, in the conditions specified above, coherence equals nonclassicality. This conclusion has an inevitable implication: not only squeezed states but also coherent states are nonclassical states. Moreover, the more energetic, the more nonclassical.

### 2.5.3 Extension to continuous basis

The next step in the analysis is to extend it to continuous bases both in finite and infinite-dimensional spaces. By a suitable generalization we consider as coherence with respect to any basis $|\phi\rangle$, even if it is continuous or nonorthogonal, the contribution of the nondiagonal terms of $\rho$, this is an expression of the form

$$\mathcal{C}_H=\mathrm{tr}\left(\sqrt{\rho}^2\right)-1. \tag{2.126}$$

as in Eq. (2.79). The question to be addressed is whether such a definition of coherence has the same geometrical meaning we have found above in the case of discrete orthogonal basis. To discuss this we focus on whether there is a proper definition of $\rho_d$ as the incoherent state closest to $\rho$. First we consider normalized nonorthogonal bases in finite-dimensional spaces, and then orthogonal nonnormalized ones in infinite-dimensional spaces.

#### 2.5.3.1 Finite-dimensional case

For definiteness, we use as the basis the set of finite-dimensional phase states

$$|\phi\rangle = \frac{1}{\sqrt{N}} \sum_{j=1}^{N} e^{ij\phi} |j\rangle, \tag{2.127}$$

where the $|j\rangle$ refers to some orthonormal number-like basis. In this scenario we may consider

$$\rho_d = \frac{N}{2\pi} \int d\phi \langle\phi|\rho|\phi\rangle |\phi\rangle\langle\phi| \tag{2.128}$$

to be the "incoherent" state of reference, no longer diagonal in the $|\phi\rangle$ basis, as we will see in the following. In addition, it is necessary to determine the meaning of the square root suitable for this continuous framework. Thus we define $\sqrt{\rho_d}$ as

$$\sqrt{\rho_d} = \sqrt{\frac{N}{2\pi}} \int d\phi \sqrt{\langle\phi|\rho|\phi\rangle} |\phi\rangle\langle\phi|, \tag{2.129}$$

so that coherence is null if $\rho = \rho_d$. After these definitions it turns out that $\mathrm{tr}\left[(\sqrt{\rho} - \sqrt{\rho_d})^2\right]$ does not reproduce Eq. (2.126) nor the Pythagorean theorem holds due to

$$\mathrm{tr}\left[(\sqrt{\rho} - \sqrt{\rho_d})\left(\sqrt{\rho_d} - I/\sqrt{N}\right)\right] \neq 0, \tag{2.130}$$

as it can be easily checked for example for the qubit state. We may ascribe this behavior to the lack of orthogonality of the phase states

$$\langle\phi'|\phi\rangle = \frac{1}{N} \sum_{j}^{N} e^{ij(\phi-\phi')} \neq 0, \tag{2.131}$$

which makes $\rho_d$ nondiagonal, meaning $\langle\phi'|\rho_d|\phi\rangle \neq 0$ for $\phi \neq \phi'$.

#### 2.5.3.2 Infinite-dimensional case

Next, we consider the case of a continuous basis made of unnormalizable orthogonal states, such as the quadrature or position eigenstates $|x\rangle$, where $x$ can take any real value. Although they are orthogonal in the sense of $\langle x'|x\rangle = \delta(x - x')$ there is the difficulty of $|x\rangle$ being no normalizable. As a consequence, any state diagonal in the

$|x\rangle$ basis is not physical since its trace diverges, in particular this is the case of the following definition of $\rho_d$:

$$\rho_d = \int_{-\infty}^{\infty} dx \langle x|\rho|x\rangle |x\rangle\langle x|. \tag{2.132}$$

As we have done above with $\rho_T$ we can try to avoid this via some kind of regularization in some proper limit. To this end, we replace $|x\rangle$ by some normalizable states, for example, displaced-squeezed states $|x\rangle_\Delta$ with quadrature-coordinate wave function

$$\langle x'|x\rangle_\Delta = \frac{1}{(2\pi\Delta^2)^{1/4}} \exp\left[-\frac{(x-x')^2}{4\Delta^2}\right] \tag{2.133}$$

so that we can define a truly unit-trace $\rho_d$ as

$$\rho_d = \int_{-\infty}^{\infty} dx \langle x|\rho|x\rangle |x\rangle_{\Delta\Delta}\langle x| \tag{2.134}$$

in the spirit of considering afterwards the limit $\Delta \to 0$. Through this definition it can be easily seen that $\lim_{\Delta\to 0}\langle x|\rho_d|x\rangle = \langle x|\rho|x\rangle$, simply by invoking the Gaussian representation of the Dirac delta function $\lim_{\Delta\to 0} |\langle x'|x\rangle_\Delta|^2 = \delta(x-x')$.

Now we introduce $\sqrt{\rho}$ and $\sqrt{\rho_d}$ respectively as

$$\sqrt{\rho} = \int_{-\infty}^{\infty}\int_{-\infty}^{\infty} dx' dx \sqrt{\langle x|\rho|x'\rangle}|x\rangle\langle x'| \text{ and } \sqrt{\rho_d} = \int_{-\infty}^{\infty} dx \sqrt{\langle x|\rho|x\rangle}|x\rangle_{\Delta\Delta}\langle x|, \tag{2.135}$$

and try to recover an expression for the coherence in Eq. (2.126) as a suitable distance, this is in terms of $\mathrm{tr}\left[\left(\sqrt{\rho}-\sqrt{\rho_d}\right)^2\right]$.

On the one hand $\mathrm{tr}\left(\sqrt{\rho_d}^2\right)$ vanish in the limit $\Delta \to 0$ since

$$\lim_{\Delta\to 0} |{}_\Delta\langle x'|x\rangle_\Delta|^2 = 2\sqrt{\pi}\Delta\delta(x-x') \to 0. \tag{2.136}$$

On the other hand, in this limit we may consider $\langle x'|x\rangle_\Delta$ and ${}_\Delta\langle x|x''\rangle$ so peaked functions hence they act as Dirac delta functions

$$\lim_{\Delta\to 0}\langle x'|x\rangle_{\Delta\Delta}\langle x|x''\rangle = 2\sqrt{2\pi}\Delta\delta(x-x')\delta(x-x''), \tag{2.137}$$

implying $\mathrm{tr}\left(\sqrt{\rho_d}\sqrt{\rho}\right) \to 2\sqrt{2\pi}\Delta\int dx\langle x|\rho|x\rangle \to 0$. All this together it emerges

$$\lim_{\Delta\to 0} \mathrm{tr}\left[\left(\sqrt{\rho}-\sqrt{\rho_d}\right)^2\right] = \mathrm{tr}\left(\sqrt{\rho}^2\right), \tag{2.138}$$

and therefore Eq. (2.126) and the geometrical meaning of coherence are essentially recovered. In view of this we wonder whether Pythagorean relation in Eq. (2.122) also holds. Note that in this continuous case $\sqrt{\rho_T}$ is defined as

$$\sqrt{\rho_T} = \int dx \sqrt{\langle x|\rho_T|x\rangle}|x\rangle_{\Delta\Delta}\langle x|. \tag{2.139}$$

This question is answered in the affirmative since the limits $\lim_{\Delta\to 0} |{}_\Delta\langle x'|x\rangle_\Delta|^2$ in Eq.

(2.136) and $\lim_{\Delta\to 0}\langle x'|x\rangle_{\Delta\Delta}\langle x|x''\rangle$ in Eq. (2.137) ensure the orthogonality condition $\mathrm{tr}\left[\left(\sqrt{\rho}-\sqrt{\rho_d}\right)\left(\sqrt{\rho_d}-\sqrt{\rho_T}\right)\right]=0$ in Eq. (2.121).

From this analysis of infinite dimensional spaces and continuous bases can be concluded that the critical point is the definition of incoherent states, and, therefore, any basis or space that does not allow a diagonal states implies a more sophisticated treatment of the idea of coherence.

### 2.5.4 Different distance-based quantifiers of nonclassicality

The importance of the preceding study lies in two main ideas, namely, the interpretation of the distance to the identity as nonclassicality, Eq. (2.108), and the relation between this concept and coherence by means of the basis properties, Eq. (2.111). Similarly to the large number of quantifiers of coherence suggested in the literature, alternative quantifiers of nonclassicality based on different distances can be considered. The question then is whether their relation to coherence remains, so comparable phytagorean equations could be obtained.

As a first example we appealed to the Hilbert-Schmidt distance,

$$d_H(\rho_1,\rho_2)=\sqrt{\mathrm{tr}[(\rho_1-\rho_2)^2]}, \tag{2.140}$$

which has already been used to quantify other magnitudes in addition to coherence [193]. By means of Eq. (2.140) it can be defined equivalent quantifiers of coherence $\mathcal{C}_{HS}=\mathrm{tr}\left[(\rho-\rho_d)^2\right]$, nonclassicality $\mathcal{NC}_{HS}=\mathrm{tr}\left[(\rho-I/N)^2\right]$ and certainty $\mathcal{S}_{HS}=\mathrm{tr}\left[(\rho_d-I/N)^2\right]$, and the corresponding Pythagoras-like equation is recovered in finite dimensional spaces:

$$\mathrm{tr}\left[(\rho-I/N)^2\right]=\mathrm{tr}\left[(\rho-\rho_d)^2\right]+\mathrm{tr}\left[(\rho_d-I/N)^2\right]. \tag{2.141}$$

We presented the study of this distance in more depth in Ref. [221]. Despite of its widespread use, Braumgratz *et al.* demonstrated in Ref. [103] that the measure of coherence based on the Hilbert-Schmid distance does not satisfy the strong monotonocity condition. This requirement reflects the intuition that coherence should not increase on average under incoherent measurements if there is the possibility of filtering the final state according to the measurement outcomes. The importance of this condition is imposed by the experimental availability of sub-selection [103, 194] and it is also applied in other resource theories [122, 193].

Alternatively we can recall the quantum relative entropy between two density matrices

$$S(\rho_1\|\rho_2)=\mathrm{tr}\left[\rho_1\log_2\rho_1\right]-\mathrm{tr}\left[\rho_1\log_2\rho_2\right]. \tag{2.142}$$

The corresponding relative entropy of coherence is considered a legitimate measurement of coherence satisfying all the requirements imposed so far [129]

$$\mathcal{C}_S = S(\rho\|\rho_d) = S(\rho_d) - S(\rho), \tag{2.143}$$

where $S(\rho) = -\text{tr}(\rho \log_2 \rho)$ is the Von Newmann entropy. Another remarkable property of this measure is that it has been demonstrated to quantify a direct physical resource, the maximum coherence distillable from a mixed state. For all these reasons, we considered it appropriate to test our model of nonclassicality. To this end, we defined the corresponding quantifiers,

$$\mathcal{NC}_S = S(\rho\|I/N), \quad \mathcal{S}_S = S(\rho_d\|I/N), \tag{2.144}$$

along with the well-established relative entropy of coherence introduced in Eq. (2.143). It is simple to obtain a Pythagorean-like relation if we consider the following simplification for the relative entropy in Eq. (2.142)

$$S(\rho\|\sigma) = S(\rho_d) - S(\rho) + S(\rho_d\|\sigma), \tag{2.145}$$

applicable when one of the states is diagonal. Thus, in finite dimensional spaces and discrete basis the relative entropy gives rise to Nonclassicality as the sum of coherence and certainty due to

$$S(\rho\|I/N) = S(\rho\|\rho_d) + S(\rho_d\|I/N). \tag{2.146}$$

The extension to infinite dimensional spaces and discrete basis takes advantage of the same definition of classical state introduced in Eq. (2.120). Since $\rho_T$ is diagonal, Eq. (2.145) remains applicable and the latter equation is straightforward reproducible

$$S(\rho\|\rho_T) = S(\rho\|\rho_d) + S(\rho_d\|\rho_T). \tag{2.147}$$

In the case of nonortogonal basis of finite dimensional spaces we faced the same difficulties caused by the definition of the closest incoherent state, see Eq. (2.131), so it results impossible to find a suitable geometrical formulation of coherence and nonclassicality in such continuous frameworks.

Finally, we considered an infinite dimensional space and continuous bases made of unnormalizable orthogonal states, where an identical definition to the incoherent state proposed in Eq.(2.134) can be utilized. In the same spirit, we define the classical state as

$$\rho_T^{\Delta} = \int dx \langle x|\rho_T|x\rangle |x\rangle_{\Delta\Delta}\langle x|, \tag{2.148}$$

diagonal in the limit $\Delta \to 0$ as it follows from Eq. (2.137). Therefore we also obtain $\mathcal{NC}_S = \mathcal{C}_S + \mathcal{S}_S$ in this context.

### 2.5.5 Concluding remarks

In Sec. 2.4, we translated an established measure of coherence into a distance between states so that distance could be utilized to quantify different magnitudes. In particular, it has been utilized to quantify two magnitudes introduced in this section, say the nonclassicality and the certainty. The connection between these three quantities turns meaningful and consistent in the analyzed scenarios except for the continuous non-orthogonal bases case, where there is no straightforward expansion of the formalism. All these conclusions are shared by the analyses made with Heillinger-like, relative entropy, and Hilbert-Schmidt distances, except in the case of continuous non-orthogonal basis.

The concordance between results when using different measures suggests that the concept of nonclassicality as the maximum coherence achievable can go beyond the specific distance-based quantifier applied, reinforcing the consistency of this approach.

The quasiprobability representation of quantum coherence introduced in Sec. 1.5 perfectly illustrates that nonclassical features can manifest in different ways depending on the definition of classicality at hand. In the explicit example of qubit states the idea of $SU(2)$ squeezing appears in many equivalent proposals, such as the ones in Refs. [238, 239, 240, 241, 242, 243]. Some of these criteria imply that every qubit is classical, as far as all qubit pure states are SU(2) coherent states with a well-behaved SU(2) $P$-function. On the other hand, according to the criterion of qubit entropic squeezing in Ref. [244], all density matrices different from the identity would show squeezing which agrees with the general formalism of nonclassicality developed in Refs. [26]. We have shown how the definition of nonclassicality based on the Hellinger-like distance is somehow able to unify the criteria by detecting nonclassicality in every state different from the identity matrix, regardless of the basis.

## 2.6 Equivalence between quantum coherence and nonclassicality

In the previous section, we found a quantitative relation between some quantifiers of coherence and nonclassicality. To conclude this thesis, we show how the very concept of nonclassicality as introduced in Chapter 1, this is, the lack of a proper joint distribution for incompatible observables, equals the concept of quantum coherence, regardless of the quantifier utilized. This deep, qualitative equivalence unifies two concepts with no so clear connections at first sight, even if both of them are at the heart of the question about what makes the world quantum. We derive this equivalence for a finite-dimensional space of dimension $N$, however, it can be extended to spaces of arbitrary dimension as introduced in [26]. We recall that the basis at hand $\{|j\rangle\}$ is defined by the eigenvectors of a given observable $J$, $J|\rangle = j|j\rangle$.

For any state, $\rho$, the *coherences* [28] are the nondiagonal terms of the density matrix,

$$\rho_{j,k} = \langle j|\rho|k\rangle, \quad j \neq k, \tag{2.149}$$

since their presence implies that $\rho$ is a coherent superposition of the states $|j\rangle$ and $|k\rangle$. Therefore, these terms define the coherence of the state regarding the corresponding basis. Based on this, one may define different functions of these terms in order to quantify the concept of coherence. We have already seen several examples, $\mathcal{C}_H = \sum |\rho_{jk}|$, $\mathcal{C}_{HS} = \sum |\rho_{jk}|^2$ or, less explicitly, $\mathcal{C}_S$ in (2.143). All of them are not null whenever any $\rho_{jk}$ is not null. Thus, in this section we refer to a state as having coherence in a certain basis when any nondiagonal element is non-zero, $\rho_{jk} \neq 0$.

On the other hand, we recall the definition of nonclassicality without any prior assumption about a definite set of states being classical [195, 196, 197, 198, 82, 26]. Instead, we need to invoke two incompatible observables to see pathologies in the common statistics which accredit the presence of nonclassicality. In this regard, we consider the observable given by the basis, $J$, and another observable, say $M$, with $[M, J] \neq 0$.

With this in mind, we demonstrate that the quantum nature of $\rho$ with respect to $J$ and $M$ lies precisely on the non-diagonal matrix elements of $\rho$ in the basis $J$. This is, we show how in the basis in which there is coherence, there is nonclassicality in the lack of joint $J - M$ distribution. However, coherence is a basis-dependent property. Nevertheless, we have seen in the previous section that for every state different from the identity you can find a basis where the *coherences* are not null. In the same spirit but regarding nonclassicality, it is also always possible to find a combination of incompatible observables for which there is no legitimate probability distribution for every $\rho \neq \dfrac{I}{N}$, [26].

**Theorem.** *A state $\rho$ is nonclassical if and only if there is a basis $\{|j\rangle\}$ such that $\langle j|\rho|k\rangle \neq 0$ for at least a pair of basis elements, $|j\rangle \neq |k\rangle$.*

**Proof.** To prove that coherence implies nonclassicality we restrict ourselves to the two-dimensional subspace spanned by the basis components $|j\rangle$ and $|k\rangle$. We can define the Pauli-like matrices

$$\begin{aligned} \sigma_z &= |j\rangle\langle j| - |k\rangle\langle k|, \\ \sigma_\phi &= e^{i\phi}|j\rangle\langle k| + e^{-i\phi}|k\rangle\langle j|, \\ \sigma_{\perp\phi} &= i(e^{i\phi}|j\rangle\langle k| - e^{-i\phi}|k\rangle\langle j|), \end{aligned} \tag{2.150}$$

being the basis of the subspace the eigenvectors of $\sigma_z$, which plays the role of $J$. Moreover we chose $\phi$ so that

$$\langle\sigma_\phi\rangle = 2|\langle j|\rho|k\rangle|, \quad \langle\sigma_{\perp\phi}\rangle = 0. \tag{2.151}$$

To address the pathologies in the statistics we apply the approach of the joint measurement of incompatible observables introduced in Chapter 1 [35, 26]. In this case, we consider the blurred measurement of $\sigma_z$, and $\sigma_{\perp\phi}$, that plays the role of $M$. The dichotomic variables $y, z = \pm 1$ are the possible outcomes of $\sigma_z$, and $\sigma_{\perp\phi}$ respectively. The POVM representing the measurement performed lies

$$\tilde{\Delta}(z, y) = \frac{1}{4}(\sigma_0 + z\gamma_z\sigma_z + y\gamma_y\sigma_{\perp\phi} + zy\gamma_{zy}\sigma_\phi) \tag{2.152}$$

where once again $\sigma_0$ is the $2\times 2$ identity matrix and the $\gamma_i$ are parameters characterizing the measurement, which are constrained to obey the relation $\gamma_y^2 + \gamma_z^2 + \gamma_{yz}^2 \leq 1$. The state, Eq. (1.13), in terms of the mean values of these Pauli-like matrices, Eq. (2.150), result as

$$\rho = \frac{1}{2}(\sigma_0 + s_z\sigma_z + s_{\perp\phi}\sigma_{\perp\phi} + s_\phi\sigma_\phi) \tag{2.153}$$

being $s_i = \mathrm{tr}(\rho\sigma_i) = \langle\sigma_i\rangle$ for $i = z, \perp\phi, \phi$. After the data inversion introduced in Eqs. (1.79) -(1.45), we obtain the inferred joint distribution for $\sigma_z$ and $\sigma_{\perp\phi}$, with exact marginal distributions for both observables,

$$p(z, y) = \frac{1}{4}(1 + z\langle\sigma_z\rangle + y\langle\sigma_{\perp\phi}\rangle + yz\frac{\gamma_{yz}}{\gamma_y\gamma_z}\langle\sigma_\phi\rangle). \tag{2.154}$$

If the state has nondiagonal terms, $|\langle j|\rho|k\rangle| \neq 0$, this is $s_\phi = \langle\sigma_\phi\rangle \neq 0$, there is always a posible combination of the $\gamma$ factors giving rise to negativities in the statistics. For example, it is easy to imagine a $\gamma_{yz} \neq 0$ together with $\gamma_y \to 0$ and $\gamma_z \to 0$, which will give negative probabilities $p(y, z) < 0$ for the outcome $y = -z = 1$ .

Finally, to prove that nonclassicality implies coherence, we note that the only way that $p(y, z) \geq 0$ in Eq. (2.154) for all $y, z$ and all the allowed $\gamma$ values is that the mean value of $\sigma_\phi$ is null, $\langle\sigma_\phi\rangle = 0$ which is only possible in the conditions established if there are not non diagonal terms, $\langle j|\rho|k\rangle = 0$. Therefore a negative joint distribution, $p(y, z) < 0$, implies necessarily any *coherence*, $\langle j|\rho|k\rangle \neq 0$. ■

### 2.6.1 Concluding remarks

Essentially, the statistical information corresponding to the observables orthogonal to the observable generating the basis is encapsulated in the nondiagonal terms of the density matrix. This is quite direct from the representation of the state in terms of Pauli matrices in Eq. (1.13). In this section, we demonstrate that this information is accessible from the nonideal joint measurement of both observables. A straightforward relationship between coherence and quantumness occurs when the definition of nonclassicality relies on the incoherent superposition of classical states. However, we have found a similar relationship in our context, without the need for a previous definition of classical states. In any case, nonclassicality and coherence of $\rho$ with respect to $J$ holds

provided that $[J, \rho] \neq 0$, where by $J$ we mean here the family of projectors $\{|j\rangle\langle j|\}$. This agrees with the recent results in Refs. [246, 247, 248], where some measures of quantumness and coherence are introduced that rely on $[J, \rho] \neq 0$.

In the previous section we demonstrated that, for every state different from the identity, the quantifier of nonclassicality is always not null since it is always possible to find a basis where the *coherences* are not null. In the same spirit but regarding the joint statistics of incompatible observables, it is also always possible to find a combination of incompatible observables for which there is no legitimate joint probability distribution [26]. This establishes a relationship between a measured statistics of two observables and the nondiagonal elements of the density matrix. Thus, we have found an equivalence between coherence and nonclassicality irrespective of the quantification of these magnitudes.

# Conclusions

*Otro día se dará peor.*
*I. A. D.*

The common thread of this thesis has been to discern the potential structural connections between different elements of the quantum theory at several levels: from the relationship between observed quantum effects, to the correspondence between key concepts of the theory itself. Always with the idea of coherence as the main element underlying nonclassical effects kept in mind. We remark in this section on the main contributions of this work to the current knowledge in the area.

From the diverse tests carried out, we conclude that the nonideal joint measurement of incompatible observables (JMIO) followed by the corresponding data inversion has been demonstrated as the essential complement to the definition of nonclassicality based on the practical detection of pathological joint probability distributions.

On the one hand, the JMIO has manifested to be suitable for investigating indirect signatures of nonclassicality, such as Bell's test, allowing to recover Fine's theorem. It has propitiated the definition of an indirect signature of nonclassicality, the inequalities for complementarity. These translate the equivalence between the failure of classical models and lack of common statistics to the single subsystem scenario with equivalent meaning and conclusions than in the bipartite scheme.

Specifically, this approach has given rise to setting the statistics separability in the spotlight even in systems without spatial separation. The failure of a factorizable model when talking about measurements on a single system points to a different element than non-locality to be considered as its cause. On the other hand, it allowed us to demonstrate the relevance of the detector in quantum effects. We came to the conclusion that the nonclassicality of the measurement element is a necessary condition to address any nonclassical statistics. This offers a different perspective on nonclassical results, joining the role of states and measurements in complete agreement with the very foundations of quantum theory.

According to this, quantumness should be seen not as a property of the state itself but as a consequence of certain measurements over certain states. Hence, what has true

meaning is the concept of nonclassical effect, which refers to the concrete combination of state and measurement that gives rise to pathological statistics. This does not mean that a state may be classical or quantum depending on the chosen measurement, in the spirit of contextuality. On the contrary, we have shown in this thesis that every state different from the identity can lead to nonclassical effects as long as the adequate measurement is performed.

Related to the importance of the measurement process, we also analyzed the implication of the coherence of the detector in the resolution of properly defined metrological processes. It has been naturally obtained that the coherence properties of the detector and those of the probe state contribute equally to the resolution of the process. The relevance of this contribution lies in the relationship between coherence and resolution itself, which was missing in the literature despite the active use of coherence to enhance precision in quantum metrology.

Regarding the connections between quantum effects, we concluded that there is a complete equivalence between polarization nonclassicality and multi-photon entanglement. This correspondence goes beyond connections previously presented in the literature since it is not restricted to polarization squeezing and relates a multi-mode property with a multi-particle feature.

The experimental feasibility of the quasiprobability representation of quantum coherence has been shown. We reported the first experimental reconstruction of this property, concluding that it is a suitable indirect signature of nonclassicality, not only from a theoretical but from an experimental point of view.

The analysis of the dependence of coherence on the basis led us to introduce a geometrical approach directly expressing the quantifier of nonclassicality in terms of the quantifier of coherence. We concluded that this quantifier of nonclassicality can be regarded as an on/off detector for coherence, being coherence in any basis a necessary and sufficient condition for the presence of nonclassicality in all basis. The link between both magnitudes is related to the properties of the corresponding basis. These results have been proven valid for several distance-based quantifiers. Thus, we have demonstrated that the approach to nonclassicality based on coherence is consistent in the framework of resource theories.

Finally, we concluded that the nondiagonal terms of the density matrix and the lack of a joint distribution for incompatible observables are equivalent concepts. This establishes a univocal relation between coherence and nonclassicality, which represents the accomplishment of the main objective of this thesis.

To sum up, we remark on the consistency of the general approach of this work: it starts from an unambiguous definition of nonclassicality, exposes a mechanism to detect it and to analyze its causes, and, ultimately, allows the conclusion that the fundamental cause of nonclassicality is coherence.

# Appendix A: List of publications derived from the thesis

- Elisa Masa, Laura Ares, Alfredo Luis, Nonclassical joint distributions and Bell measurements, Physics Letters A 384, 126416 (2020).
- Alfredo Luis and Laura Ares, Apparatus contribution to observed nonclassicality, Physical Review A 102, 022222 (2020).
- Laura Ares and Alfredo Luis, Signal estimation and coherence, Optics Letters 46, 5409-5412 (2021).
- Elisa Masa, Laura Ares, Alfredo Luis, Inequalities for complementarity in observed statistics, Physics Letters A 427, 127914 (2022).
- Laura Ares and Alfredo Luis, Distance-based approach to quantum coherence and nonclassicality, Physical Review A 106, 012415 (2022).
- Laura Ares and Alfredo Luis, Beam Splitter as quantum coherence-maker, Physica Scripta 98, 015101 (2022).

# Bibliography


[1] F. Laloë, Do We Really Understand Quantum Mechanics (Cambridge University Press, Cambridge, 2019).

[2] B. Drummond, Violation of Bell Inequalities: Mapping the Conceptual Implications, International Journal of Quantum Foundations **7**, (2021).

[3] L. Masanes, T.D. Galley, and M.P. Müller, The measurement postulates of quantum mechanics are operationally redundant. Nat Commun **10**, 1361 (2019).

[4] G. Carcassi, L. Maccone, and C. A. Aidala, Four Postulates of Quantum Mechanics Are Three Phys. Rev. Lett. **126**, 110402 (2021).

[5] M. Schlosshauer, Quantum decoherence, Physics Reports**831**, 1-57 (2019).

[6] O. C. Stoica, Standard quantum mechanics without observers, Phys. Rev. A **103**, 032219 – (2021).

[7] N. Korolkova and G. Leuchs, Quantum correlations in separable multi-mode states and in classically entangled light Rep. Prog. Phys. 82 056001 (2019).

[8] Alfred Wünsche, About the nonclassicality of states defined by nonpositivity of the P-quasiprobability, J. Opt. B: Quantum Semiclass. Opt. **6**, 159 (2004).

[9] S.-L. Liu *et al.*, Classical analogy of a cat state using vortex light, Communications Physics volume **2**, 75 (2019).

[10] I. H. Deutsch, Harnessing the Power of the Second Quantum Revolution, PRX QUANTUM **1**, 020101 (2020).

[11] W. Ge *et al.*, Operational resource theory of nonclassicality via quantum metrology, Phys. Rev. Research **2**, (2020).

[12] M. O. Scully and M. S. Zubairy, *Quantum Optics* (Cambridge University Press, 1997).

[13] G. Greenstein and A. G. Zajonc, The Quantum Challenge: Modern Research on the Foundations of Quantum Mechanics,(Jones & Bartlett Learning, 2005).

[14] G. García, L. Ares and A. Luis, Phase space quantum–classical hybrid model, Annals of Physics **411**, 167961 (2019).

[15] J. Braden, M. C. Johnson, H. V. Peiris, A. Pontzen and S. Weinfurtner, New Semiclassical Picture of Vacuum Decay, Phys. Rev. Lett. **123**, 031601 (2019).

[16] L. Mandel and E. Wolf, *Optical Coherence and Quantum Optics* (Cambridge University Press, 1995).

[17] E. Wigner, On the Quantum Correction For Thermodynamic Equilibrium,Phys. Rev. 40, 749 (1932).

[18] U. M. Titulaer and R. J. Glauber, Phys. Rev. **140**, B676 (1965).

[19] L. Mandel and E. Wolf, Optical Coherence and Quantum Optics, Cambridge University Press, (1995).

[20] R. J. Glauber, The Quantum Theory of Optical Coherence, Phys. Rev. **130**, 2529–2539 (1963).

[21] R. Glauber, Coherent and Incoherent States of the Radiation Field, Phys. Rev. **131**, 2766–2788 (1963).

[22] E. C. G. Sudarshan Equivalence of Semiclassical and Quantum Mechanical Descriptions of Statistical Light Beams, Phys. Rev. Lett. **10**, 277 (1963).

[23] W. Vogel and D.-G. Welsch, Quantum Optics, 3rd Ed. (Wiley-VCH, Weinheim, 2006).

[24] T. Kiesel, Classical and quantum-mechanical phase-space distributions,Phys. Rev. A **87**, 062114 (2013).

[25] A. Fine, Hidden Variables, Joint Probability, and the Bell Inequalities, Phys. Rev. Lett **48**, 291–295 (1982).

[26] A. Luis and L. Monroy, Nonclassicality of coherent states: Entanglement of joint statistics, Phys. Rev A **96**, 063802 (2017).

[27] J. Sperling et *al.*, Wave-particle duality revisited: Neither wave nor particle, arXiv:1907.09836 [quant-ph]

[28] C. Cohen-Tannoudji, D. Bernard, & F. Laloë, Quantum mechanics Vol 1, 5 ed. Germany: De Gruyter (2020).

[29] A. Peres, Quantum Theory: Concepts and Methods, 1st edn (Springer, 2002).

[30] W. M. Muynck, Foundations of Quantum Mechanics, an Empiricist Approach, (Kluwer Academic Publishers, 2002).

[31] E. B. Davies and J. T. Lewis, An Operational Approach to Quantum Probability, Commun. math. Phys. **17**, 239—260 (1970).

[32] A.S. Holevo, Probabilistic and Statistical Aspects of Quantum Theory, vol. 1, Springer Science & Business Media, (2011).

[33] P. Busch, Unsharp reality and joint measurements for spin observables, Phys. Rev. D **33**, 2253 (1986).

[34] P. Busch, Some Realizable Joint Measurements of Complementary Observables, Found.Phys., **17**, 905 (1987).

[35] A. Luis, Nonclassical light revealed by the joint statistics of simultaneous measurements, Opt. Lett. **41**, 1789–92 (2016).

[36] Klyshko, D. N. Observable signs of nonclassical light,Phys. Lett. A **213**, 7–15 (1996).

[37] J. Bell, Speakable and Unspeakable in Quantum Mechanics, (Cambridge: Cambridge University Press 1993).

[38] J. F. Clauser and M. A. Horne, Experimental consequences of objective local theories, Phys. Rev. D **10**, 526–535 (1974).

[39] J. S. Bell, On the Einstein Podolsky Rosen paradox, Physics **1**, 195–200 (1964).

[40] A. Einstein, B. Podolsky and N. Rosen, Can Quantum Mechanical Description of Physical Reality Be Considered Complete?, Phys. Rev. **47**, 777-780 (1935).

[41] S. J. Freedman and J. F. Clauser, Experimental Test of Local Hidden-Variable Theories, Phys. Rev. Lett. **28**, 938 (1972).

[42] A. Aspect, J. Dalibard, and G. Roger, Experimental Test of Bell's Inequalities Using Time-Varying Analyzers,Phys. Rev. Lett. **49**, 1804 (1982)

[43] J. W. Pan D. Bouwmeester, H. Weinfurter, and A. Zeilinger, Experimental entanglement swapping: Entangling photons that never interacted, Phys. Rev. Lett. **80**, 3891 (1998).

[44] A. Fine, Antinomies of Entanglement: The Puzzling Case of the Tangled Statistics, The Journal of Philosophy **79**, 733-747 (1982).

[45] Joe Henson, Non-separability Does Not Relieve the Problem of Bell's Theorem, Found Phys **43**, 1008–1038 (2013).

[46] A. Shafiee and F. Taher Ghahramani, On the meaning of locality: the overlapping assumptions. Quantum Stud.: Math. Found. 2, 435–448 (2015).

[47] J. A. de Barros, J. V. Kujala and G. Oas, Negative probabilities and contextuality, J. Math. Psychol. **74**, 34–45 (2016).

[48] W. M. Muynck and O. Abu-Zeid, On an alternative interpretation of the Bell inequalities, Phys. Lett. A **100**, 485–489 (1984).

[49] M. Czachor, On some class of random variables leading to violations of the Bell inequality, Phys. Lett. A **129**, 291–294 (1988); Erratum, Phys. Lett. A **134**, 512(E) (1989).

[50] A. Rivas, On the role of joint probability distributions of incompatible observables in Bell and Kochen–Specker Theorems, Ann. of Phys. **411**, 167939 (2019).

[51] A. Khrennikov, Can There be Given Any Meaning to Contextuality Without Incompatibility? Int. J. Theor. Phys. **60**, 106—114 (2021).

[52] E. Masa, L. Ares and A. Luis, Inequalities for complementarity in observed statistics, Phys. Lett. A **427**, 127914 (2022).

[53] M.J.W.Hall, The Significance of Measurement Independence for Bell Inequalities and Locality. In: Asselmeyer-Maluga, T. (eds) At the Frontier of Spacetime. Fundamental Theories of Physics, vol 183. Springer, Cham. (2016).

[54] A. Cabello, Bell Non-locality and Kochen–Specker Contextuality: How are They Connected?, Found Phys **51**, 61 (2021).

[55] R. Galazo, I. Bartolomé, L. Ares, and A. Luis, Classical and quantum complementarity, Phys. Lett. A **384**, 126849 (2020).

[56] M. Markiewicz, D. Kaszlikowski, P. Kurzyński *et al.*, From contextuality of a single photon to realism of an electromagnetic wave, npj Quantum Information 5, 5 (2019).

[57] Bell's theorem: Critique of proofs with and without inequalities, AIP Conference Proceedings **750**, 150 (2005).

[58] A. Matzkin, Is Bell's theorem relevant to quantum mechanics. On locality and non-commuting observables, AIP Conference Proceedings 1101, 339 (2009).

[59] T. M. Nieuwenhuizen, Is the Contextuality Loophole Fatal for the Derivation of Bell Inequalities?, Found. Phys. **41**, 580 (2011).

[60] A. Khrennikov, CHSH Inequality: Quantum Probabilities as Classical Conditional Probabilities, Found. of Phys. **45**, 711–725 (2015).

[61] A. Khrennikov, Non-Kolmogorov probability models and modified Bell's inequality, J. Math. Phys. **41**, 1768 (2000).

[62] E. Masa, L. Ares, and A. Luis A, Nonclassical joint distributions and Bell measurements, Phys. Lett. A **384**, 126416 (2020).

[63] W. M. de Muynck and H. Martens, Joint measurement of incompatibles observables and ,the Bell inequalities, Phys. Lett. A **142**, 187–190 (1989).

[64] W. Son, E. Andersson, S. M. Barnett, and M. S. Kim, Joint measurements and Bell inequalities, Phys. Rev. A **72**, 052116 (2005).

[65] Y. Ben-Aryeh and A. Mann, Explicit constructions of all separable two-qubits density matrices and related problems for three-qubits systems, arXiv:1510.07222 [quant-ph].

[66] N. G. Walker, Quantum theory of multiport optical homodyning, J. Mod. Opt. **34**, 15 (1987).

[67] A. Luis and J. Peřina, Generalized measurements in eight-port homodyne detection, Quantum Semiclass. Opt. **8**, 873 (1996).

[68] L. Ares and A. Luis, Semiclassical violation of Bell inequalities,Phys. Lett. A **459**, 128586 (2023).

[69] L. Mandel, Non-Classical States of the Electromagnetic Field, Phys. Scr. **T12**, 34-42 (1986)

[70] A. Luis and L. Ares, Apparatus contribution to observed nonclassicality, Phys. Rev. A **102**, 022222 (2020).

[71] C. L. Mehta, Diagonal Coherent-State Representation of Quantum Operators, Phys. Rev. Lett. **18** 752 (1967).

[72] W. M. de Muynck, Information in neutron interference experiments Phys. Lett. A **182**, 201 (1993).

[73] A. Luis and L. L. Sánchez-Soto, Complete Characterization of Arbitrary Quantum Measurement Processes, Phys. Rev. Lett. **83**, 3573 (1999).

[74] A. Luis, Quantum tomography of input-output processes Phys. Rev. A **62**, 054302 (2000).

[75] J. S. Lundeen, *et al.*, tomography of quantum detectors Nature Physics **5**, 27 (2009).

[76] K. Kim, Effect of van der Waals interaction on the structural and cohesive properties of black phosphorus, J. Korean Phys. Soc. **64**, 155 (2014).

[77] P. Grangier, G. Roger and A. Aspect, Experimental Evidence for a Photon Anticorrelation Effect on a Beam Splitter: A New Light on Single-Photon Interferences, Europhys. Lett. **1**, 173 (1986).

[78] C. T. Lee, Measure of the nonclassicality of nonclassical states, Phys. Rev. A **44**, R2775 (1991).

[79] B. L. Schumaker, Noise in homodyne detection, Opt. lett. **9**, 189 (1984).

[80] J. P. Amiet and S. Weigert, Discrete Q- and P -symbols for spin s, J. Opt. B Opt. **2**, 118 (2000).

[81] S. Heiss and S. Weigert, Discrete Moyal-type representations for a spin, Phys. Rev. A **63**, 012105 (2000).

[82] A. Luis and N. Korolkova, Polarization squeezing and nonclassical properties of light,Phys. Rev. A **74**, 043817 (2006).

[83] S. Ryl, J. Sperling, E. Agudelo, M. Mraz, S. Köhnke, B. Hage, and W. Vogel, Unified nonclassicality criteria, Phys. Rev. A **92**, 011801(R) (2015).

[84] C. Carmeli, T. Heinosaari and A. Toigo, Quantum Incompatibility Witnesses, Phys. Rev. Lett. **122**, 130402 (2019).

[85] E. Chitambar, G. Gour, K. Sengupta, and R. Zibakhsh, Quantum Bell nonlocality as a form of entanglement, Phys. Rev. A **104**, 052208 (2021).

[86] D-D. Dong, G-B. Wei, X-K. Song, D. Wang and L. Ye, Unification of coherence and quantum correlations in tripartite systems, Phys. Rev. A **106**, 042415 (2022)

[87] J. Sperling and I. A. Walmsley, Quasiprobability representation of quantum coherence, Phys. Rev. A **97**, 062327 (2018).

[88] J. Sperling and W. Vogel, Representation of entanglement by negative quasiprobabilities, Phys. Rev. A **79**, 042337 (2009).

[89] F. T. Arecchi, E. Courtens, R. Gilmore, and H. Thomas, Atomic coherent states in quantum optics, Phys. Rev. A **6**, 2211-2237 (1972).

[90] A. Luis, Polarization in quantum optics, Prog. Opt. **61**, 283–331 (2016).

[91] Aaron Z. Goldberg *et al.*, Quantum concepts in optical polarization, Adv. Opt. Photon. **13**, 1-73 (2021).

[92] P. W. Atkins and J. C. Dobson, Angular momentum coherent states, Proceedings of the Royal Society of London Series A **321**, 321–340 (1971).

[93] R. Demkowicz–Dobrzański, M. Jarzyna, and J. Kołodynski, Quantum limits in optical interferometry, Progress in Optics **60**, 345 (2015).

[94] A. Luis, Nonclassical polarization states, Phys. Rev. A **73**, 063806 (2006).

[95] M. Kitagawa and M. Ueda, Squeezed spin states, Phys. Rev. A **47**, 5138 (1993).

[96] A. Sørensen, LM. Duan, J. Cirac, and P. Zoller, Many-particle entanglement with Bose–Einstein condensates, Nature **409**, 63–66 (2001).

[97] N. Korolkova *et al.*, Polarization squeezing and continuous-variable polarization entanglement, Phys. Rev. A **65**, 052306 (2002).

[98] J. Sperling, E. Agudelo, Entanglement of particles versus entanglement of fields: independent quantum resources, arXiv:2204.06245.

[99] A. Rivas, On the role of joint probability distributions of incompatible observables in Bell and Kochen–Specker Theorems, Ann. Phys. **411**, 167939 (2019).

[100] J. Peřina, Coherence of Light (Van Nostrand Reinhold, 1971) pp. 26-27.

[101] R. H. Brown and R. Twiss, Correlation between photons in two coherent beams of light, Nature **177**, 27–29 (1956).

[102] C. Cohen-Tannoudji, J. Dupont-Roc, and G. Grynberg, Atom–Photon Interactions, (Wiley, New York 1992).

[103] T. Baumgratz, M. Cramer, and M. B. Plenio, Quantifying Coherence, Phys. Rev. Lett. **113** 140401 (2014).

[104] S. Kim, C. Xiong, A. Kumar, and J. Wu, Converting coherence based on positive-operator-valued measures into entanglement, Phys. Rev. A **103**, 052418 (2021).

[105] Z.-X. Wang, S. Wang, T. Ma et al. Gaussian entanglement generation from coherence using beam-splitters, Sci. Rep. **6**, 38002 (2016).

[106] J. Ma *et al.*, Converting Coherence to Quantum Correlations, Phys. Rev. Let. **116**, 160407 (2016).

[107] A. Karnieli *et al.*, The coherence of light is fundamentally tied to the quantum coherence of the emitting particle, Sci. Adv. **7**, 18 (2021).

[108] X. Yuan *et al.*, Quantum Coherence and Intrinsic Randomness, Adv. Quantum Technol. **2**, 1900053 (2019).

[109] M. Schlosshauer, Decoherence, the measurement problem, and interpretations of quantum mechanics, Rev. Mod. Phys. **76**, 4 (2004).

[110] F. Caravelli *et al.*, Energy storage and coherence in closed and open quantum batteries, Quantum **5**, 505 (2021).

[111] M.T. Mitchison, Quantum thermal absorption machines: refrigerators, engines and clocks, Contemporary Physics **60**, 164-187 (2019).

[112] C. Lüders *et al.*, Quantifying Quantum Coherence in Polariton Condensates, PRX Quantum **2**, 030320 (2021).

[113] P. Cimavilla-Román *et al.*, Influence of silica aerogel particles on the foaming process and cellular structure of rigid polyurethane foams, European Polymer Journal **135**, 109884 (2020).

[114] P. Álvarez-Zapatero, A. Vega, A. Aguado, A neural network potential for searching the atomic structures of pure and mixed nanoparticles. Application to ZnMg nanoalloys with an eye on their anticorrosive properties, Acta Materialia, **220**, 117341 (2021).

[115] M. Herreras-Giralda, *et al.*, Thermal emission in the successive orders of scattering (SOS) radiative transfer approach, Journal of Quantitative Spectroscopy and Radiative Transfer **291**, 108327 (2022).

[116] A. Acín *et al.*, The quantum technologies roadmap: a European community view, New J. Phys. **20**, 080201, (2018)

[117] S. Pirandola *et al.*, Advances in quantum cryptography, Adv. Opt. Photon. **12**, 1012-1236 (2020)co.

[118] A.J. Daley *et al.*, Practical quantum advantage in quantum simulation, Nature **607**, 667–676 (2022).

[119] F. Poggiali, P. Cappellaro, and N. Fabbri, Optimal Control for One-Qubit Quantum Sensing, Phys. Rev. X 8, 021059 – Published 7 June 2018

[120] R. Horodecki, P. Horodecki, M. Horodecki, and K. Horodecki, Quantum entanglement, Rev. Mod. Phys. **81**, 865 (2009).

[121] A. Streltsov, H. Kampermann, S. Wölk, M. Gessner, and D. Bruß, Maximal coherence and the resource theory of purity, New J. Phys. **20**, 053058 (2018).

[122] Tan, K.C.; Jeong, H. Resource Theories of Nonclassical Light, Quantum Reports, **1**, 151-161, (2019).

[123] C. Sparaciari, The first law of general quantum resource theories, Quantum **4**, 259 (2020)

[124] T. Theurer, N. Killoran, D. Egloff, and M. B. Plenio, Resource Theory of Superposition, Phys. Rev. Lett. **119**, 230401 (2017).

[125] YQ Nie *et al.*, Quantum Coherence Witness with Untrusted Measurement Devices, Phys. Rev. Lett. **123**, 090502 (2019).

[126] E. Chitambar, and G. Gour, Comparison of incoherent operations and measures of coherence, Phys. Rev. A **94**, 052336 (2016).

[127] W. GE *et al.*, Operational resource theory of nonclassicality via quantum metrology, Phys. Rev. Res. **2**, 023400 (2020).

[128] S. Köhnke et al., Quantum Correlations beyond Entanglement and Discord, Phys. Rev. Lett. **126**, 170404 (2021).

[129] A. Streltsov, G. Adesso and M. B. Plenio, Colloquium: Quantum coherence as a resource, Rev. Mod. Phys. **89** 041003 (2017).

[130] A.H. Tavabi, C.B. Boothroyd, E. Yücelen, *et al.*, The Young-Feynman controlled double-slit electron interference experiment. Sci Rep **9**, 10458 (2019).

[131] S. Gerlich, *et al*, Quantum interference of large organic molecules, Nat Commun **2**, 263 (2011).

[132] E. Schrödinger, The Present Status of Quantum Mechanics, Die Naturwissenschaften **23**, 48 (1935).

[133] H. M. Wiseman, S. J. Jones, and A. C. Doherty, Steering, Entanglement, Nonlocality, and the Einstein-Podolsky-Rosen Paradox, Phys. Rev. Lett. **98**, 140402 (2007).

[134] M. Fadel, L. Ares, A. Luis, and Q. He, Number-phase entanglement and Einstein-Podolsky-Rosen steering, Phys. Rev. A **101**, 052117 (2020).

[135] A. Smirne, D. Egloff, M. G. Díaz, M. B. Plenio and S. F. Huelga, Coherence and non-classicality of quantum Markov processes, Quantum Sci. Technol. **4**,01LT01 (2019) .

[136] G. Pérez-Callejo *et al.*, TIA: A forward model and analyzer for Talbot interferometry experiments of dense plasmas Physics of Plasmas **29**, 043901 (2022).

[137] N. P. de Leon, K. M. Itoh, D. Kim, K. K. Mehta, T. E. Northup, H. Paik, B. S. Palmer, N. Samarth, S. Sangtawesin, and D. W. Steuerman, Materials challenges and opportunities for quantum computing hardware, Science **372**, 6539 (2021).

[138] F. Ahnefeld, T. Theurer, D. Egloff, J. Mauricio Matera, and M. B. Plenio, Coherence as a Resource for Shor's Algorithm, Phys. Rev. Lett. **129**, 120501 (2022).

[139] L. Gerster, F. Martńez-Garcá, P. Hrmo, *et al.*, Experimental Bayesian Calibration of Trapped-Ion Entangling Operations, PRX Quantum **3**, 020350 (2022).

[140] K.-D. Wu, A. Streltsov, B. Regula, G.-Y. Xiang, C.-F. Li and G.-C. Guo, Experimental Progress on Quantum Coherence: Detection, Quantification, and Manipulation, Adv. Quantum Technol., **4** 2100040 (2021).

[141] Z. Ding, R. Liu, C. Radhakrishnan, W. Ma, X. Peng, Y. Wang, T. Byrnes, F. Shi and J. Du, Experimental study of quantum coherence decomposition and trade-off relations in a tripartite system, npj Quantum Information **7**, 145 (2021).

[142] J. Sperling, E. Meyer-Scott, S. Barkhofen, B. Brecht, and C. Silberhorn, Experimental Reconstruction of Entanglement Quasiprobabilities, Phys. Rev. Lett. **122**, 053602 (2019).

[143] G. M. D'Ariano, M. G. A. Paris and M. F. Sacchi, Quantum tomography, Adv. Imag. Electron. Phys. **128**, 205–308 (2003).

[144] C.R. Müller, B. Stoklasa, C. Peuntinger, C. Gabriel, J. Řeháček, Z. Hradil, A. B. Klimov, G. Leuchs, Ch. Marquardt and L. L. Sánchez–Soto, Quantum polarization tomography of bright squeezed light,New Journal of Physics **14**, 085002 (2012).

[145] L. Wu, H. J. Kimble, J. L. Hall, and H. Wu, Generation of Squeezed States by Parametric Down Conversion, Phys. Rev. Lett. 57, 2520 (1986).

[146] P. Kok and S. L. Braunstein, Detection devices in entanglement-based optical state preparation, Phys. Rev. A **63**, 033812 (2001).

[147] J. Tiedau, M. Engelkemeier, B. Brecht, J. Sperling, and C. Silberhorn, Statistical Benchmarking of Scalable Photonic Quantum Systems Phys. Rev. Lett 126, 023601 (2021)

[148] C. Radhakrishnan, Z. Ding, F. Shi, J. Du, T. Byrnes, Basis-independent quantum coherence and its distribution, Ann. Phys. **409**, 167906 (2019).

[149] Adi Ben-Israel, The Moore of the Moore–Penrose inverse, Electron. J. Linear Algebra **9**, 150–157 (2002).

[150] J. Rubio, J. Anders , L. A. Correa, Global Quantum Thermometry, Phys. Rev. Lett. **127**, 190402 (2021).

[151] V. Villa-Ortega, T. Dent, A. Curiel Barroso, Rapid source classification and distance estimation for compact binary mergers with PyCBC live, Monthly Notices of the Royal Astronomical Society **515**, 5718–5729 (2022).

[152] W. H. Zurek, Decoherence and the Transition from Quantum to Classical – Revisited,Progress in Mathematical Physics, **48**, 1-31 (2006).

[153] V. Giovannetti, S. Lloyd, and L. Maccone, Advances in quantum metrology, Nat. Photon. **5**, 222–229 (2011).

[154] Z. Ficek and R. Tanaś, Quantum–Limit Spectroscopy, Springer Series in Optical Sciences 200 (Springer, 2017).

[155] M. Napolitano and M. W. Mitchell, Nonlinear metrology with a quantum interface, New J. Phys. **12**, 093016 (2010).

[156] M. W. Mitchell, J. S. Lundeen and A. M. Steinberg, Super–resolving phase measurements with a multiphoton entangled state, Nature **429**, 161–164 (2004).

[157] D. Braun, Quantum-enhanced measurements without entanglement, Rev. Mod. Phys. **90** (2018).

[158] A. Luis, Nonlinear transformations and the Heisenberg limit, Phys. Lett. A **329**, 8–13 (2004).

[159] E. Chitambar and G. Gour, Quantum resource theories, Rev. Mod. Phys. **91**, 025001 (2019).

[160] H. Kwon *et al.*, Nonclassicality as a Quantifiable Resource for Quantum Metrology, Phys. Rev. Lett. **122**, 040503 (2019).

[161] A. Luis, Coherence versus interferometric resolution, Phys. Rev. A **81**, 065802 (2010).

[162] P. Giorda and M. Allegra, Coherence in quantum estimation, J. Phys. A: Math. Theor. **51**, 025302 (2018).

[163] H. Kwon, K. Chuan Tan, S. Choi, y H. Jeong, Quantum Fisher information on its own is not a valid measure of the coherence, Results in Physics **9**, 1594-1595 (2018).

[164] L. Li, Q.-W. Wang, S.-Q. Shen, and M. Li, and Ming Li, Quantum coherence measures based on Fisher information with applications, Phys. Rev. A **103**, 012401 (2021).

[165] Paloma López-Reyes, *et al.*, Optimization of the deposition parameters of MgF2/LaF3 narrowband reflective FUV multilayers, Opt. Mater. Express **11**, 1678-1691 (2021).

[166] M. Vara-Lubiano *et al.*, The multichord stellar occultation on 2019 October 22 by the trans-Neptunian object (84922) 2003 VS2, A&A, 663 (2022)

[167] C. Brif and A. Mann, Phase-space formulation of quantum mechanics and quantum-state reconstruction for physical systems with Lie-group symmetries, Phys. Rev. A **59**, 971 (1999).

[168] V. Bužek, C. H. Keitel, and P. L. Knight, Sampling entropies and operational phase-space measurement. I. General formalism, Phys. Rev. A **51**, 2575 (1995).

[169] J. Rubio, Non-asymptotic quantum metrology: extracting maximum information from limited data, Doctoral thesis (PhD) University of Sussex, (2020).

[170] F. Martínez-García, Harnessing Bayesian Optimization for Quantum Information Processing, thesis (PhD) Swansea University (2022)

[171] N. Bohr, The Quantum Postulate and the Recent Development of Atomic Theory, Nature **121**, 580–590 (1928).

[172] L. De Broglie, Waves and Quanta, Nature 112, 540 (1923).

[173] P.A.M. Dirac, The Quantum Theory of the Emission and Absorption of Radiation, Proc. R. Soc. Lond. A **114**,243 (1927).

[174] J. A. Wheeler and W.H. Zurek, Quantum Theory and Measurement, Princeton: Princeton University Press, 1983.

[175] M. Jacob and J. A. Bergou, Quantitative complementarity relations in bipartite systems: Entanglement as a physical reality, Opt. Commun. **283**, 827-830 (2010).

[176] X.-F. Qian, K. Konthasinghe, S. K. Manikanda, D. Spiecker, A. N. Vamivakas, and J. H. Eberly, Turning off quantum duality, Phys. Rev. Research **2**, 012016(R) (2020).

[177] T. H. Yoon and M. Cho, Quantitative complementarity of wave-particle duality, Science Advances **7**, 34 (2021).

[178] Y.-R. Zhang, L.-H. Shao, Y. Li, and H. Fan, Quantifying coherence in infinite-dimensional systems, Phys. Rev. A **93**, 012334 (2016).

[179] A. Luis and L. L. Sánchez-Soto, A quantum description of the beam splitter, Quantum Semiclass. Opt. **7**, 153–160 (1995).

[180] M. J. Holland and K. Burnett, Interferometric Detection of Optical Phase Shifts at the Heisenberg Limit, Phys. Rev. Lett. **71**, 1355–1358 (1993).

[181] M. Ban, Decomposition formulas for su(1, 1) and su(2) Lie algebras and their applicationsin quantum optics, J. Opt. Soc. Am. B **10**, 1347–1359 (1993).

[182] F.T. Arecchi, E. Courtens, R. Gilmore, and H. Thomas, Atomic Coherent States in Quantum Optics, Phys. Rev. A **6**, 2211–2237 (1972).

[183] G.S. Agarwal and R.R. Puri, Atomic states with spectroscopic squeezing, Phys. Rev. A **49**, 4968–4971 (1994).

[184] C. Brif and A. Mann, Nonclassical interferometry with intelligent light, Phys. Rev. A **54**, 4505–4518 (1996).

[185] H. F. Hofmann, All path-symmetric pure states achieve their maximal phase sensitivity in conventional two-path interferometry, Phys. Rev. A **79**, 033822 (2009).

[186] M. García-Díaz, D. Egloff, and M. B. Plenio, A note on coherence power of n-dimensional unitary operators, Quantum Info. Comput. **16**, 1282–1294 (2016).

[187] S. Ataman, Quantum Fisher information maximization in an unbalanced interferometer, Phys. Rev. A **105**, 012604 (2022).

[188] K.K. Mishra and S. Ataman, Optimal phase sensitivity of an unbalanced Mach-Zehnder interferometer, Phys. Rev. A **106**, 023716 (2022).

[189] L. Ares and A. Luis, Beam splitter as quantum coherence-maker, Phys. Scr. **98**, 015101 (2022).

[190] A. Luis, Quantum-classical correspondence for visibility, coherence, and relative phase for multidimensional systems, Phys. Rev. A **78**, 025802 (2008).

[191] A. Luis, Coherence and visibility for vectorial light, J. Opt. Soc. Am. A **27**, 1764–1769 (2010).

[192] A. S. M. Patoary, G. Kulkarni, and A. K. Jha, Intrinsic degree of coherence of classical and quantum states, J. Opt. Soc. Am. B **36**, 2765-2776 (2019).

[193] M. Ozawa, Entanglement measures and the Hilbert-Schmidt distance, Phys. Lett. A **268** 158–160 (2000).

[194] H. Zhao, Cs. Yu, Coherence measure in terms of the Tsallis relative $\alpha$ entropy. Sci Rep **8**, 299 (2018).

[195] J. Vaccaro, Number-phase Wigner function on Fock space, Phys. Rev. A **52**, 3474 (1995).

[196] L. M. Johansen, Nonclassical properties of coherent states, Phys. Lett. A **329**, 184 (2004).

[197] L. M. Johansen, Nonclassicality of thermal radiation, J. Opt. B **6**, L21 (2004).

[198] L. M. Johansen and A. Luis, Nonclassicality in weak measurements, Phys. Rev. A **70**, 052115 (2004).

[199] L. E. Ballentine, Quantum Mechanics (Prentice Hall, Englewood Cliffs, 1990). Chapter 20.

[200] A. Luis and J. Peřina, Optimum phase-shift estimation and the quantum description of the phase difference, Phys. Rev. A **54**, 4564–4570 (1996).

[201] S. L. Braunstein, How large a sample is needed for the maximum likelihood estimator to be approximately Gaussian?, J. Phys A: Math. Gen. **25**, 3813–3826 (1992).

[202] Z.X. Jin, S.M. Fei, Quantifying quantum coherence and non-classical correlation based on Hellinger distance, Phys. Rev. A **97**, 062342 (2018).

[203] Carolin Lüders, Matthias Pukrop, Elena Rozas, Christian Schneider, Sven Höfling, Jan Sperling, Stefan Schumacher, and Marc Aßmann, Quantifying Quantum Coherence in Polariton Condensates, PRX Quantum **2**, 030320 (2021).

[204] K. Baek, Quantifying coherence of quantum measurements, New J. Phys. **22**, 093019 (2020).

[205] L. Ares and A. Luis, Signal estimation and coherence, Optics Letters **46**, 5409-5412 (2021).

[206] M. Born and E. Wolf, Principles of Optics Cambridge University, 7th ed, (1999).

[207] L. Mandel, Fluctuations of Photon Beams: The Distribution of the Photo-Electrons, Proc. Phys. Soc., **74**, 233 (1959).

[208] L. Mandel and E Wolf, The Measures of Bandwidth and Coherence Time in Optics, Proc. Phys. Soc. **80**, 894 (1962).

[209] A. Rényi, On the measures of entropy and information, Proc. 4th Berkeley Symp. on Mathematics and Statistical Probability, Vol. 1, University of California Press (1961), pp. 547-561.

[210] I. Bialynicki-Birula, Formulation of the uncertainty relations in terms of the Rényi entropies, Phys. Rev. A **74**, 052101 (2006).

[211] A. Luis, G. M. Bosyk, and M. Portesi, Entropic measures of joint uncertainty: Effects of lack of majorization, Physica A **444**, 905-913 (2016).

[212] H. Cramér, Mathematical methods of statistics, Princeton University Press, (1946).

[213] B.R. Frieden, Physics from Fisher information: A Unification, Cambridge U.Press, (1999).

[214] G. D'Ariano, C. Macchiavello, and M. Sacchi, On the general problem of quantum phase estimation, Phys. Lett. A. **248**, 103–108 (1998).

[215] B. P. Abbott *et al.* (LIGO Scientific Collaboration and Virgo Collaboration), Observation of Gravitational Waves from a Binary Black Hole Merger, Phys. Rev. Lett. **116**, 061102 (2016).

[216] R. Lynch, The quantum phase problem: A critical review, Phys. Rep. 256, 367–436 (1995).

[217] V. Peřinová, A. Lukš, J. Peřina, Phase in Optics (World Scientific, Singapore 1998).

[218] A. Álvarez-Marcos and A. Luis, Phase-space quantum Wiener–Khintchine theorem, Opt. Lett. **47**, 4604-4607 (2022).

[219] F. Herbut, A quantum measure of coherence and incompatibility, J. Phys. A: Math. Gen. **38**, 2959–2974 (2005).

[220] W. Roga, D. Spehner, and F. Illuminati1, Geometric measures of quantum correlations: characterization, quantification, and comparison by distances and operations, J. Phys. A: Math. Theor. **49**, 235301 (2016).

[221] L. Ares and A. Luis, Distance-based approach to quantum coherence and nonclassicality, Phys. Rev. A **106**, 012415 (2022).

[222] Y.R. Zhang, L.H. Shao, Y. Li, and H. Fan, Quantifying coherence in infinite-dimensional systems, Phys. Rev. A **93**, 012334 (2016).

[223] S. Cheng and M. J. W. Hall, Complementarity relations for quantum coherence, Phys. Rev. A **92**, 042101 (2015).

[224] Y. Yao, G. H. Dong, X. Xiao, and C. P. Sun, Frobenius-norm-based measures of quantum coherence and asymmetrt, Sci Rep **6**, 32010 (2016).

[225] A. Luis and L. L. Sánchez–Soto, Quantum phase difference, phase measurements and Stokes operators, Progress in Optics, edited by E. Wolf (Elsevier, Amsterdam, 2000) **41**, 421–481 (2000).

[226] L. Susskind and L. Glogower, Quantum mechanical phase and time operator, Physics Physique Fizika **1**, 49 (1964).

[227] A. Luis, Squeezed coherent states as feasible approximations to phase-optimized states, Phys. Lett. A **354**, 71–78 (2006).

[228] M.-L. Hu and H. Fan, Relative quantum coherence, incompatibility, and quantum correlations of states, Phys. Rev. A **95**, 052106 (2017).

[229] L. Ferro, R. Fazio, F. Illuminati, G. Marmo, V. Vedral, and S. Pascazio, Measuring quantumness: from theory to observability in interferometric setups, Eur. Phys. J. D **72**, 219 (2018).

[230] A. Luis, Complementarity and duality relations for finite-dimensional systems, Phys. Rev. A **67**, 032108 (2003).

[231] A. Rènyi, in Proceeding of the 4th Berkeley Symposium on Mathematical Statistics and Probability **1**, 547 (1961).

[232] S. Dürr, Quantitative wave-particle duality in multibeam interferometers, Phys. Rev. A **64**, 042113 (2001).

[233] A. Streltsov, H. Kampermann, S. Wölk, M. Gessner, and D. Bruß, Maximal coherence and the resource theory of purity, New J. Phys. **20** 053058, (2018).

[234] J. Xu, Quantifying coherence of Gaussian states, Phys. Rev. A **93**, 032111 (2016).

[235] A. Ferraro *et al.*, Almost all quantum states have nonclassical correlations, Phys. Rev. A **81**, 052318 (2010).

[236] H. Dai and S. Luo, Information-theoretic approach to atomic spin nonclassicality, Phys. Rev. A, **100**, 062114 (2019).

[237] Y. Zhang and S. Luo, Spin nonclassicality via variance, Theor. Math. Phys. **208**, 916–925 (2021).

[238] D. F. Walls and P. Zoller, Reduced Quantum Fluctuations in Resonance Fluorescence, Phys. Rev. Lett. **47**, 709–711 (1981).

[239] P. K. Aravind, Mixed-state SU(2) squeezing and its occurrence in two quantum optical models, J. Opt. Soc. Am. B **3**, 1712-1717 (1986).

[240] M. Kitagawa and M. Ueda, Squeezed spin states, Phys. Rev. A **47**, 5138–5143 (1993).

[241] M.-F. Fang, P. Zhou, and S. Swain, Entropy squeezing for a two-level atom, J. Mod. Opt. **47**, 1043-1053 (2000).

[242] Sørensen, L.-M. Duan, J. I. Cirac, and P. Zoller, Many-particle entanglement with Bose–Einstein condensates, Nature (London) 409, 63–66 (2001).

[243] N. Korolkova and R. Loudon, Nonseparability and squeezing of continuous polarization variables, Phys. Rev. A **71**, 032343 (2005).

[244] A.-S. F. Obada, N. A. Alshehri, E. M. Khalil, S. Abdel-Khalek, and H.F. Habeba, Entropy squeezing and atomic Wehrl density for the interaction between SU(1,1) Lie algebra and a three-level atom in presence of laser field, Results in Physics **30**, 104759 (2021).

[245] L. Ares and A. Luis, Coherence, nonclassicality and metrological resolution, arXiv:2109.04046 [quant-ph].

[246] S. Luo and Y. Sun, Quantum coherence versus quantum uncertainty, Phys. Rev. A **96**, 022130 (2017).

[247] S. Luo, Classicality versus quantumness in Born's probability, Phys. Rev. A **96**, 052126 (2017).

[248] Y. Zhang and S. Luo, Quantum states as observables: Their variance and nonclassicality, Phys. Rev. A **102**, 062211 (2020).